The anaerobic monoterpene metabolism in *Castellaniella defragrans* 65Phen

Dissertation

Zur Erlangung des Grades eines

Doktors der Naturwissenschaften

- Dr. rer. nat. -

Dem Fachbereich Biologie/Chemie der

Universität Bremen

vorgelegt von

Edinson A. Puentes Cala

Bremen, März 2018

Die vorliegende Arbeit wurde in der Zeit von April 2014 bis März 2018 am Max Planck Institut für marine Mikrobiologie in Bremen angefertigt.

1. Gutachter: Prof. Dr. Jens Harder

2. Gutachter: Prof. Dr. Michael Friedrich

1. Prüfer: Prof. Dr. Rudolf Amann

2. Prüfer: Dr. Jan-Hendrik Hehemann

Tag des Promotionskolloquiums: 19.Apr.2018

Table of contents

Chapter VI

Appendix

Summary

The betaproteobacterium *Castellaniella defragrans* 65Phen belongs to a handful of bacterial strains able to mineralize monoterpenes under anaerobic denitrifying conditions. It utilizes acyclic, monocyclic and bicyclic monoterpenes as sole carbon and energy sources. Whether *C. defragrans* uses parallel pathways for the degradation of the different monoterpene families or whether the metabolism of all its substrates is centralized in a single pathway was elucidated in this study.

A mutant with a defective monocyclic monoterpene degradation pathway was used to identify the initial biotransformation of the bicyclic monoterpenes α-pinene, 3-carene and sabinene. Monocyclic monoterpenes were formed in cell cultures and in *in vitro* assays using cell lysates. This enzyme activity was stimulated by ATP and the first evidence suggested a membrane association. Besides the accumulation of monocyclic intermediates, transposon mutants and the proteome of bicyclic monoterpene-degrading cells supported that the cyclic monoterpene degradation pathway is used for the degradation of all monoterpenes in *C. defragrans*.

Additional evidence was provided by the *in vitro* formation of monocyclic monoterpene intermediates from monoterpene alcohols. Here, the *in vitro* dehydration of α-terpineol and terpinen-4-ol was observed for the first time. This dehydratase activity together with a second alcohol dehydratase acting on linalool were partially purified and characterized.

An anaerobic limonene dehydrogenase (CtmAB) was purified and characterized from limonene-grown *C. defragrans*. CtmAB is a heterodimeric enzyme and carries two tightly-bound flavins per dimer. These two unique features differentiate CtmAB from other proteins of the family of the phytoene dehydrogenases (COG1233). CtmAB catalyzes the reversible anaerobic hydroxylation of limonene to perillyl alcohol. The oxidation was detected with ferrocenium as electron acceptor, whereas DTT served as reductant for perillyl alcohol reduction to limonene. CtmAB reduced ferrocenium ions using several other monocyclic monoterpenes including those formed during acyclic and bicyclic monoterpene degradation. Thus, *C. defragrans* channels all monocyclic monoterpene dienes with a

sp^2-hybridized C_1 atom via the limonene dehydrogenase into the monocyclic monoterpene degradation pathway for their mineralization.

Insertion mutants unable to grow on monoterpenes often carried the transposable element on membrane-associated and membrane integral proteins. A novel efflux pump of the Resistance-Nodulation Division (RND) superfamily was analyzed to prove its function as a monoterpene detoxification mechanism in *C defragrans*. The RND transporter encoded by genes *ameABCD* is likely forming a proton gradient-dependent tetrapartite efflux complex which spans from the inner membrane, through the periplasm and the outer membrane to the extracellular space. The deletion of genes *ameABCD* significantly reduced *C. defragrans*' tolerance towards monoterpene hydrocarbons and increased intracellular accumulation of the fluorescent dye Nile Red. Thus, we suggest that AmeABCD is actively exporting monoterpenes and other non-polar substrates.

Zusammenfassung

Das Betaproteobakterium *Castellaniella defragrans* 65Phen gehört zu einigen wenigen Bakterienstämmen, die in der Lage sind, Monoterpene unter anaeroben, denitrifizierenden Bedingungen zu mineralisieren. Es verwendet azyklische, monozyklische und bizyklische Monoterpene als alleinige Kohlenstoff- und Energiequelle. In dieser Doktorarbeit wurde untersucht, ob *C. defragrans* parallele Stoffwechselwege für den Abbau unterschiedlicher Monoterpenfamilien nutzt, oder ob der Metabolismus aller seiner Substrate in einem einzigen Stoffwechselweg zentralisiert ist.

Ein Mutant mit defektem monozyklischen Monoterpenabbauweg wurde genutzt, um die anfängliche Biotransformation der bizyklischen Monoterpene α-Pinene, 3-Caren und Sabinen zu identifizieren. Monozyklische Monoterpene wurden in Zellkulturen und *in vitro* Untersuchungen mit Zelllysaten hergestellt. Diese enzymatische Aktivität wurde durch ATP stimuliert und erste Beweise deuten auf eine Membranassoziation hin. Die Ansammlung von monozyklischen Intermediaten, Transposonmutanten, sowie das Proteom von bizyklischen monoterpenabbauenden Zellen unterstützten die Schlussfolgerung, dass der zyklische Monoterpenabbauweg für den Abbau aller Monoterpene in *C. defragrans* verwendet wird.

Zusätzliche Beweise lieferte die *in vitro* Bildung von monozyklischen Monoterpenintermediaten von Monoterpenalkoholen. Die Dehydrierung von α-Terpineol und Terpinen-4-ol wurde zum ersten Mal beobachtet. Die Aktivität dieser Dehydratase zusammen mit einer zweiten Alkohol-Dehydratase, die auf Linalool wirkt, wurde teilweise aufgereinigt und charakterisiert.

Eine anaerobe Limonen-Dehydrogenase (CtmAB) wurde von auf Limonen gewachsenen *C. defragrans* aufgereinigt und charakterisiert. CtmAB ist ein heterodimerisches Enzym, welches zwei kovalent gebundene Flavine pro Dimer besitzt. Diese zwei Eigenschaften unterscheiden CtmAB von anderen Proteinen der Familie der Phytoen-Dehydrogenasen (COG1233). CtmAB katalysiert die reversible anaerobische Hydroxylierung von Limonen zu Perillaalkohol. Die Oxidation wurde mit Ferrocenium als Elektronenakzeptor entdeckt, wohingegen DTT als Reduktionsmittel für

Perillaalkohol zu Limonen diente. CtmAB reduzierte Ferrocenium-Ionen mit Hilfe verschiedener monozyklischer Monoterpene, inklusive solcher, die während des Abbaus azyklischer und bizyklischer Monoterpene gebildet wurden. Daher leitet *C. defragrans* alle monozyklischen Monoterpendiene mit einem sp^2-hybridisierten Kohlenstoffatom über die Limonen-Dehydrogenase in den monozyklischen Monoterpenabbauweg weiter, um sie zu mineralisieren.

Insertionsmutanten die nicht auf Monoterpenen wachsen konnten, trugen oft das mobile Element auf membranassoziierten oder integralen Membranproteinen. Eine neue Efflux-Pumpe aus der Superfamilie der „Resistance-Nodulation-Division“ (RND) wurde analysiert, um ihre Funktion im Monoterpenentgiftungsmechanismus in *C defragrans* zu beweisen. Dieser RND Transporter wird durch *ameABCD* Gene kodiert, die einen vom Protonengradienten abhängigen aus vier Komponenten bestehenden Efflux-Komplex bilden, welcher von der inneren Membran durch das Periplasma und die äußere Membran bis zum extrazellulären Raum reicht. Das Ausschalten von *ameABCD* Genen reduzierte die Toleranz von *C. defragrans* gegenüber Monoterpen-Hydrogenkarbonaten signifikant und steigert die Akkumulation des Fluoreszenzfarbstoffes Nile Red. Deshalb schlagen wir vor, dass AmeABCD aktiv Monoterpene und andere nicht polare Substrate exportiert.

Chapter I: Introduction

1.1 Terpenes and monoterpenes

Terpenes constitute a naturally occurring and chemically diverse group of hydrocarbons present in organisms of all domains of life (Davis and Croteau 2000). Despite their ubiquitous distribution, terpenes attain their greatest abundance and structural diversity in plants. The term "terpene" derives from the German word for turpentine, *Terpentin*, the viscous balsam obtained by carving the bark of several pine trees (*Pinaceae*). The ever growing number of terpene compounds identified to date has reached over 80,000 (Pemberton *et al*. 2017), comprising the largest and most diverse family of natural products known. Structurally, terpenes, also called isoprenoids, consist of repetitions of the five-carbon building block isoprene (C_5H_8, 2-methyl-buta-1,3-diene) (Ruzicka 1953). Terpenes are classified based on the length of their carbon skeleton into hemi- (C5), mono- (C10), sesqui- (C15), di- (C20), tri- (C30), tetra- (C40) and polyterpenes (>C40) (Figure 1) (Ashour *et al*. 2010). During synthesis, the linear carbon chain undergoes rearrangements and cyclization reactions resulting in a-, mono-, bi-, tri-, tetra- and polycyclic products with multiple stereocenters. Additionally, functionalization with oxygen yields alcohols, aldehydes, acids, ketones, esters and epoxides.

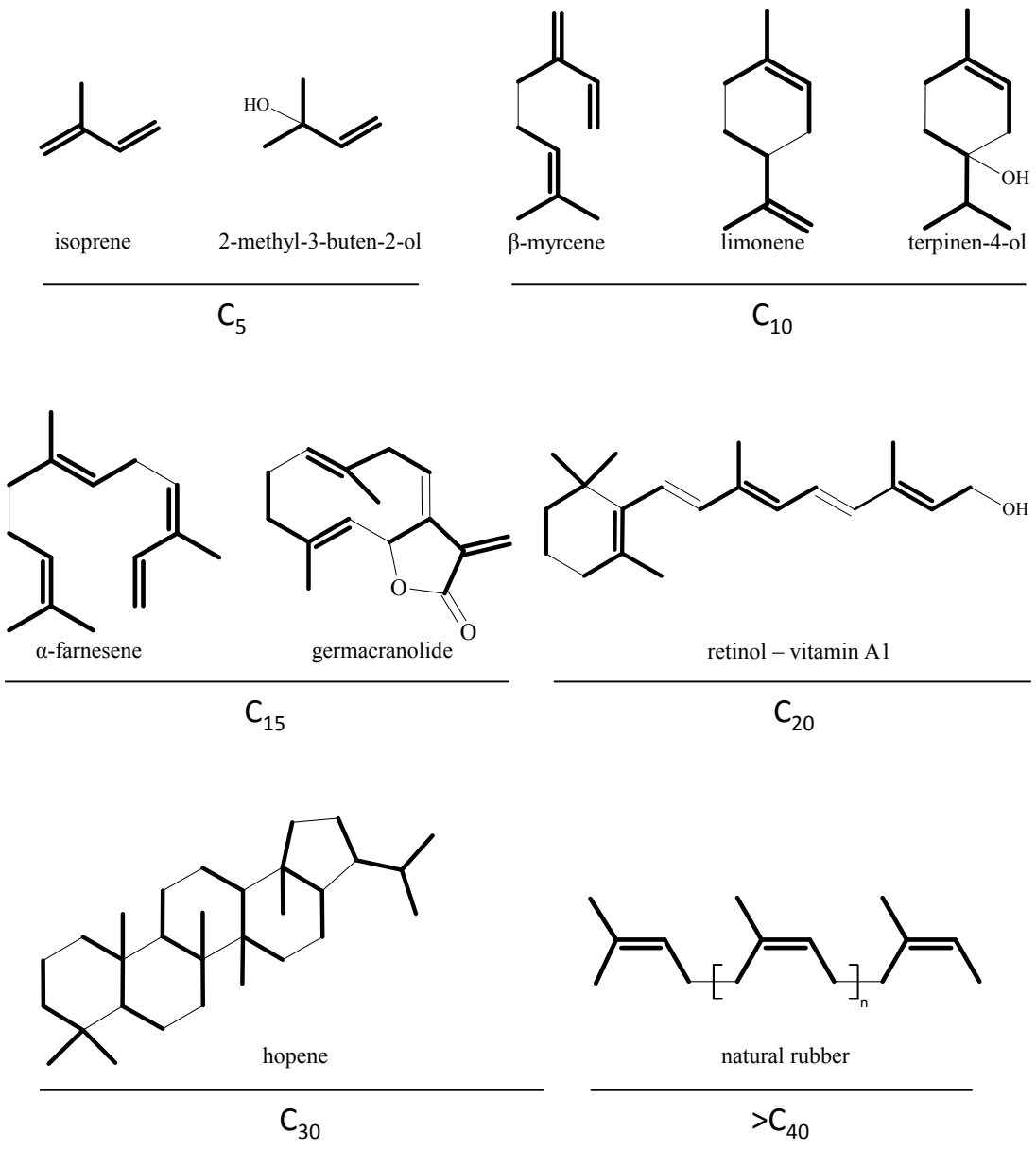

Figure 1. Selected structures of natural terpenes classified by their carbon chain length. C_5, hemiterpenes; C_{10}, monoterpenes; C_{15}, sesquiterpenes; C_{20}, diterpenes; C_{30}, triterpenes and $>C_{40}$, politerpenes. Constitutive isoprene repetitions are highlighted on each structure.

Due to their large diversity terpenes have been attributed with a myriad of biological functions both as primary and secondary metabolites, while in many cases their function still remains unelucidated. Some intracellular roles of terpenes include hormones (cytokinins, gibberellins), pigments (carotenoids), components of electron transfer systems (ubiquinone, plastoquinone) and membrane fluidity determinants (sterols) (Pichersky and Raguso 2016). Interestingly, the vast majority of the

terpenes have ecological functions such as toxins or repellants to herbivores, as antimicrobial agents and as allelochemicals in insect-insect, plant-insect and plant-plant interactions (Gershenzon and Dudareva 2007; Singh and Sharma 2015). Humans have profited from the wide array of biological functions of terpenes for millennia. These have been used in preservation of foods, for embalmment and as antimicrobial, anti-inflammatory, sedative, analgesic, spasmolytic and anesthetic remedies (Bakkali *et al*. 2008; Brettell *et al*. 2017). Throughout history human dependency on terpenes has not changed much; instead it has further expanded for satisfying the needs for plastics (rubber), biofuels, chemical precursors and fragrances.

Terpenes are synthesized in three major steps: (i) the formation of the universal precursors isopentenyl diphosphate (IPP) and dimethylallyl diphosphate (DMAPP); (ii) the condensation of the precursors to linear polyprenyl diphosphates of varying lengths; and (iii) intramolecular rearrangements of the polyprenyl diphosphates resulting in a highly diverse group of terpene end products (Bian *et al*. 2017; Pichersky *et al*. 2006). IPP and DMAPP can be synthesized via two compartmentalized pathways: the cytosol/peroxisome-localized mevalonate pathway (MVA) and the mostly plastid-localized 2-*C*-methyl-D-erythritol-4-phosphate pathway (MEP) (Figure 2). The MVA pathway is present in the majority of the organisms including animals, yeast, *Archaea* and some Gram-positive bacteria (Kovacs *et al*. 2002; Smit and Mushegian 2000; Wilding *et al*. 2000), whereas the MEP pathway is used by most Gram-negative bacteria, cyanobacteria and green algae (Disch *et al*. 1998; Rohmer *et al*. 1993; Vranova *et al*. 2013a). Remarkably, both pathways are present and used in higher plants and some algae (e.g., *Cyanidium caldarium* and *Ochromonas danica*), which is considered as a legacy of early endosymbiotic events between eukaryotic hosts and cyanobacterial (endo-)symbionts (Keeling 2010; Lichtenthaler 2010; Lohr *et al*. 2012). In the MVA pathway, the condensation of three acetyl-CoA units leads to the synthesis of 3-hydroxy-3-methylglutaryl-CoA (Miziorko 2011). The reduction of this compound by the corresponding reductase yields mevalonate, which is pyrophosphorylated in two successive ATP-dependent steps and finally decarboxylated to yield IPP. The formation of DMAPP in the MVA pathway is catalyzed by an isopentenyl diphosphate:dimethylallyl diphosphate isomerase (IDI) (Lohr *et al*. 2012; Singh and Sharma 2015). The more recently elucidated MEP pathway, also referred to as the 1-deoxy-D-xylulose-5-phosphate (DXP) pathway, starts by the fusion of pyruvate

and glyceraldehyde-3-phosphate in a transketolase-like condensation (Lange *et al*. 1998). The resulting product DXP is isomerized and reduced to 2-*C*-methyl-D-erythritol-4-phosphate (MEP). The transformation of MEP into 4-hydroxy-3-methyl-2-(E)-butenyl-diphosphate (HMBPP) is catalyzed in a cascade of four enzymatic steps (Lichtenthaler 2010). The enzyme HMBPP reductase yields both IPP and DMAPP, usually in ratios between 3:1 and 5:1 (Rohdich *et al*. 2002; Tritsch *et al*. 2010). Depending on metabolic demands, the ratio of IPP and DMAPP is balanced out by a second IDI enzyme within the plastid (Lichtenthaler 2010).

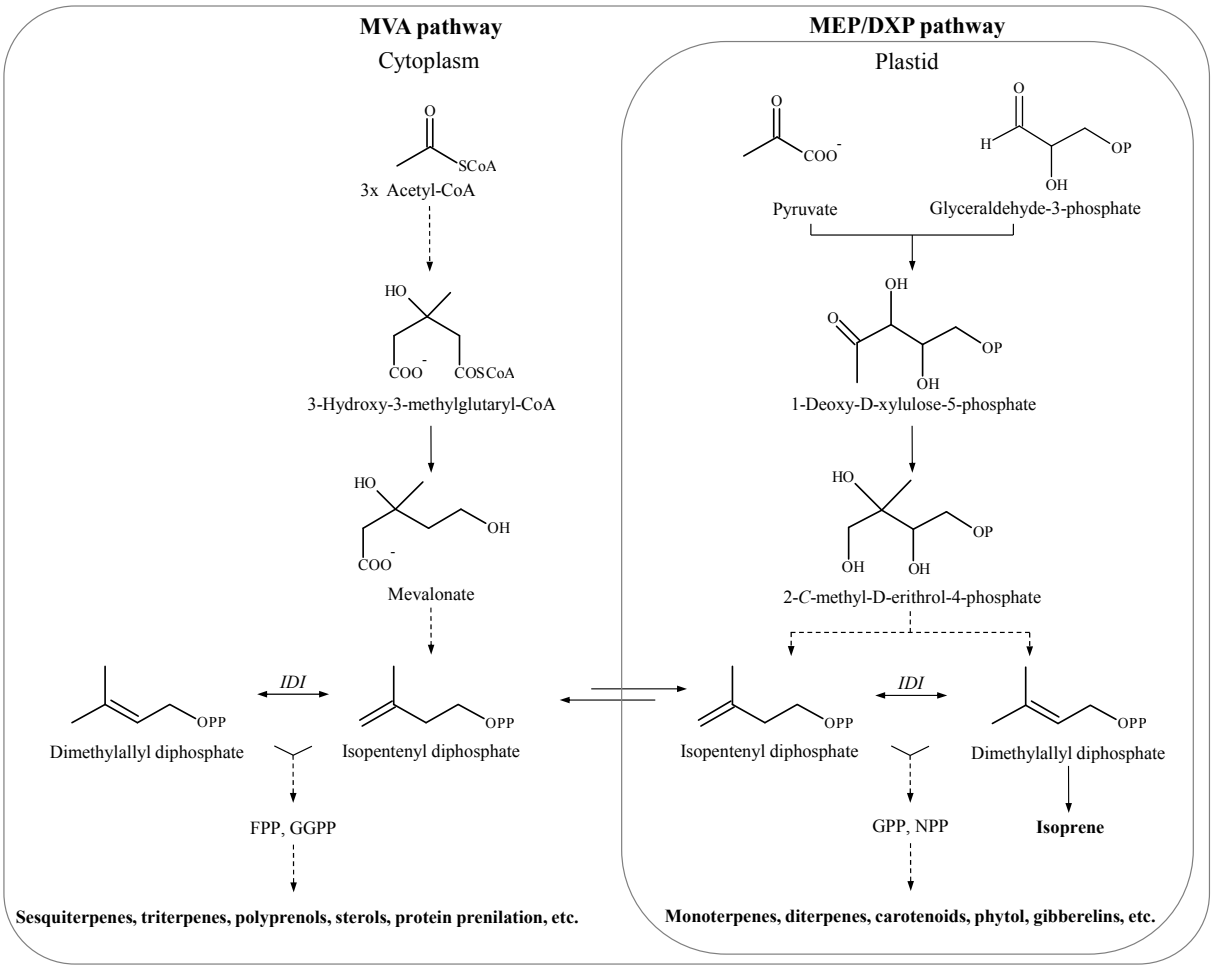

Figure 2. Overview of the compartmentalized pathways for terpene biosynthesis as described for plants. The cytoplasmic mevalonate (MVA) pathway and the plastidic 2-*C*-methyl-D-erythritol-4-phosphate (MEP) pathway, also known as the 1-deoxy-D-xylulose-5-phosphate (DXP) pathway, synthesize the universal C_5 precursors isopentenyl diphosphate and dimethylallyl diphosphate. The corresponding isoenzymes isopentenyl diphosphate:dimethylallyl diphosphate isomerases (IDI)

catalyze the interconversion of the precursors based on physiological demands. The depletion of C_5 precursors in one of the pathways is compensated by transport across compartments by a still unidentified transporter (Vranova *et al*. 2012). The condensation of the C_5 precursors yields geranyl diphosphate (GPP), neryl diphosphate (NPP), farnesyl diphosphate (FPP) and geranyl geranyl diphosphate (GGPP). These are the branch point for the subsequent synthesis of all terpenes.

Both pathways result in the formation of the two universal precursors for terpene synthesis isopentenyl diphosphate (IPP) and dimethylallyl diphosphate (DMAPP). In plants reduced IPP or DMAPP production by one of the pathways can be compensated by transport of either of the precursors across the plastidic membrane (Pellaud and Mene-Saffrane 2017; Vranova *et al*. 2013b). The condensation of IPP and DMAPP results in the synthesis of a wide array of terpene compounds. In a second stage of terpene biosynthesis, prenyltransferases catalyze the 1'-4 (head to tail) condensation of DMAPP and IPP. These enzymes determine the *cis*- or *trans*- stererochemistry of the C10 product, namely neryl diphosphyte (NPP) and geranyl diphosphate (GPP), respectively (Gutensohn *et al*. 2014; Vranova *et al*. 2013a). Further addition of IPP to NPP and GPP results in the formation of all *cis*- and all *trans*-farnesyl diphosphate (FPP). Altogether NPP, GPP, all *cis*-FPP and all *trans*-FPP are the branch point for the subsequent synthesis of all isoprenoids. The last step in terpene biosynthesis proceeds through the formation and rearrangement of carbocationic intermediates within the active site of specialized terpene synthases (Christianson 2017). These enzymes generally fall into two main classes depending on the strategy for carbocation formation: class I enzymes generate a comparatively stable allylic carbocation by the release of the pyrophosphate group, whereas class II enzymes generate a tertiary carbocation by protonating a C–C double bond or an epoxide ring (Schmidt-Dannert 2015). The former includes the prenyl transferases, the monoterpene and sesquiterpene cyclases and many diterpene cyclases (Gao *et al*. 2012; Wendt and Schulz 1998). Class II synthases include mainly the triterpene and tetraterpene cyclases involved in cholesterol and β-carotene biosynthesis.

Terpenes play important roles in the climate system, the atmospheric chemistry and the carbon cycle. They account for 70-85% of the biogenic volatile organic compounds (BVOC) emitted yearly (760-1000 Tg C yr^{-1}) (Bai *et al*. 2017; Sindelarova *et al*. 2014). Mostly emitted by land plants, the

hemiterpene isoprene (400-500 Tg C yr^{-1}) and a small group of monoterpenes (95-157 Tg C yr^{-1}) are the main components of the global BVOC flux (Guenther *et al*. 2012; Muller *et al*. 2008). Ferns, mosses, gymnosperms and angiosperms all include members that emit high amounts of isoprene and monoterpenes to the atmosphere (Bohlmann *et al*. 1998; Sharkey *et al*. 2008). The cost for terpene emission in terms of carbon loss is compensated by the proposed photosystem protection conferred by these metabolites via heat dissipation and tolerance against reactive oxygen species (Holopainen 2004; Penuelas and Llusia 2003; Sharkey *et al*. 2008). In the atmosphere, volatile terpenes rapidly undergo photo-oxidation resulting in less volatile products known as secondary organic aerosols (SOA) (Emanuelsson *et al*. 2014). SOA production promotes cloud condensation, affects tropospheric ozone chemistry and reduces the overall oxidizing capacity of the lower troposphere (Jokinen *et al*. 2015; Kroll and Seinfeld 2008; Librando and Tringali 2005). SOAs persist in the atmosphere until their total oxidation to CO_2 takes place or until atmospheric deposition on land and aquatic systems occurs.

Monoterpenes released from decomposing ground litter and root exudates can be found in soils and sediments (Hayward *et al*. 2001; Lin *et al*. 2007). These belowground monoterpenes permeate the soil through air-filled pores and are known to influence macro- and microorganisms in a rather complex and intricate manner. The inhibition of seed germination and plant growth by α- and β-pinene, limonene, camphene and other monoterpenes has been amply documented (De Martino *et al*. 2010; Muller and Muller 1964; Vokou *et al*. 2003; Wenke *et al*. 2010). The allelopathy extends also to animals which respond positively or negatively to the underground volatile blends (Weissteiner and Schütz 2006). The selective attraction of organisms that are endoparasitic to attacking hervibores is a common feature in the soil arms race (Bertin *et al*. 2003; Langenheim 1994). Root volatiles are important in the regulation of surrounding microbial populations. Monoterpenes such as β-phellandrene and 1,8-cineol emitted by the roots and rhizomes of numerous phylogenetically unrelated plants exhibit antimicrobial activity against several of their bacterial and fungal pathogens (Cobb *et al*. 1968; Dudareva *et al*. 2006; Vilela *et al*. 2009; Wenke *et al*. 2010). Despite their low solubility and high cytotoxicity, monoterpenes are growth substrates to aerobic and anaerobic microorganisms. Such biodegradation carries ecological repercussions since it alleviates the allelopathic effects of soil monoterpenes (Ehlers 2011).

1.2 Monoterpene biodegradation

As it is the case for other hydrocarbons, the microbial mineralization of monoterpenes requires the introduction of functional groups suitable for biological activity. The most recurrent functionalization reactions in monoterpene metabolism are (i) allylic oxygenation, (ii) oxygenation on a double bond and (iii) water addition (Madyashta 1984; Marmulla and Harder 2014). These reactions are commonly catalyzed by mono- and dioxygenases, and other monoterpene hydroxylases (Rojo 2009). These yield primary or secondary alcohols and epoxides as products. For the last half a century, several monoterpene biotransformation reactions including functionalizations, oxidations and molecular rearrangements have been reported in the literature (de Carvalho and da Fonseca 2006; Li and Lan 2011; Marmulla and Harder 2014). However, information regarding complete metabolic pathways is scarce. Nonetheless, the regio- and enantioselectivity of several of such enzymatic reactions pose great potential for biotechnological applications in medicine and the perfume, cosmetics and food industries (Balcerzak *et al*. 2014; Bicas *et al*. 2009; Krings and Berger 2010). The use of abundant and inexpensive monoterpenes such as α/β-pinene and limonene as precursors for the synthesis of more valuable compounds is subject of intensive research (Bian *et al*. 2017; Leavell *et al*. 2016; Linares *et al*. 2009; Molina *et al*. 2013).

The aerobic mineralization of several monoterpenes has been thoroughly investigated in species of *Pseudomonas*. A partial degradation pathway for the primary monoterpene alcohols geraniol, nerol and citronellol was described in *P. citronellolis* as early as the 1960s (Seubert 1960; Seubert and Fass 1964). Later, this pathway was found to be widely distributed in other *Pseudomonas* species (Cantwell *et al*. 1978; Prakash *et al*. 2007; Vandenbergh and Wright 1983), and recently has been completely described (Figure 3) (Forster-Fromme *et al*. 2006; Forster-Fromme and Jendrossek 2010). Briefly, the degradation of acyclic monoterpene alcohols in *Pseudomonas* sp. can be outlined in four phases: (i) the oxidation of the substrate to a carboxylic acid followed by its activation to a CoA-thioester; (ii) the elimination of the β-methyl group by carboxylation and subsequent de-acetylation, also known as the acyclic utilization terpene (Atu) pathway; (iii) the cleavage of two acetyl-CoA units by β-oxidation

producing methyl crotonyl-CoA and (iv) the further degradation to C2 units in the leucine/isovalerate utilization pathway (Liu pathway).

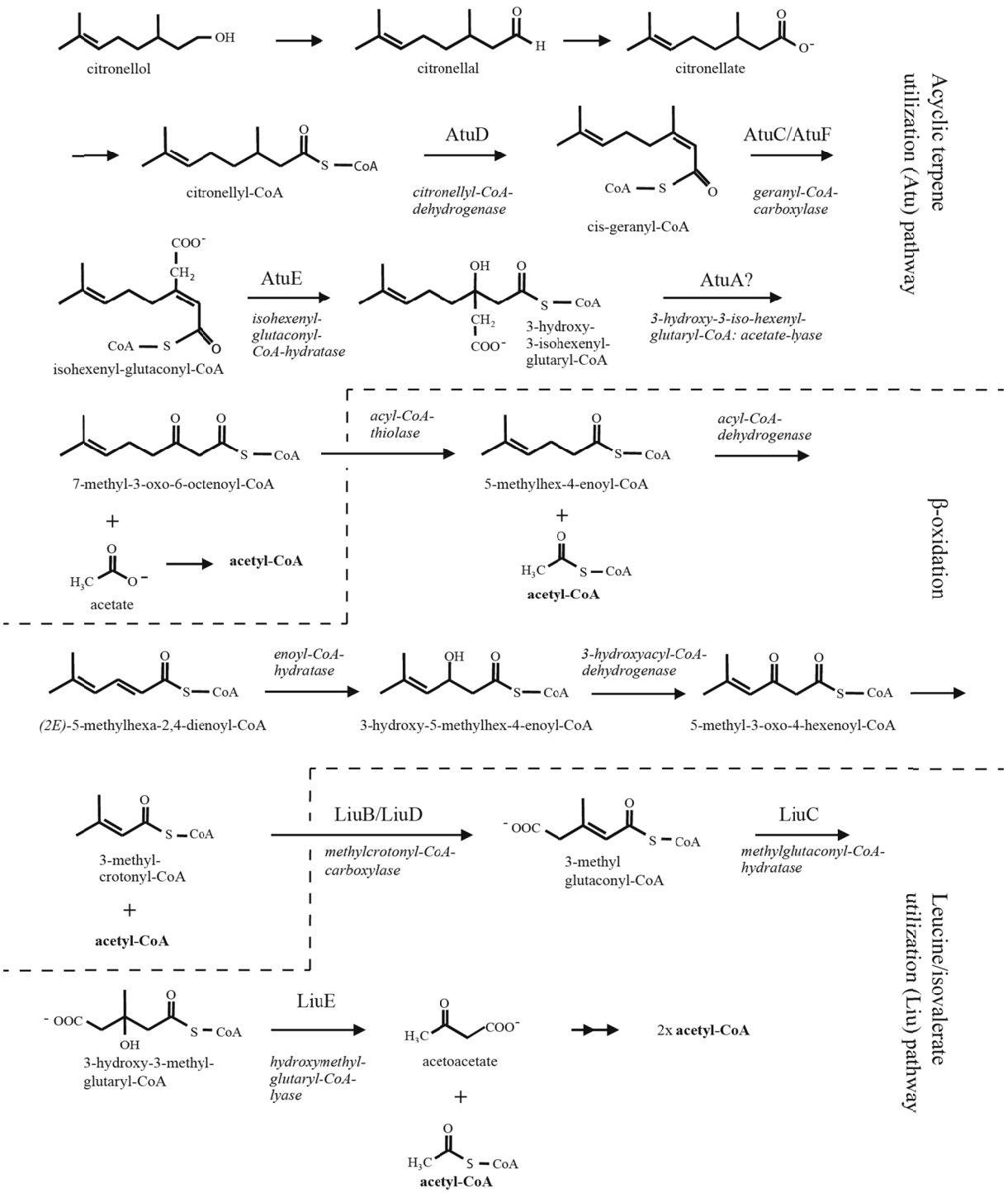

Figure 3. Degradation pathway for acyclic monoterpenes used by several strains of *Pseudomonas*. Taken and modified from (Forster-Fromme and Jendrossek 2010).

Additional pathways for the mineralization of the monoterpenes myrcene, linalool, limonene, *p*-cymene, camphor and pinene have been disclosed in *Pseudomonas* (Duetz *et al*. 2003; Iwaki *et al*. 2013; Linares *et al*. 2009; Soares-Castro and Santos 2015). Other model organisms in monoterpene degradation are *Rhodococcus erythropolis* DCL14 and *R. opacus* PWD4. Numerous members of this genus can grow on several hydrocarbons and monoterpenes, including limonene, as sole carbon and energy sources (Chatterjee 2004; de Carvalho and da Fonseca 2005). *R. erythropolis* DCL14 attacks the cyclohexene ring in limonene with two different mono-oxygenases forming either limonene-1,2-epoxide or *trans*-carveol (van der Werf and Boot 2000; van der Werf *et al*. 1999). The latter is also formed by *R. opacus* PWD4 (Duetz *et al*. 2001). Subsequent oxidation steps result in the formation of monoterpene lactone intermediates which are hydrolyzed to linear carboxylic acids. After their activation to the respective CoA thioesters the intermediates are further degraded via β-oxidation.

The anaerobic mineralization of monoterpene substrates was first reported in denitrifying enrichments from forest soil and activated sludge samples (Harder and Probian 1995). The isolation of the microbes allowed the characterization of seven strains affiliating to *Betaproteobacteria*. The strains distributed into three novel species within the genera *Thauera* and *Castellaniella* (ex *Alcaligenes*) (Foss and Harder 1998; Foss *et al*. 1998; Kampfer *et al*. 2006). The strain *Thauera terpenica* 58Eu^T grows on the bicyclic monoterpene epoxide eucalyptol, and several monocyclic and bicyclic monoterpene dienes, as well as on α-terpineol and terpinen-4-ol. The monocyclic monoterpenes (−)-menthol, (−)-menthone, (+)-isomenthol, (−)-isopulegol and (+)-pulegone and the acyclic 3,7-dimethyl-octan-1-ol supported growth of *T. terpenica* 21Mol. In this organism, a pathway involving the formation of a dione as an intermediate for the cyclohexane ring-opening of its cyclic substrates has been proposed (Hylemon and Harder 1998). The characterization of the strain 47Lol^T resulted in the description of a second *Thauera* species, namely *T. linaloolentis*, which specializes in growth on acyclic monoterpene alcohols. In this organism, the membrane associated linalool isomerase catalyses the regioselective isomerization of the tertiary alcohol linalool to geraniol (Foss and Harder 1997; Marmulla *et al*. 2016). Geraniol is oxidized to geranial and then to geranic acid by the corresponding alcohol and aldehyde dehydrogenases. The further oxidation of geranic acid has been suggested to

occur via a pathway analogous to the Atu pathway described in *Pseudomonas* (Figure 3) (Forster-Fromme and Jendrossek 2010; Marmulla *et al*. 2016).

The placement of the strains 51Men, 54Pin^T, 62Car and 65Phen was originally proposed in a new species within the genus *Alcaligenes*, namely *Alcaligenes defragrans* (Foss *et al*. 1998). Upon further phylogenetic and chemotaxonomic analysis relocation into the novel genus *Castellaniella* within the family *Alcaligenaceae* was proposed (Kampfer *et al*. 2006). *Castellaniella defragrans* strains 51Men and 65Phen were isolated using the monocyclic monoterpenes (+)-menthene and α-phellandrene, respectively, as sole carbon and energy source (Harder and Probian 1995). On the other hand, strains 54Pin and 62Car were isolated on the bicyclic compounds α-pinene and 2-carene, respectively. All four strains are reported to grow on the monocyclic substrates (+)-*p*-menth-1-ene, (+)-limonene, α-phellandrene, α-terpinene, γ-terpinene, terpinolene, (+)-α-terpineol and (+)-terpinen-4-o1, as well as on the bicyclic (+)-sabinene, (+)-2-carene, (+)-3-carene, (-)-α-pinene and (-)-β-pinene. Additionally, all except 54Pin can grow on the monocyclic β-myrcene.

1.3 *Castellaniella defragrans* 65Phen

C. defragrans 65Phen is a motile, rod-shaped (1.3-1.8 µm x 0.5-0.6 µm) mesophile with a facultative and strictly respiratory metabolism (Foss *et al*. 1998). Apart from molecular oxygen, it uses nitrate, nitrite and nitrous oxide as electron acceptor. As carbon and energy sources it can use selected amino acids and short-chain fatty acids, as well as several acyclic, monocyclic and bicyclic monoterpenes. Noticeably, the mineralization of the cyclic monoterpene substrates requires the presence of a sp^2 hybridized C1 atom (Heyen and Harder 1998). Other compound families such as alkanes, carbohydrates and aromatics are not metabolized.

In *C. defragrans* 65Phen, the degradation of the acyclic monoterpene β-myrcene is initiated by hydration of the methylene double bond forming the tertiary alcohol linalool (Figure 4). Linalool is then isomerized to the primary alcohol geraniol. Both reactions are catalyzed by the bifunctional enzyme linalool dehydratase/isomerase (Ldi) (Brodkorb *et al*. 2010; Lüddeke and Harder 2011). Ldi is a periplasmic homopentameric enzyme, which carries out the dehydratase and hydroxyl mutase

reactions in strict anaerobic conditions without the need for soluble cofactors or prosthetic groups. Its recently elucidated crystal structure revealed the existence of three catalytic centers in the enzyme's active center, which coordinate the protonation and hydration of the double bond and determine the regioselectivity of the isomerization reaction (Nestl *et al*. 2017; Weidenweber *et al*. 2016). As a primary alcohol, geraniol is subject to oxidation first to geranial and then to geranic acid by specific geraniol and geranial dehydrogenases (GeoA and GeoB, respectively) (Lüddeke *et al*. 2012b). The discovery and characterization of GeoA and GeoB confirmed the previous detection of geranic acid in cultures and cell suspensions supplied with β-myrcene and other monoterpenes (Heyen and Harder 2000). Thus far, the fate of geranic acid in *C. defragrans* has not been resolved. Genes analogous to the Atu pathway from *Pseudomonas* (Figure 3) have not been found in *C. defragrans*. In fact, experiments with a deletion mutant lacking the gene for the linalool dehydratase/isomerase have suggested the existence of an alternative pathway for linalool metabolism and a link between the cyclic and acyclic monoterpene degradation (Figure 4) (Lüddeke *et al*. 2012a; Marmulla 2015).

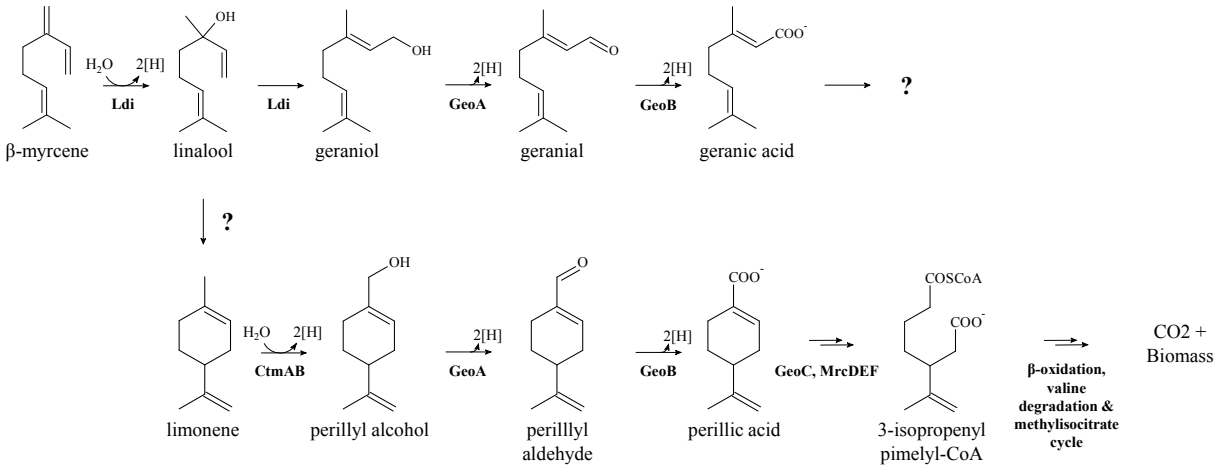

Figure 4. Proposed pathways for the degradation of acyclic and monocyclic monoterpenes in *C. defragrans* 65Phen. The main reactions are catalyzed by the linalool dehydratase/isomerase (Ldi), geraniol dehydrogenase (GeoA), geranial dehydrogenase (GeoB), limonene dehydrogenase (CtmAB), perillate-CoA ligase (GeoC), perillyl-CoA hydratase (MrcF), 2-hydroxy-4-isopropenylcyclohexane-1-carboxyl-CoA dehydrogenase (MrcD), 4-isopropenyl-2-oxo-cyclohexane-1-carboxyl-CoA hydrolase (MrcE). The fate of geranic acid has thus far not been experimentally disclosed. Recent results have

suggested a link between the acyclic and monocyclic monoterpene degradation pathways, being the biotransformation of linalool the linking step (Marmulla 2015).

Recently, a pathway for the complete mineralization of monocyclic monoterpenes has been proposed (Figure 4) (Petasch *et al*. 2014). The oxidation of limonene is started by the oxygen-independent hydroxylation of the allylic methyl group, a reaction catalyzed by the genetic product of genes *ctmAB* (Harder and Marmulla 2017; Petasch *et al*. 2014). This limonene dehydrogenase CtmAB is predicted to be a flavoenzyme related to the phytoene dehydrogenases (COG1233). Members of the phytoene dehydrogenases, also known as desaturases, are a group of enzymes that introduce double bonds into specific allylic groups of phytoene, a precursor in carotenoid biosynthesis. The product of limonene hydration is perillyl alcohol, a primary alcohol that serves as substrate to the geraniol dehydrogenase - GeoA. This enzyme exhibited comparable K_M values for geraniol and perillyl alcohol, but a higher overall catalytic efficiency for the latter (Lüddeke *et al*. 2012b). Perillyl aldehyde, the product of GeoA, is further oxidized to perillic acid by the geranial dehydrogenase GeoB which is also involved in the myrcene degradation (Petasch *et al*. 2014). Its product, perillic acid, is likely activated by the ATP-dependent ligase GeoC to the corresponding CoA thioester. A cascade of oxidation reactions on the cyclohexene double bond by enzymes MrcF, MrcD and MrcE results in the formation of the acyclic intermediate 3-isopropenyl pimelyl-CoA, a suitable substrate for β-oxidation. Three acetyl-CoA eliminations via β-oxidation yield the formation of the C_4 compound methacrylyl-CoA, an intermediate of the valine degradation pathway. After further oxidation and decarboxylation, the product, propionyl-CoA, is incorporated into the tricarboxylic acid cycle via the methyl isocitrate cycle.

The genome of *C. defragrans* 65Phen has recently been made available in public databases (NCBI HG916765) (Petasch *et al*. 2014). Its analysis revealed the existence of a 70 kb genetic island where several of the enzymes involved in monoterpene degradation are encoded. The island includes the genes for the linalool dehydratase/isomerase, the geraniol and geranial dehydrogenases, the perillate-CoA ligase, the cyclic terpene metabolism cluster *ctmABCDEFG* and the monoterpene ring cleavage

cluster *mrcABCDEFGH*. Within the island several electron transfer proteins, proteins related to fatty acid metabolism and hypothetical proteins await for further characterization.

1.4 Aims of the study

Due to the versatility of its metabolism towards monoterpene substrates *Castellaniella defragrans* 65Phen has become a model organism for the study of the anaerobic monoterpene degradation. The initial steps of the acyclic monoterpene metabolism and the complete mineralization of limonene, as representative for monocyclic substrates, have been elucidated (Harder and Marmulla 2017). Several bicyclic monoterpenes also support growth of *C. defragrans* in culture media. However, apart from isolated experiments, the physiology and enzymology of bicyclic monoterpene degradation has not been studied comprehensively. Therefore, the first aim of this study [**Chapter II**] was to elucidate the biochemistry of the bicyclic monoterpene metabolism. Based on the evidence gathered from proteomics analysis and experiments with deletion and transposon mutants we propose for the first time a mechanism for the anaerobic degradation of bicyclic monoterpenes.

The molecular oxygen-independent hydroxylation of the allylic methyl group is the first step in limonene degradation in *C. defragrans* (Petasch *et al*. 2014). The functionalization of the molecule by the limonene dehydrogenase CtmAB enables its oxidation and ultimately facilitates its mineralization. In **Chapter III** we purified this enzyme to homogeneity from limonene-grown *C. defragrans* and characterized its catalytic properties. The heterologous expression of genes *ctmA* and *ctmB* showed only partial enzymatic activity. The wild-type enzyme showed several unique features within the family of the phytoene dehydrogenases (COG1233) and exhibited a wide substrate spectrum among monoterpene substrates.

In addition to pure monoterpene hydrocarbons *C. defragrans* utilizes several monoterpene alcohols as growth substrates. Recently, growth on linalool of a mutant lacking the *ldi* gene suggested the existence of an alternative pathway for linalool degradation (Lüddeke *et al*. 2012a). Additionally, a linalool- and ATP-dependent formation of cyclic monoterpene dienes was detected in crude cell lysates of the same mutant (Marmulla 2015). Besides linalool *C defragrans* mineralizes the

monocyclic monoterpene alcohols α-terpineol and terpinen-4-ol whose fate we aimed to disclose. In this study we discovered a novel catalytic activity that uses α-terpineol and terpinen-4-ol as substrates. In **Chapter IV** we aimed for the purification of these two novel dehydratase activities acting on acyclic and monocyclic monoterpene alcohols. The reactions yield monocyclic monoterpene hydrocarbons as products which justifies the metabolic versatility of *C. defragrans* towards monoterpene substrates.

Monoterpenes are known to be toxic to microorganisms. Due to their hydrophobicity they tend to accumulate in cellular membranes causing instability and loss of proton gradient. Tolerance mechanisms towards monoterpenes in *C. defragrans* include modification of the membrane composition and monoterpene biotransformation. Proteins of a putative efflux transporter were highly up-regulated in α-phellandrene-grown *C. defragrans* (Petasch *et al*. 2014). In **Chapter V** we aimed to investigate the role of this efflux transporter in monoterpene metabolism and tolerance. We characterized this novel component of the monoterpene metabolism by conducting bioinformatics analysis and growth and fluorometric experiments with the wild-type and a deletion mutant.

1.5 Manuscript and publication outline

Chapter II: 'Anaerobic degradation of bicyclic monoterpenes in *Castellaniella defragrans*'

Edinson Puentes-Cala, Manuel Liebeke, Stephanie Markert, Jens Harder.

Published in Metabolites 8 (2018):12; doi:10.3390/metabo8010012.

Authors' contribution:

EPC and JH conceived and designed the experiments; EPC performed the experiments; EPC and ML performed hydrocarbon GC-MS; SM performed MALDI-ToF; EPC and JH analyzed the data and wrote the manuscript.

Contribution of EPC:

Experimental concept and design: 50%; Acquisition of experimental data: 85%; Data analysis and interpretation: 85%; Preparation of figures and tables: 90%; Writing of the manuscript: 70%.

Chapter III: 'Limonene dehydrogenase, a hydroxylating flavoenzyme in the anaerobic monocyclic monoterpene degradation'

Edinson Puentes-Cala, Manuel Liebeke, Stefanie Markert, Jens Harder.

Submitted to the Journal of Biological Chemistry.

Authors' contribution:

EPC and JH conceived and designed the experiments; EPC performed microbiological and biochemical experiments; ML and SM performed mass spectrometry determinations; EPC and JH analyzed the data and wrote the manuscript.

Contribution of EPC:

Experimental concept and design: 40%; Acquisition of experimental data: 90%; Data analysis and interpretation: 60%; Preparation of figures and tables: 80%; Writing of the manuscript: 60%.

Chapter IV: 'Initial purification of novel monoterpene synthases from *Castellaniella defragrans*'

Edinson Puentes-Cala, Elizabeth Engler-Hüsch, Manuel Liebeke, Jens Harder.

Manuscript in preparation.

Authors' contribution:

EPC and JH conceived and designed the experiments; EPC and EEN performed the experiments; ML performed mass spectrometry determinations; EPC and JH analyzed the data and wrote the manuscript.

Contribution of EPC:

Experimental concept and design: 50%; Acquisition of experimental data: 50%; Data analysis and interpretation: 60%; Preparation of figures and tables: 70%; Writing of the manuscript: 70%.

Chapter V: 'An RND transporter in the monoterpene metabolism of *Castellaniella defragrans*'

Edinson Puentes-Cala, Jens Harder.

Manuscript in preparation.

Authors' contribution:

EPC and JH conceived and designed the experiments; EPC performed the experiments; EPC and JH analyzed the data and wrote the manuscript.

Contribution of EPC:

Experimental concept and design: 80%; Acquisition of experimental data: 100%; Data analysis and interpretation: 80%; Preparation of figures and tables: 95%; Writing of the manuscript: 70%.

1.6 Contributed work

Appendix: 'The anaerobic linalool metabolism in *Thauera linaloolentis* 47 Lol'

Robert Marmulla, Edinson Puentes-Cala, Stephanie Markert, Thomas Schweder, and Jens Harder.

Published in BMC Microbiology 16 (2016);76; doi:10.1186/s12866-016-0693-8

Authors' contribution:

RM, EPC and JH conceived and designed the experiments; RM conducted growth experiments, enzyme assays and bioinformatics work; EPC performed transposon mutagenesis experiments; SM performed MALDI-ToF; RM and JH wrote the manuscript.

Contribution of EPC:

Experimental concept and design: 20%; Acquisition of experimental data: 20%; Data analysis and interpretation: 20%; Preparation of figures and tables: 0%; Writing of the manuscript:. 0%.

References

Ashour M, Wink M, Gershenzon J (2010) Biochemistry of terpenoids: monoterpenes, sesquiterpenes and diterpenes. In: Annual Plant Reviews Volume 40: Biochemistry of Plant Secondary Metabolism. Wiley-Blackwell, pp 258-303

Bai JH, Guenther A, Turnipseed A, Duhl T, Greenberg J (2017) Seasonal and interannual variations in whole-ecosystem BVOC emissions from a subtropical plantation in China. Atmos Environ 161:176-190

Bakkali F, Averbeck S, Averbeck D, Idaomar M (2008) Biological effects of essential oils--a review. Food Chem Toxicol 46:446-475

Balcerzak L, Lipok J, Strub D, Lochynski S (2014) Biotransformations of monoterpenes by photoautotrophic micro-organisms. J Appl Microbiol 117:1523-1536

Bertin C, Yang XH, Weston LA (2003) The role of root exudates and allelochemicals in the rhizosphere. Plant Soil 256:67-83

Bian G, Deng Z, Liu T (2017) Strategies for terpenoid overproduction and new terpenoid discovery. Curr Opin Biotechnol 48:234-241

Bicas JL, Dionisio AP, Pastore GM (2009) Bio-oxidation of terpenes: an approach for the flavor industry. Chem Rev 109:4518-4531

Bohlmann J, Meyer-Gauen G, Croteau R (1998) Plant terpenoid synthases: molecular biology and phylogenetic analysis. Proc Natl Acad Sci USA 95:4126-4133

Brettell R, Martin W, Atherton-Woolham S, Stern B, McKnight L (2017) Organic residue analysis of Egyptian votive mummies and their research potential- Stud Conserv 62:68-82

Brodkorb D, Gottschall M, Marmulla R, Lüddeke F, Harder J (2010) Linalool dehydratase-isomerase, a bifunctional enzyme in the anaerobic degradation of monoterpenes. J Biol Chem 285:30436-30442

Cantwell SG, Lau EP, Watt DS, Fall RR (1978) Biodegradation of acyclic isoprenoids by pseudomonas species. J Bacteriol 135:324-333

Chatterjee T (2004) Biotransformation of geraniol by *Rhodococcus* sp strain GR3. Biotechnol Appl Bioc 39:303-306

Christianson DW (2017) Structural and chemical biology of terpenoid cyclases. Chem Rev 117:11570-11648

Cobb FW, Jr., Kristie M, Zavarin E, Barber HW, Jr. (1968) Inhibitory effects of volatile oleoresin components on *Fomes annosus* and four *Ceratocystis* species. Phytopathol 58:1327-1335

Davis EM, Croteau R (2000) Cyclization enzymes in the biosynthesis of monoterpenes, sesquiterpenes, and diterpenes. Top Curr Chem 209:53-95

de Carvalho CCCR, da Fonseca MMR (2005) The remarkable *Rhodococcus erythropolis*. Appl Microbiol Biot 67:715-726

de Carvalho CCCR, da Fonseca MMR (2006) Biotransformation of terpenes. Biotechnol Adv 24:134-142

De Martino L, Mancini E, de Almeida LF, De Feo V (2010) The antigerminative activity of twenty-seven monoterpenes. Molecules 15:6630-6637

Disch A, Schwender J, Muller C, Lichtenthaler HK, Rohmer M (1998) Distribution of the mevalonate and glyceraldehyde phosphate/pyruvate pathways for isoprenoid biosynthesis in unicellular algae and the cyanobacterium *Synechocystis* PCC 6714. Biochem J 333:381-388

Dudareva N, Negre F, Nagegowda DA, Orlova I (2006) Plant volatiles: recent advances and future perspectives. Crit Rev Plant Sci 25:417-440

Duetz WA, Bouwmeester H, van Beilen JB, Witholt B (2003) Biotransformation of limonene by bacteria, fungi, yeasts, and plants. Appl Microbiol Biot 61:269-277

Duetz WA, Fjallman AHM, Ren SY, Jourdat C, Witholt B (2001) Biotransformation of D-limonene to (+) trans-carveol by toluene-grown *Rhodococcus opacus* PWD4 cells. Appl Environ Microbiol 67:2829-2832

Ehlers BK (2011) Soil microorganisms alleviate the allelochemical effects of a thyme monoterpene on the performance of an associated grass species. Plos One 6:e26321

Emanuelsson EU, Mentel TF, Watne AK, Spindler C, Bohn B, Brauers T, Dorn HP, Hallquist AM, Häseler R, Kiendler-Scharr A, Müller KP, Pleijel H, Rohrer F, Rubach F, Schlosser E, Tillmann R, Hallquist M (2014) Parameterization of thermal properties of aging secondary

organic aerosol produced by photo-oxidation of selected terpene mixtures. Environ Sci Technol 48:6168-6176

Forster-Fromme K, Hoschle B, Mack C, Bott M, Armbruster W, Jendrossek D (2006) Identification of genes and proteins necessary for catabolism of acyclic terpenes and leucine/isovalerate in *Pseudomonas aeruginosa*. Appl Environ Microbiol 72:4819-4828

Forster-Fromme K, Jendrossek D (2010) Catabolism of citronellol and related acyclic terpenoids in pseudomonads. Appl Microbiol Biot 87:859-869

Foss S, Harder J (1997) Microbial transformation of a tertiary allylalcohol: regioselective isomerisation of linalool to geraniol without nerol formation FEMS Microbiol Lett 149

Foss S, Harder J (1998) *Thauera linaloolentis* sp. nov. and *Thauera terpenica* sp. nov., isolated on oxygen-containing monoterpenes (linalool, menthol, and eucalyptol) and nitrate. Syst Appl Microbiol 21:365-373

Foss S, Heyen U, Harder J (1998) *Alcaligenes defragrans* sp. nov., description of four strains isolated on alkenoic monoterpenes ((+)-menthene, alpha-pinene, 2-carene, and alpha-phellandrene) and nitrate. Syst Appl Microbiol 21:237-244

Gao Y, Honzatko RB, Peters RJ (2012) Terpenoid synthase structures: a so far incomplete view of complex catalysis. Nat Prod Rep 29:1153-1175

Gershenzon J, Dudareva N (2007) The function of terpene natural products in the natural world. Nat Chem Biol 3:408-414

Guenther AB, Jiang X, Heald CL, Sakulyanontvittaya T, Duhl T, Emmons LK, Wang X (2012) The Model of Emissions of Gases and Aerosols from Nature version 2.1 (MEGAN2.1): an extended and updated framework for modeling biogenic emissions. Geosci Model Dev 5:1471-1492

Gutensohn M, Nguyen TT, McMahon RD, Kaplan I, Pichersky E, Dudareva N (2014) Metabolic engineering of monoterpene biosynthesis in tomato fruits via introduction of the non-canonical substrate neryl diphosphate. Metab Eng 24:107-116

Harder J, Marmulla R (2017) Catabolic pathways and enzymes involved in the anaerobic degradation of terpenes. In: Boll M (ed) Anaerobic utilization of hydrocarbons, oils, and lipids. Springer International Publishing, Cham, pp 1-15

Harder J, Probian C (1995) Microbial degradation of monoterpenes in the absence of molecular oxygen. Appl Environ Microbiol 61:3804-3808

Hayward S, Muncey RJ, James AE, Halsall CJ, Hewitt CN (2001) Monoterpene emissions from soil in a Sitka spruce forest. Atmos Environ 35:4081-4087

Heyen U, Harder J (1998) Cometabolic isoterpinolene formation from isolimonene by denitrifying *Alcaligenes defragrans.* FEMS Microbiol Lett 169:67-71

Heyen U, Harder J (2000) Geranic acid formation, an initial reaction of anaerobic monoterpene metabolism in denitrifying *Alcaligenes defragrans.* Appl Environ Microbiol 66:3004-3009

Holopainen JK (2004) Multiple functions of inducible plant volatiles. Trends Plant Sci 9:529-533

Hylemon PB, Harder J (1998) Biotransformation of monoterpenes, bile acids, and other isoprenoids in anaerobic ecosystems. FEMS Microbiol Rev 22:475-488

Iwaki H, Grosse S, Bergeron H, Leisch H, Morley K, Hasegawa Y, Lau PCK (2013) Camphor pathway redux: functional recombinant expression of 2,5-and 3,6-diketocamphane monooxygenases of *Pseudomonas putida* ATCC 17453 with their cognate flavin reductase catalyzing Baeyer-Villiger reactions. Appl Environ Microbiol 79:3282-3293

Jokinen T, Berndt T, Makkonen R, Kerminen VM, Junninen H, Paasonen P, Stratmann F, Herrmann H, Guenther AB, Worsnop DR, Kulmala M, Ehn M, Sipilä M. (2015) Production of extremely low volatile organic compounds from biogenic emissions: Measured yields and atmospheric implications. Proc Natl Acad Sci USA 112:7123-7128

Kampfer P, Denger K, Cook AM, Lee ST, Jackel U, Denner EBM, Busse HJ (2006) *Castellaniella* gen. nov., to accommodate the phylogenetic lineage of *Alcaligenes defragrans*, and proposal of *Castellaniella defragrans* gen. nov., comb. nov and *Castellaniella denitrificans* sp nov. Int J Syst Evol Micr 56:815-819

Keeling PJ (2010) The endosymbiotic origin, diversification and fate of plastids. Philos Trans R Soc Lond B Biol Sci 365:729-748

Kovacs WJ, Olivier LM, Krisans SK (2002) Central role of peroxisomes in isoprenoid biosynthesis. Prog Lipid Res 41:369-391

Krings U, Berger RG (2010) Terpene bioconversion - how does its future look?. Nat Prod Commun 5:1507-1522

Kroll JH, Seinfeld JH (2008) Chemistry of secondary organic aerosol: formation and evolution of low-volatility organics in the atmosphere. Atmos Environ 42:3593-3624

Lange BM, Wildung MR, McCaskill D, Croteau R (1998) A family of transketolases that directs isoprenoid biosynthesis via a mevalonate-independent pathway. Proc Natl Acad Sci USA 95:2100-2104

Langenheim JH (1994) Higher-plant terpenoids - a phytocentric overview of their ecological roles. J Chem Ecol 20:1223-1280

Leavell MD, McPhee DJ, Paddon CJ (2016) Developing fermentative terpenoid production for commercial usage. Curr Opin Biotechnol 37:114-119

Li HJ, Lan WJ (2011) Biotransformation of limonene by microorganisms. Prog Chem 23:2318-2325

Librando V, Tringali G (2005) Atmospheric fate of OH initiated oxidation of terpenes. Reaction mechanism of alpha-pinene degradation and secondary organic aerosol formation. J Environ Manage 75:275-282

Lichtenthaler HK (2010) The non-mevalonate DOXP/MEP (deoxyxylulose-5-phosphate/methylerythritol-4-phosphate) pathway of chloroplast isoprenoid and pigment biosynthesis. Adv Photosynth Resp 31:95-118

Lin C, Owen SM, Penuelas J (2007) Volatile organic compounds in the roots and rhizosphere of *Pinus* spp. Soil Biol Biochem 39:951-960

Linares D, Fontanille P, Larroche C (2009) Exploration of alpha-pinene degradation pathway of *Pseudomonas rhodesiae* CIP 107491. Application to novalic acid production in a bioreactor. Food Res Int 42:461-469

Lohr M, Schwender J, Polle JEW (2012) Isoprenoid biosynthesis in eukaryotic phototrophs: A spotlight on algae. Plant Sci 185:9-22

Lüddeke F, Dikfidan A, Harder J (2012a) Physiology of deletion mutants in the anaerobic beta-myrcene degradation pathway in *Castellaniella defragrans.* BMC Microbiol 12:192-202

Lüddeke F, Harder J (2011) Enantiospecific (*S*)-(+)-linalool formation from beta-myrcene by linalool dehydratase-isomerase. Z Naturforsch C 66:409-412

Lüddeke F, Wülfing A, Timke M, Germer F, Weber J, Dikfidan A, Rahnfeld T, Linder D, Meyerdierks A, Harder J (2012b) Geraniol and geranial dehydrogenases induced in anaerobic monoterpene degradation by *Castellaniella defragrans.* Appl Environ Microbiol 78:2128-2136

Madyashta KM (1984) Microbial transformations of acyclic monoterpenes. P Indian Acad Sci - Chem Sci 93:677-686

Marmulla R (2015) The anaerobic linalool metabolism in the betaproteobacteria *Castellaniella defragrans* 65Phen and *Thauera linaloolentis* 47Lol. Disseration. University Bremen.

Marmulla R, Cala EP, Markert S, Schweder T, Harder J (2016) The anaerobic linalool metabolism in *Thauera linaloolentis* 47 Lol. BMC Microbiol 16:76-83

Marmulla R, Harder J (2014) Microbial monoterpene transformations-a review. Front Microbiol 5:346-359

Miziorko HM (2011) Enzymes of the mevalonate pathway of isoprenoid biosynthesis. Arch Biochem Biophys 505:131-143

Molina G, Pimentel MR, Pastore GM (2013) *Pseudomonas*: a promising biocatalyst for the bioconversion of terpenes. Appl Microbiol Biot 97:1851-1864

Muller JF, Stavrakou1 T, Wallens S, de Smedt I, van Roozendael M, Potosnak MJ, Rinne J, Munger B, Goldstein A, Guenther AB (2008) Global isoprene emissions estimated using MEGAN, ECMWF analyses and a detailed canopy environment model. Atmos Chem Phys 8:1329-1341

Muller WH, Muller CH (1964) Volatile growth inhibitors produced by *Salvia* species. Bull Torrey Bot Club 91:327-330

Nestl BM, Geinitz C, Popa S, Rizek S, Haselbeck RJ, Stephen R, Noble MA, Fischer MP, Ralph EC, Hau HT, Man H, Omar M, Turkenburg JP, van Dien S, Culler SJ, Grogan G; Hauer B (2017)

Structural and functional insights into asymmetric enzymatic dehydration of alkenols. Nat Chem Biol 13:275-281

Pellaud S, Mene-Saffrane L (2017) Metabolic origins and transport of vitamin E biosynthetic precursors. Front Plant Sci 8:1959-1966

Pemberton TA *et al*. (2017) Exploring the influence of domain architecture on the catalytic function of diterpene synthases. Biochemistry 56:2010-2023

Penuelas J, Llusia J (2003) BVOCs: plant defense against climate warming?. Trends Plant Sci 8:105-109

Petasch J, Disch EM, Markert S, Becher D, Schweder T, Hüttel B, Reinhardt R, Harder J (2014) The oxygen-independent metabolism of cyclic monoterpenes in *Castellaniella defragrans* 65Phen. BMC Microbiol 14:164-176

Pichersky E, Noel JP, Dudareva N (2006) Biosynthesis of plant volatiles: nature's diversity and ingenuity. Science 311:808-811

Pichersky E, Raguso RA (2016) Why do plants produce so many terpenoid compounds? New Phytol https://doi.org/10.1111/nph.14178

Prakash O, Kumari K, Lal R (2007) *Pseudomonas delhiensis* sp nov., from a fly ash dumping site of a thermal power plant. Int J Syst Evol Micr 57:527-531

Rohdich F, Hecht S, Gärtner K, Adam P, Krieger C, Amslinger S, Arigoni D, Bacher A, Eisenreich W (2002) Studies on the nonmevalonate terpene biosynthetic pathway: metabolic role of IspH (LytB) protein. Proc Natl Acad Sci USA 99:1158-1163

Rohmer M, Knani M, Simonin P, Sutter B, Sahm H (1993) Isoprenoid biosynthesis in bacteria: a novel pathway for the early steps leading to isopentenyl diphosphate. Biochem J 295:517-524

Rojo F (2009) Degradation of alkanes by bacteria. Environ Microbiol 11:2477-2490

Ruzicka L (1953) The isoprene rule and the biogenesis of terpenic compounds. Experientia 9:357-367

Schmidt-Dannert C (2015) Biosynthesis of terpenoid natural products in fungi. Adv Biochem Eng Biotechnol 148:19-61

Seubert W (1960) Degradation of isoprenoid compounds by micro-organisms. I. Isolation and characterization of an isoprenoid-degrading bacterium, *Pseudomonas citronellolis* n. sp. J Bacteriol 79:426-434

Seubert W, Fass E (1964) Untersuchungen über den bakteriellen Abbau von Isoprenoiden .V. Der Mechanismus des Isoprenoidabbaues. Biochem Z 341:35-44

Sharkey TD, Wiberley AE, Donohue AR (2008) Isoprene emission from plants: why and how. Ann of Bot 101:5-18

Sindelarova K, Granier C, Bouarar I; Guenther A, Tilmes S, Stavrakou S, Müller JF, Kuhn U, Stefani P, Knorr W (2014) Global data set of biogenic VOC emissions calculated by the MEGAN model over the last 30 years. Atmos Chem Phys 14:9317-9341

Singh B, Sharma RA (2015) Plant terpenes: defense responses, phylogenetic analysis, regulation and clinical applications. Biotech 5:129-151

Smit A, Mushegian A (2000) Biosynthesis of isoprenoids via mevalonate in *Archaea*: the lost pathway. Genome Res 10:1468-1484

Soares-Castro P, Santos PM (2015) Deciphering the genome repertoire of *Pseudomonas* sp M1 toward beta-myrcene biotransformation. Genome Biol Evol 7:1-17

Tritsch D, Hemmerlin A, Bach TJ, Rohmer M (2010) Plant isoprenoid biosynthesis via the MEP pathway: *in vivo* IPP/DMAPP ratio produced by (*E*)-4-hydroxy-3-methylbut-2-enyl diphosphate reductase in tobacco BY-2 cell cultures. FEBS Lett 584:129-134

van der Werf MJ, Boot AM (2000) Metabolism of carveol and dihydrocarveol in *Rhodococcus erythropolis* DCL14. Microbiol 146:1129-1141

van der Werf MJ, Swarts HJ, de Bont JAM (1999) *Rhodococcus erythropolis* DCL14 contains a novel degradation pathway for limonene. Appl Environ Microbiol 65:2092-2102

Vandenbergh PA, Wright AM (1983) Plasmid involvement in acyclic isoprenoid metabolism by *Pseudomonas putida.* Appl Environ Microbiol 45:1953-1955

Vilela GR, Almeida GS, Regitano D'Arcea MA, Duarte-Moraes ME, Brito JO, das G.F. da Silva MF, Cruz-Silva S, de Stefano-Piedade SM, Calori-Domingues MA, Micotti da Gloria E (2009) Activity of essential oil and its major compound, 1,8-cineole, from *Eucalyptus globulus*

Labill., against the storage fungi *Aspergillus flavus* Link and *Aspergillus parasiticus* Speare. J Stored Prod Res 45:108-111

Vokou D, Douvli P, Blionis GJ, Halley JM (2003) Effects of monoterpenoids, acting alone or in pairs, on seed germination and subsequent seedling growth. J Chem Ecol 29:2281-2301

Vranova E, Coman D, Gruissem W (2012) Structure and dynamics of the isoprenoid pathway metwork. Mol Plant 5:318-333

Vranova E, Coman D, Gruissem W (2013a) Network analysis of the MVA and MEP pathways for isoprenoid synthesis. Ann Rev Plant Biol 64:665-700

Vranova E, Coman D, Gruissem W (2013b) Network analysis of the MVA and MEP pathways for isoprenoid synthesis. Ann Rev Plant Biol 64:665-700

Weidenweber S, Marmulla R, Ermler U, Harder J (2016) X-ray structure of linalool dehydratase/isomerase from *Castellaniella defragrans* reveals enzymatic alkene synthesis. FEBS Lett 590:1375-1383

Weissteiner S, Schütz S (2006) Are different volatile pattern influencing host plant choice of belowground living insects? Mitt Dtsch Ges Allg Angew Ent 15:51-55

Wendt KU, Schulz GE (1998) Isoprenoid biosynthesis: manifold chemistry catalyzed by similar enzymes. Structure 6:127-133

Wenke K, Kai M, Piechulla B (2010) Belowground volatiles facilitate interactions between plant roots and soil organisms. Planta 231:499-506

Wilding EI, Brown JR, Bryant AP, Chalker AF, Holmes DJ, Ingraham KA, Iordanescu S, So CY, Rosenberg M, Gwynn MN (2000) Identification, evolution, and essentiality of the mevalonate pathway for isopentenyl diphosphate biosynthesis in gram-positive cocci. J Bacteriol 182:4319-4327

Chapter II: Manuscript 1

Anaerobic degradation of bicyclic monoterpenes in *Castellaniella defragrans*

Edinson Puentes-Cala[1], Manuel Liebeke[2], Stephanie Markert[3] and Jens Harder[1]*

[1]Dept. of Microbiology, Max Planck Institute for Marine Microbiology, Celsiusstr. 1, 28359 Bremen, Germany; epuentes@mpi-bremen.de

[2]Dept. of Symbiosis, Max Planck Institute for Marine Microbiology, Celsiusstr. 1, 28359 Bremen, Germany; mliebeke@mpi-bremen.de

[3]Pharmaceutical Biotechnology, University Greifswald, Felix-Hausdorff-Straße, 17489 Greifswald, Germany; stephanie.markert@uni-greifswald.de

*To whom correspondence should be addressed: Jens Harder, Dept. of Microbiology, Max Planck Institute for Marine Microbiology, Celsiusstr. 1, D-28359 Bremen, Germany, Tel.: ++49 421 2028-750; Fax: ++49 421 2028-790; e-mail: jharder@mpi-bremen.de

Published in *Metabolites* (2018) 8:12-24. DOI: 10.3390/metabo8010012.

metabolites

MDPI

Article

Anaerobic Degradation of Bicyclic Monoterpenes in *Castellaniella defragrans*

Edinson Puentes-Cala [1], Manuel Liebeke [2], Stephanie Markert [3] and Jens Harder [1,*]

[1] Department of Microbiology, Max Planck Institute for Marine Microbiology, Celsiusstr. 1, 28359 Bremen, Germany; epuentes@mpi-bremen.de
[2] Department of Symbiosis, Max Planck Institute for Marine Microbiology, Celsiusstr. 1, 28359 Bremen, Germany; mliebeke@mpi-bremen.de
[3] Pharmaceutical Biotechnology, University Greifswald, Felix-Hausdorff-Straße, 17489 Greifswald, Germany; stephanie.markert@uni-greifswald.de
* Correspondence: jharder@mpi-bremen.de; Tel.: +49-421-2028-750

Received: 23 January 2018; Accepted: 2 February 2018; Published: 7 February 2018

Abstract: The microbial degradation pathways of bicyclic monoterpenes contain unknown enzymes for carbon–carbon cleavages. Such enzymes may also be present in the betaproteobacterium *Castellaniella defragrans*, a model organism to study the anaerobic monoterpene degradation. In this study, a deletion mutant strain missing the first enzyme of the monocyclic monoterpene pathway transformed cometabolically the bicyclics sabinene, 3-carene and α-pinene into several monocyclic monoterpenes and traces of cyclic monoterpene alcohols. Proteomes of cells grown on bicyclic monoterpenes resembled the proteomes of cells grown on monocyclic monoterpenes. Many transposon mutants unable to grow on bicyclic monoterpenes contained inactivated genes of the monocyclic monoterpene pathway. These observations suggest that the monocyclic degradation pathway is used to metabolize bicyclic monoterpenes. The initial step in the degradation is a decyclization (ring-opening) reaction yielding monocyclic monoterpenes, which can be considered as a reverse reaction of the olefin cyclization of polyenes.

Keywords: monoterpene; anaerobic metabolism; ring-opening reactions; carbon–carbon lyase; isoprenoid degradation

1. Introduction

Monoterpenes are a diverse family of biogenic (C10) hydrocarbons. They are synthesized by the condensation of two activated isoprene (C5) units [1,2], primarily as secondary metabolites in higher plants. In addition, some bacteria, fungi, algae and animals are minor monoterpene producers [3]. Global estimates for monoterpene emissions into the atmosphere range from 95 to 157 Tg C a^{-1}, a considerable contribution to the total biogenic organic volatiles (760–1000 Tg C a^{-1}) [4–7]. Monoterpenes contained in foliage are transported into soils, sediments and aquatic habitats, where they become growth substrates for microorganisms [8,9]. Most studies on monoterpene biodegradation since the first report in 1960 were focused on aerobic microorganisms [10–12]. The anaerobic degradation of these biogenic hydrocarbons was discovered in the mid-1990s in denitrifying strains [13], later described as *Castellaniella* (ex *Alcaligenes*) *defragrans*, *Thauera linaloolentis* and *Thauera terpenica* [14–16].

C. defragrans metabolizes more than a dozen structurally diverse monoterpenes to carbon dioxide [15], while most studied aerobic bacteria metabolize one or two closely related substrates [17]. For this reason, over the years, *C. defragrans* (particularly strain 65Phen) has become a model organism to study the anaerobic mineralization of monoterpenes. Several enzymatic steps of the degradation of acyclic and monocyclic monoterpenes have been characterized [18–21]. The hydration of β-myrcene

to (*S*)-linalool, an oxygen-independent reaction catalyzed by the linalool dehydratase/isomerase, has raised interest for its industrial potential in the production of alkenes [18,22,23]. Another novelty is the anaerobic hydroxylation of limonene to perillyl alcohol, the first step in the oxidation of monocyclic monoterpenes [19,20]. A 70 kb genetic island in *C. defragrans*' genome seems to contain all genes necessary for the biotransformation of several monoterpenes including myrcene, linalool, geraniol, α-phellandrene, limonene and pinene to central metabolites, e.g., of the citrate cycle [19,21].

In contrast to acyclic and monocyclic monoterpenes, the enzymology of bicyclic monoterpene degradation in *C. defragrans* has not been investigated. Traces of monoterpenes were detected during growth on bicycles in the past, but a systematic study has not yet been conducted. Here, we studied the transformation of the bicyclic monoterpenes α-pinene, sabinene and 3-carene, using several experimental approaches including the metabolite accumulation in mutants with a defect in the degradation pathway for monocyclic monoterpenes.

2. Results

2.1. Metabolite Formation in Cultures

In order to identify possible intermediates in the metabolism of the bicyclic monoterpenes, cultures of *C. defragrans* strains 65Phen (wild-type, rifampicin-resistant) and 65Phen Δ*ctmAB* were grown in liquid artificial freshwater (AFW) medium with 20 mM acetate and 3 mM of either sabinene, 3-carene or α-pinene as carbon sources and 10 mM nitrate as electron acceptor. Under these conditions, the limitation of nitrate may allow the accumulation of metabolites. Cultures without inoculum or with acetate as substrate served as control experiments. Cultures were harvested in early stationary phase, and hydrophobic substances were extracted and analyzed by gas chromatography with flame ionization detection (GC-FID) for quantification and with mass spectrum detection (GC-MS) for identification. Bicyclic monoterpenes were consumed by both strains, wild-type and Δ*ctmAB* (Table 1). Sabinene concentrations were reduced to half, while only a small portion of 3-carene or α-pinene was consumed.

Table 1. Recovery of bicyclic monoterpenes from cultures of *C. defragrans* wild-type and Δ*ctmAB*.

Monoterpene Co-Substrate	Monoterpene (mM), (Monoterpene Consumed (%))	
	Wild-Type	**Δ*ctmAB***
sabinene	1.6 ± 0.6 (47%)	1.44 ± 0.11 (52%)
3-carene	2.65 ± 0.15 (12%)	2.68 ± 0.02 (11%)
α-pinene	2.95 ± 0.03 (2%)	2.69 ± 0.06 (10%)

The decrease of bicyclic monoterpenes coincided with the formation of monocyclic monoterpenes and monoterpene alcohols in the cultures (Figure 1). These compounds were identified by retention time comparison with authentic standards and GC-MS analysis. Although both strains accumulated the same metabolites, their concentrations in wild-type cultures were considerably lower (in no case higher than 115 µM) than in cultures of the deletion mutant. The co-metabolism of acetate and sabinene in Δ*ctmAB* cultures led to the accumulation of the monoterpenes γ-terpinene (368 ± 35 µM) and α-terpinene (57 ± 7 µM), and of the monoterpene alcohol terpinen-4-ol (78 ± 11 µM) (Figure 1A). Cultures consuming 3-carene accumulated 37 ± 8 µM of limonene and 23 ± 14 µM of α-terpineol (Figure 1B). Coinciding with the disappearance of α-pinene, 227 ± 39 µM of α-terpinene, 32 ± 10 µM of limonene and 18 ± 9 µM of α-terpineol were detected in Δ*ctmAB* cultures (Figure 1C).

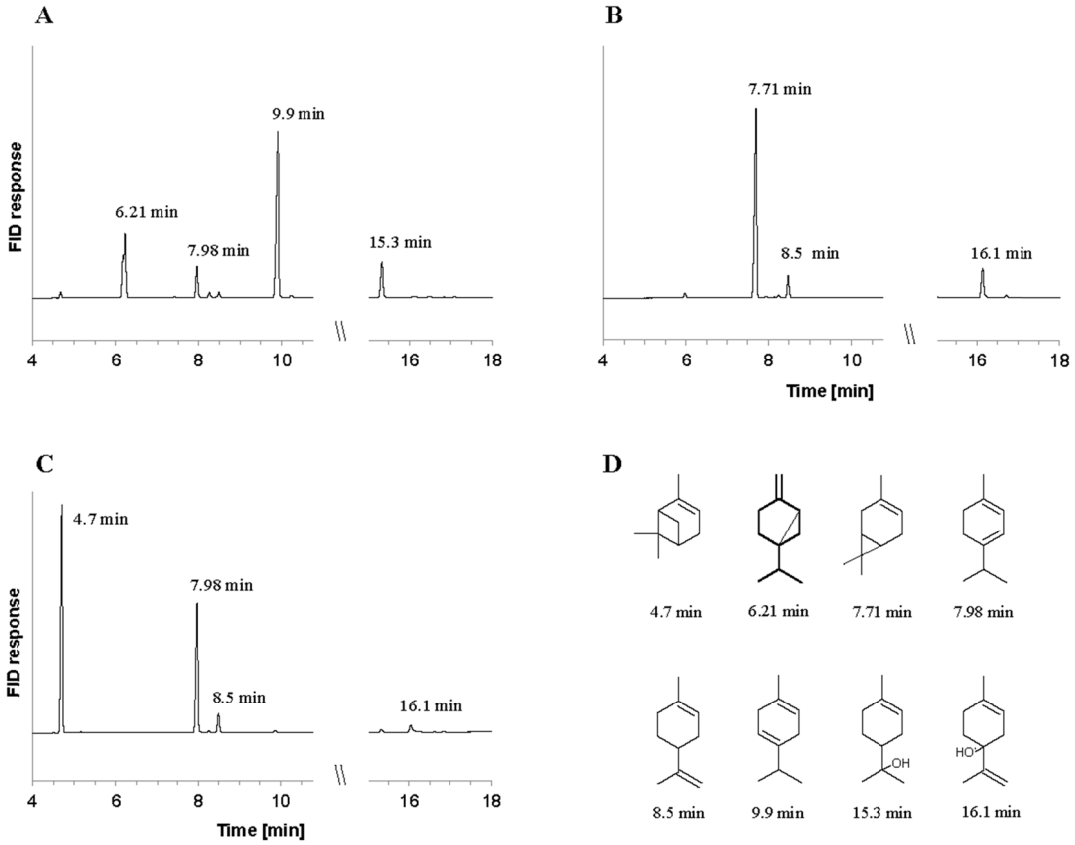

Figure 1. Metabolites formed in cultures of *C. defragrans* 65Phen Δ*ctmAB* grown on acetate in co-metabolism with sabinene (**A**), 3-carene (**B**) and α-pinene (**C**). Monoterpenes were identified by retention time and mass spectrum. The retention times of monoterpenes (**D**) are: α-pinene (4.7 min), sabinene (6.21 min), 3-carene (7.71 min), α-terpinene (7.98 min), limonene (8.5 min), γ-terpinene (9.9 min), terpinen-4-ol (15.3 min) and α-terpineol (16.1 min).

2.2. Metabolite Formation in Cell Lysates

The in vitro biotransformation of bicyclic monoterpenes was assayed in cell lysates of *C. defragrans* 65Phen grown on α-pinene. Several monocyclic products in the presence of each of the three bicycles as detected in hexane extracts by GC-FID (Figure 2). The main product of α-pinene isomerization was terpinolene. The formation of this product was slightly stimulated by the addition of Mg^{2+}, Mn^{2+} and ATP, from 2066 to 2334 fkat mg^{-1}. After removal of endogenous low-molecular weight compounds by dialysis of the cell lysate, terpinolene formation decreased and, in addition, a limonene formation appeared. The apparent enzyme activity for terpinolene synthesis increased from 957 to 2508 fkat mg^{-1} and for limonene from 110 to 196 fkat mg^{-1} after addition of the cofactors. EDTA counteracted this stimulation suggesting an essential role of the divalent ions (Figure 2B). Separate assays showed that Ca^{2+} is also a suitable enzyme cofactor (data not shown). The isomerization of sabinene and 3-carene was observed in crude and dialyzed cell lysates and also stimulated by the cofactor mixture. Incubations with sabinene yielded γ-terpinene as main product (3863 fkat mg^{-1}) followed by α-terpinene (702 fkat mg^{-1}) and terpinolene (445 fkat mg^{-1}) (Figure 2C). The decyclization of 3-carene yielded α-terpinene (1146 fkat mg^{-1}), limonene (1162 fkat mg^{-1}) and terpinolene (476 fkat mg^{-1}) (Figure 2D). The ring-opening of the bicyclic monoterpenes was observed in cell lysates, but not in the soluble or the membrane fraction obtained after separation by ultracentrifugation (230,000× *g* for 40 min at 4 °C). The recombination of the resuspended 75 Svedberg membrane pellet with the

supernatant did not restore enzyme activity. This suggests an irreversible disruption of an enzyme complex and may be considered in future attempts to purify the enzyme.

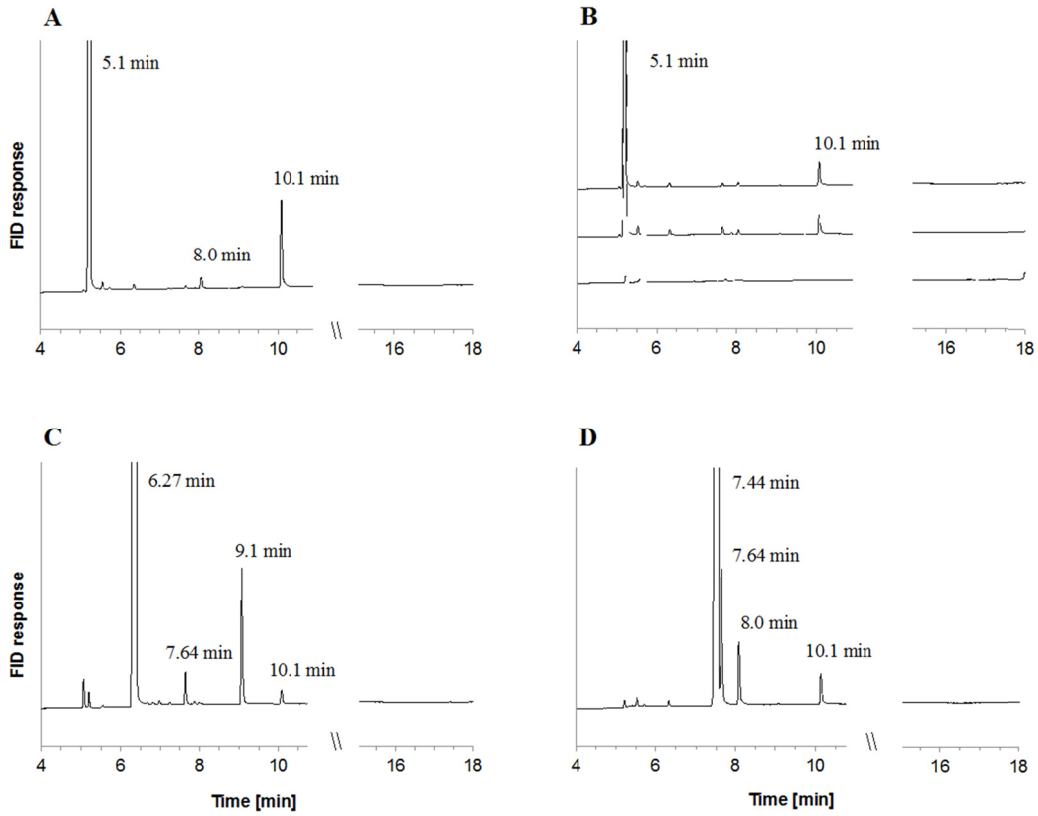

Figure 2. Metabolites formed in vitro from α-pinene (**A**,**B**), sabinene (**C**) and 3-carene (**D**) by dialyzed cell lysates of pinene-grown *C. defragrans* 65Phen. The *y*-axis has the same scale in all graphs; (**B**) terpinolene formation from α-pinene was hampered after EDTA addition (25 mM) (solid line) or in the absence of divalent cations and ATP (dashed line); the cell lysate did not contain monoterpenes (dotted line). Monoterpenes were identified by GC-MS, standard addition analysis and retention time comparison with authentic standards: α-pinene (5.1 min), sabinene (6.27 min), 3-carene (7.44 min) α-terpinene (7.64 min), limonene (8.0 min), γ-terpinene (9.1 min) and terpinolene (10.1 min).

2.3. *Differential Proteomics*

Growth of wild-type *C. defragrans* in α-phellandrene resulted in the upregulated content of 107 proteins in comparison to the proteome of acetate-grown cells [19]. In this study, we investigated the proteomes of *C. defragrans* 65Phen grown on acetate or on one of the monoterpenes R-(+)-limonene, sabinene and α-pinene as single carbon source to identify links between the metabolism of bicyclic and monocyclic monoterpenes. Soluble proteins were separated by anion exchange chromatography and one-dimensional denaturing gel electrophoresis and then protein bands were identified by MALDI-ToF-MS. This approach detected 33 proteins with higher concentration in monoterpene-grown cells (Table 2).

Table 2. Proteins of *C. defragrans* 65Phen present in larger amounts in cells grown on monoterpenes compared to cells grown on acetate. Proteins were fractionated with anion exchange chromatography, semi-quantified by SDS-PAGE (In-gel protein band intensity: +, observable; (+) weakly observable; -, not visible) and identified by MALDI-ToF-MS. Carbon source: L, R-(+)-limonene (monocyclic); S, sabinene (bicyclic); P, α-pinene (bicyclic).

Accession Number	Annotation	Growth Substrate		
		L	S	P
CDM22609	Translation elongation factor Tu	+	-	-
CDM22610	Translation elongation factor G	+	+	+
CDM22641	Translation elongation factor Tu	+	-	-
CDM22907	Copper-containing nitrite reductase	+	+	+
CDM23001	Aconitate hydratase	+	+	+
CDM23572	Methylmalonate-semialdehyde dehydrogenase	+	+	+
CDM23679	Heat shock protein 60 family chaperone GroEL	+	+	+
CDM23795	Chaperone protein DnaK	+	+	+
CDM23915	3-methylmercaptopropionyl-CoA dehydrogenase DmdC	+	+	+
CDM24415	Hypothetical protein	+	+	+
CDM24550	Glutamine synthetase type I	+	+	+
CDM24733	Isoleucyl-tRNA synthetase	+	+	+
CDM24892	Membrane alanine aminopeptidase N	-	+	+
CDM24998	Transcription termination protein NusA	+	-	+
CDM25009	Acetoacetyl-CoA reductase	+	+	+
CDM25072	Citrate synthase	+	+	+
CDM25085	Aconitate hydratase 2	+	+	+
CDM25210	Polyribonucleotide nucleotidyltransferase	(+)	+	+
CDM25241	Acyl-CoA dehydrogenase	+	+	+
CDM25246	3-hydroxyacyl-CoA dehydrogenase	(+)	+	+
CDM25251	4-isopropenyl-2-oxo-cyclohexane-1-carboxyl-CoA hydrolase MrcE	(+)	+	+
CDM25253	2,4-enoyl-CoA reductase MrcC	+	+	+
CDM25259	RND efflux transporter component	+	+	+
CDM25260	RND efflux transporter component	+	+	+
CDM25267	Geraniol dehydrogenase GeoA	(+)	+	+
CDM25281	Geranial dehydrogenase GeoB	-	+	+
CDM25285	NADH:ferredoxin oxidoreductase CtmF	+	+	+
CDM25289	Limonene dehydrogenase CtmB	+	+	+
CDM25290	Limonene dehydrogenase CtmA	+	+	+
CDM25340	Branched-chain amino acid aminotransferase	-	+	+
CDM25770	Protein export cytoplasm protein SecA	-	-	+
CDM25844	Heat shock protein 60 family chaperone GroEL	+	+	+
CDM26013	Glutamate aspartate periplasmic binding protein precursor GltI	+	+	+

Twenty-seven of the identified proteins were present in larger concentrations in all three monoterpene substrates. Among them were several proteins encoded in the genomic island for monoterpene degradation and known to participate in the metabolism of monocyclic monoterpenes. Proteins CtmA, CtmB and CtmF (CDM25290, CDM25289 and CMD25285, respectively) are synthesized from the gene cluster *ctmABCDEFG*, known to be responsible for the hydroxylation of limonene to perillyl alcohol [19,21]. GeoA (CDM25267) and GeoB (CDM25281) catalyze the oxidation of perillyl alcohol and perillyl aldehyde, respectively, resulting in the formation of perillic acid [20]. These and another eight proteins (CDM23572, CDM24415, CDM25009, CDM25241, CDM25246, CDM25251, CDM25259 and CDM25260) were previously detected as proteins with a higher cellular concentration during growth of *C. defragrans* on the monocyclic monoterpene α-phellandrene [19]. These findings link the pathway for bicyclic monoterpene degradation with that for monocyclic monoterpenes. Still, these experiments did not identify a candidate protein responsible for the cycloisomerization of the bicyclic substrates.

2.4. Transposon Conjugants Affected Growth on Monoterpenes

To discover the genes involved in bicyclic monoterpene metabolism, random transposon mutagenesis was performed by means of the mini-Tn5 transposon hosted in the vector

pRL27 [24]. Delivery into *C. defragrans* 65Phen by biparental conjugation resulted in the generation 8896 transconjugants growing with acetate on solid media. These strains were screened on solid medium replacing acetate by one of the monoterpenes limonene, sabinene, α-pinene, or 3-carene supplied via the gas phase. Forty-two of the transconjugants showed impaired growth on at least one of the monoterpenes. Thirty-five unique transposon insertion sites were identified by bidirectional sequencing after rescue cloning (Table 3). The mutation rate of 3.93×10^{-3} was in the range previously observed in similar transposon studies [19,24,25]. Three transposon insertions occurred within the genetic island for monoterpene degradation affecting proteins CDM25252, CDM25285 and CDM25290 (genes *mrcD*, *ctmF* and upstream of *ctmA*, respectively) [19]. Insertions in other genes involved in β-oxidation-like reactions, amino acid degradation and the methylisocitrate cycle (CDM25923, CDM22783 and CDM25080, respectively) also resulted in low to no bacterial growth on monoterpenes (Table 3).

Four ABC transporter genes were inactivated in six transconjugants. The corresponding proteins CDM23032 and CDM23105 had been annotated as components of nutrient uptake systems, whereas CDM23018 and CDM24629 were associated to the export of toxins and antibiotics. Inactivated was also a fifth transporter (CDM24678) that affiliated to the superfamily of proton-driven drug/metabolite transporters. Other transposon insertions took place in genes related to miscellaneous amino acid metabolism (CDM22986, CDM24922), cell wall synthesis (CDM24591), water homeostasis (CDM23452, CDM24706) and several other genes, which currently cannot be linked to monoterpene metabolism, but may contribute to the integrity of the cell in the presence of toxic monoterpenes. Remarkably, several transposon insertions occurred in non-coding regions in front of genes. Seven out of 11 of these insertions were more than 250 bp upstream of the start codon. For the remaining four mutants (CDM22986, CDM23110, CDM25290 and CDM25994), the insertion occurred less than 100 bp upstream of the respective transcription start sites, which might have affected gene expression.

Table 3. Genetic and physiological features of C. *defragrans* 65Phen transconjugants affected in the metabolism of monoterpenes. Growth on monoterpenes was tested on solid and in liquid media. Carbon sources: L, R-(+)-limonene; S, sabinene; P, α-pinene; C, 3-carene. Growth quantification in liquid was based on ΔOD_{600}: + = $\Delta OD_{600} \geq 0.15$; (+) ≥ 0.05; - < 0.05.

Affected Protein (acc. no.)	Gen Length [bp]	Insertion Position [bp]	Annotation	Growth on Solid Media				Growth in Liquid Media			
				L	S	P	C	L	S	P	C
Wild-Type	-	-	-	+	+	+	+	+	+	+	+
CDM22783	1217	1023	Cystathionine beta-lyase	-	-	-	-	-	-	-	-
CDM23032	702	793	Glutamate ABC transporter permease (periplasmic component)	-	-	-	-	+	-	-	-
CDM23105	930	627	High-affinity branched-chain amino acid transport system (permease protein) LivH	-	-	-	-	-	-	-	-
CDM23105	930	161	High-affinity branched-chain amino acid transport system (permease protein) LivH	(+)	(+)	-	-	+	-	-	-
CDM23279	2793	411	Inositol phosphate phosphatase	(+)	-	-	-	-	(+)	(+)	-
CDM23452	1230	150	Fused spore maturation proteins A and B	(+)	-	-	(+)	(+)	(+)	-	(+)
CDM23960	1230	765	Glycolate dehydrogenase (iron-sulfur subunit)	-	-	-	-	+	-	-	(+)
CDM24063	279	243	HigB toxin protein	-	-	-	(+)	(+)	-	-	(+)
CDM24591	3630	889	*O*-antigen biosynthesis protein	(+)	-	-	-	(+)	-	-	-
CDM24600	1029	1012	Glycosyl transferase, family 2	-	-	-	(+)	+	+	-	-
CDM24629	1116	11	ABC transport system (permease component) YbhR	-	-	-	-	-	-	-	(+)
CDM24629	1116	1104	ABC transport system (permease component) YbhR	-	-	-	-	-	-	-	-
CDM24678	897	388	Permease of the drug/metabolite transporter superfamily	-	-	(+)	(+)	-	-	(+)	(+)
CDM24706	3387	2695	Trehalose synthase	-	-	-	-	-	-	-	-
CDM24919	3840	1904	Putative ATP-dependent helicase	-	-	-	-	-	-	-	-
CDM24922	1356	1253	*N*-acetylglutamate synthase	-	-	(+)	(+)	(+)	+	-	-
CDM25080	900	88	Methylisocitrate lyase	(+)	-	-	-	(+)	+	+	-
CDM25154	525	334	Hypothetical protein	(+)	-	-	-	+	+	-	+
CDM25252	771	497	2-hydroxy-4-isopropenyl-cyclohexane-1-carboxyl-CoA dehydrogenase MrcD	(+)	-	-	-	-	-	-	-
CDM25285	1230	492	NADH:ferredoxin oxidoreductase CtmF	-	-	-	-	-	-	-	-
CDM25322	999	468	Hypothetical protein	-	(+)	-	-	+	(+)	(+)	-
CDM25752	849	330	Glucose-1-phosphate thymidylyltransferase	(+)	+	-	-	+	+	-	-
CDM25923	777	223	Enoyl-CoA hydratase	-	-	-	-	-	-	-	-
CDM26084	1514	1428	Putative transposase	-	-	-	(+)	(+)	-	(+)	+
Non-coding region	-	−500	Upstream of CDM22657: single-stranded DNA-binding protein	-	-	-	(+)	+	+	(+)	-
Non-coding region	-	−10	Upstream of CDM22986: phenylacetate-CoA ligase	(+)	-	-	-	+	+	-	-
Non-coding region	-	26	Downstream of CDM23018: auxin efflux transporter	-	-	-	(+)	-	-	-	+
Non-coding region	-	−387	Upstream of CDM23059: hypothetical protein	-	-	-	-	-	-	-	-
Non-coding region	-	−97	Upstream of CDM23110: glutamate ABC transporter (periplasmic component)	-	-	-	-	+	-	-	-
Non-coding region	-	−281	Upstream of CDM23992: hypothetical transcriptional regulator	-	(+)	-	-	(+)	(+)	-	-
Non-coding region	-	−559	Upstream of CDM23992: putative transposase	(+)	-	-	(+)	+	-	-	-
Non-coding region	-	−270	Upstream of CDM23993: putative transcriptional regulator	(+)	-	-	-	+	+	-	-
Non-coding region	-	−78	Usptream of CDM25290: limonene dehydrogenase CtmA	(+)	(+)	(+)	-	-	(+)	-	-
Non-coding region	-	−40	Upstream of CDM25994: thiamin-phosphate pyrophosphatase	-	-	-	-	-	-	-	-
Non-coding region	-	−295	Upstream of CDM26087: putative transposase	(+)	-	-	-	+	-	-	-

3. Discussion

In the past, traces of α-terpinene, cymene and limonene (4–20 µM) were observed in cultures of *C. defragrans* grown with bicyclic monoterpenes [13]. Here, we elevated the concentrations of intermediate metabolites using a mutant strain unable to mineralize monocyclic monoterpenes and a cometabolic metabolism with acetate as growth substrate. The mutant strain formed larger amounts than the wild type strain, but the pattern of the monoterpene metabolites remained stable. We observed the formation and accumulation of several monocyclic monoterpenes (18–368 µM), which all support as individual substance growth of *C. defragrans* [15]. These observations indicate that the traces of monoterpenes found in wild-type cultures indeed are not accidental side-products, but true intermediates of the degradation pathways.

The isomerization of the bicyclic substrates into monocyclic monoterpenes requires the opening of the cyclopropyl ring present in carene and sabinene as well as the cyclobutyl ring in pinene. This process is expected to involve a transient carbocation intermediate [26,27]. In 1968, Shukla and Bhattacharyya proposed a carbocation as precursor for all monocyclic products of an aerobic *Pseudomonas* strain metabolizing α- and β-pinene [28], a hypothesis that has since gained additional evidence [26,29,30]. The products detected in *C. defragrans* suggest the transient formation of terpinen-4-yl and α-terpinyl carbocations, yielding either monocyclic olefins via deprotonation (limonene, terpinolene) or monoterpene alcohols via combination with hydroxide ions or water. The stimulating role of divalent cations and ATP in the synthesis of unsubtituted monocyclic monoterpenes is an aim for future research, but may involve enzyme modifications or the dehydroxylation of these alcohol intermediates via phosphorylation and elimination of phosphate or pyrophosphate (Figure 3).

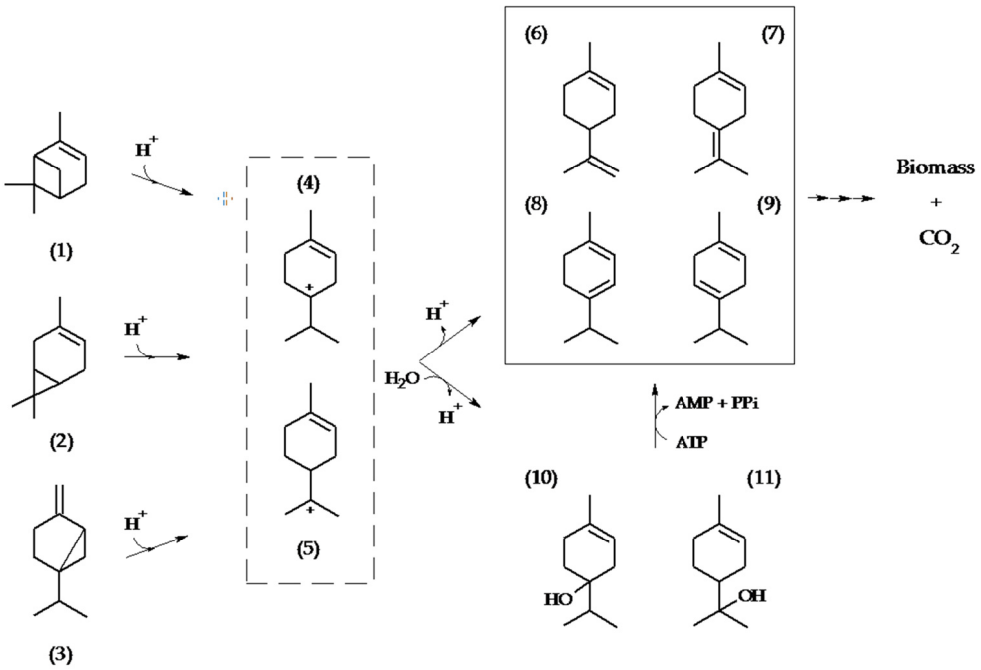

Figure 3. Proposed pathway for the degradation of the bicyclic monoterpenes α-pinene (1), 3-carene (2) and sabinene (3) in *C. defragrans* 65Phen. Electrophilic attack on the allylic double bond and an intramolecular rearrangement generates the monocyclic transient carbocations terpinen-4-yl (4) and α-terpinyl (5). These can deprotonate into monocyclic monoterpene olefins such as (6), (7), (8), (9) or hydroxylated to (10) and (11) by water addition. The alcohols may be dehydrated via an ATP-dependent reaction to monoterpene olefins.

The detection of several proteins involved in monocyclic monoterpene degradation provided additional indirect evidence for the mineralization of bicyclic monoterpenes via monocyclic intermediates. In addition, insertion mutations affecting growth on bicyclic monoterpenes were identified in genes (or upstream of genes) required for the mineralization of monocyclic monoterpenes. Transposon mutants were also affected in genes predicted to be part of defense or detoxification mechanisms such as outer membrane components or membrane permeases, linking the phenotypes to the toxicity of monoterpenes [19,25]. In summary, our observations suggest an isomerization of bicyclic monoterpenes into monocyclic intermediates, prior to their complete mineralization via the monocyclic monoterpene pathway [19]. These decyclization reactions were stimulated by divalent ions and ATP, but a detailed understanding has to await the isolation of the enzyme. So far, the involvement of α-terpinyl and terpinen-4-yl carbocations does best explain the formation of monocyclic monoterpenes.

4. Methods

4.1. Bacterial Cells

The strains and plasmids used in this study are listed in Table 4.

Table 4. List of bacterial strains used in this study.

Strain	Genotype	Source
C. defragrans 65Phen	Rifampicin-resistant (Ra^R)	[31]
C. defragrans 65Phen Δ*ctmAB*	65Phen, Ra^R, Δ*ctmAB*	This work
E. coli BW20767	RP4-2-*tet*::Mu-1, *kan*::Tn*7* integrant, *leu-63*::*IS10*, *recA1*, *creC510*, *hsdR17*, *endA1*, *zbf-5*, *uidA*, (Δ*MluI*)::*pir*$^+$ *thi*	[32]
Plasmid		
pRL27	Tn*5* with Km^R, R6K *ori*, *oriT*, RP4, *tnpA*	[24]

The in-frame deletion mutant Δ*ctmAB* was prepared as described elsewhere [31] and kindly provided by Jan Petasch (Max Planck Institute for Marine Microbiology, Bremen, Germany).

4.2. Culture Conditions

Liquid cultures of *Castellaniella defragrans* 65Phen and all mutants thereof grew under anoxic denitrifying conditions in Artificial Fresh Water (AFW) medium as described [19]. Unless otherwise indicated, 20 mM of sodium acetate or 3 mM of monoterpene was provided as carbon sources. Monoterpenes were supplied in liquid cultures by means of the carrier phase 2,2,4,4,6,8,8-heptamethylnonane (HMN). Cultures were incubated at 28 °C under constant shaking (60 rpm). *E. coli* BW20767 was grown at 37 °C under constant shaking (140 rpm) in Luria Bertani (LB) broth. The plasmid pRL27 was maintained in cultures containing 25 μg mL^{-1} of kanamycin.

4.3. Metabolite Analysis

C. defragrans strains 65Phen and Δ*ctmAB* were inoculated in 10 ml liquid AFW medium containing 20 mM acetate and 3 mM of sabinene, 3-carene or α-pinene. The monoterpenes were dissolved in a filter-sterilized 10% *v*/*v* Tween 20 solution. Tween 20 was not a growth substrate and had a final concentration of 0.5% *v*/*v* in the medium. After 7 days of culture growth, the metabolites were salted out from the aqueous phase by addition of 500 μL of isopropanol, followed by the addition of 5 g of K_2CO_3. The suspension was homogenized for 20 min at 60 rpm for and then stood vertically 10 min for phase separation. One μL of the upper (organic) phase was analyzed in a gas chromatograph (Perkin Elmer Auto System XL, Überlingen, Germany) equipped with an Optima®-5 column (0.25-μm film thickness, 50 m × 0.32-mm inner diameter; Macherey-Nagel, Düren, Germany) and coupled to a flame ionization detector (FID). The temperature program was: injection port 250 °C; column

for 2 min at 40 °C, increate at a rate of 4 °C min^{-1} until 100 °C, constant for 0.1 min, at a rate of 45 °C min^{-1} up to 320 °C, and constant at 320 °C for 3 min; detection temperature 350 °C. The split ratio was 1:9. FID responses for R-(+)-limonene, α- and γ-terpinene, terpinolene and α-terpineol were 5.26 ± 0.24 mV*s per picomol carbon. For terpinen-4-ol, the response was 4.1 mV*s per picomol carbon. Calibration curves for monoterpene dienes were linear within the range of 0.1–10 nmol of injected monoterpene. For terpinen-4-ol and α-terpineol, linearity ranged between 0.5 and 10 nmol. In all cases, the coefficient of determination (R^2) was higher than 0.99. Monoterpene concentrations refer to their theoretical concentrations in the aqueous phase. Metabolite identity initially defined by retention time was confirmed by GC-MS analysis on an Agilent 7890B gas chromatograph (Agilent, Santa Clara, CA, USA) connected to an Agilent 5977A Mass-selective detector. Analyte separation was performed on an Agilent 30 m DB5-MS column with a 10 m DuraGuard column applying the following temperature program: injection port temperature at 250 °C, initial column temperature 40 °C for 1 min, increasing to 160 °C at 4 °C min^{-1} further to 280 °C at 30 °C min^{-1} and hold for 1 min. For verification, mass spectra of monoterpene standards were recorded as reference. Metabolites were then identified by their mass spectra.

4.4. Enzyme Assays

All activity experiments were performed in the absence of oxygen. Cells of wild-type *C. defragrans* grown anaerobically on α-pinene were resuspended in 25 mM Tris-Cl, pH 8.0 and disrupted by two passages through a French-Press cell disrupter (SLM Aminco, Rochester, NY, USA) at 8.6 MPa. The crude cell lysate, as well as the soluble and pelleted fractions obtained after ultracentrifugation (230,000× *g* for 30 min at 4 °C), were dialyzed in anoxic 25 mM Tris-Cl, pH 8.0 ($1:10^6$) and tested for enzyme activity. A 500 µL assay contained 2.5–5 mg protein, 2 mM dithiothreitol, 5 mM Mg^{2+}, 10 mM Mn^{2+}, 10 mM ATP, 0.5% Tween 20 and 60 mM of a bicyclic monoterpene. When indicated, divalent cations were replaced for 10 mM Ca^{2+} supplied as $CaCl_2$. The reactions were initiated by monoterpene addition and incubated for 16–18 h at 28 °C. Hydrophobic metabolites were extracted with 100 µL *n*-hexane and analyzed by GC-FID as aforementioned. Retention times shown in Figures 1 and 2 are shifted due to column shortening during equipment maintenance. Monoterpene identity was confirmed by analysis with internal standards and GC-MS analysis.

4.5. Differential Proteomics: Preparation of Cell Lysates, Soluble Protein Fractionation and MALDI-ToF Analysis

Cells of *C. defragrans* were cultivated in 10 mL of AFW medium supplemented with either 20 mM acetate or 3 mM of R-(+)-limonene, 3-carene, sabinene or α-pinene and sodium nitrate (10 mM). Growth was determined as increase in optical density at 600 nm. Transfers to fresh medium were carried out once a week with an inoculum of 2% vol/vol. After at least 5 consecutive transfers, 5 mL of 5 to 7 days-grown cultures were transferred into 2000 mL of fresh AFW. At this scale, nitrate concentration was increased to 20 mM and the monoterpenes were added without a carrier phase. The biomass was harvested at late exponential phase and resuspended in 10 mM potassium phosphate, pH 8.0. After cell disruption, soluble proteins were separated from cell debris by ultracentrifugation at 230,000× *g* for 40 min at 4 °C. Protein concentration was determined by the method of Bradford [33] with bovine serum albumin as the standard. 20 to 40 mg of the soluble proteins were loaded onto a Resource™ Q column (GE Healthcare, Freiburg, Germany) with a 1 mL bed volume installed in an ÄKTA purifier system (GE Healthcare, Freiburg, Germany) that was equilibrated with 10 mM potassium phosphate, pH 8.0. Protein fractionation was performed by applying a salinity gradient from 0–500 mM KCl over 50 nominal column volumes (flow rate: 0.5 mL min^{-1}) with a collection in 25 fractions of 2 mL. Unbound proteins (flow-through) were collected as a single additional fraction. Each fraction was separated by size and stained in one-dimensional SDS-PAGE as described by Laemmli [34]. A comparison identified proteins present in different amounts. These were excised, subjected to tryptic in-gel digestion and analyzed on an AB SCIEX TOF/TOF™ 5800 Analyzer (AB Sciex, Darmstadt, Germany).

4.6. Transposon Mutagenesis

The generation of transposon insertion mutants and the evaluation of their ability to grow on monoterpenes proceeded as described by Petasch et al. [19]. Mutants with low to no growth on limonene, 3-carene, sabinene and/or α-pinene were selected for further examination. The genomic localization of the Tn5 mini-transposon in each mutant was determined by sequencing after rescue cloning. DNA was extracted from mutant cells from over-night cultures grown in LB medium [35]. One µg of genomic DNA was digested with BamHI (Thermo Fisher Scientific, Waltham, MA, USA) and purified with the GeneJET PCR Purification Kit (Thermo Fisher Scientific). The BamHI fragments were circularized with T4 DNA ligase (Thermo Fisher Scientific). The circularized DNA fragments were transformed into chemically competent *E. coli* BW20767 (*pir*$^+$). Clones with the ability to grow on kanamycin-containing LB medium were selected and plasmids were extracted (QIAprep Spin Miniprep Kit, QIAGEN, Hilden, Germany). Sequencing reactions were prepared with 100 to 200 ng of plasmid DNA and the BigDye Terminator v3.1 Cycle Sequencing Kit (Applied Biosystems, Life Technologies Corporation, Carlsbad, CA, USA). The oligonucleotides tpnRL17-1 (AACAAGCCAGGGATGTAA) and tpnRL 13-2 (CAGCAACACCTTCTTCACGA) were used to prime the reactions [24]. The temperature program used was 96 °C for 5 min, 99 cycles of 96 °C for 20 s, 55 °C for 10 s and 60 °C for 5 min. The DNA sequences were read on an ABI Prism 3130*xl* Genetic Analyzer (Applied Biosystems Life Technologies Corporation, Carlsbad, CA, USA).

Acknowledgments: We thank Jan Petasch for generously supplying us with the strain *C. defragrans* 65Phen Δ*ctmAB*. E.P.C. was funded by the Colombian national education ministry, the Corporación para la Investigación de la Corrosión (Colombia) and the German academic exchange service (DAAD). The project was financed by the Max Plank Society.

Author Contributions: Edinson Puentes-Cala and Jens Harder conceived and designed the experiments; Edinson Puentes-Cala performed the experiments; Edinson Puentes-Cala and Manuel Liebeke performed hydrocarbon GC-MS; Stephanie Markert performed MALDI-ToF of protein bands; Edinson Puentes-Cala and Jens Harder analyzed the data and wrote the manuscript.

Conflicts of Interest: The authors declare no conflict of interest.

References

1. Kesselmeier, J.; Staudt, M. Biogenic volatile organic compounds (VOC): An overview on emission, physiology and ecology. *J. Atmos. Chem.* **1999**, *33*, 23–88. [CrossRef]
2. Sharkey, T.D.; Wiberley, A.E.; Donohue, A.R. Isoprene emission from plants: Why and how. *Ann. Bot.* **2008**, *101*, 5–18. [CrossRef] [PubMed]
3. Chizzola, R. Regular monoterpenes and sesquiterpenes (essential oils). In *Natural Products: Phytochemistry, Botany and Metabolism of Alkaloids, Phenolics and Terpenes*; Ramawat, K.G., Mérillon, J.-M., Eds.; Springer: Berlin/Heidelberg, Germany, 2013; pp. 2973–3008.
4. Lathiere, J.; Hauglustaine, D.A.; Friend, A.D.; De Noblet-Ducoudre, N.; Viovy, N.; Folberth, G.A. Impact of climate variability and land use changes on global biogenic volatile organic compound emissions. *Atmos. Chem. Phys.* **2006**, *6*, 2129–2146. [CrossRef]
5. Laothawornkitkul, J.; Taylor, J.E.; Paul, N.D.; Hewitt, C.N. Biogenic volatile organic compounds in the earth system. *New Phytol.* **2009**, *183*, 27–51. [CrossRef] [PubMed]
6. Guenther, A.B.; Jiang, X.; Heald, C.L.; Sakulyanontvittaya, T.; Duhl, T.; Emmons, L.K.; Wang, X. The Model of Emissions of Gases and Aerosols from Nature version 2.1 (MEGAN2.1): An extended and updated framework for modeling biogenic emissions. *Geosci. Model. Dev.* **2012**, *5*, 1471–1492. [CrossRef]
7. Muller, J.F.; Stavrakou, T.; Wallens, S.; De Smedt, I.; Van Roozendael, M.; Potosnak, M.J.; Rinne, J.; Munger, B.; Goldstein, A.; Guenther, A.B. Global isoprene emissions estimated using MEGAN, ECMWF analyses and a detailed canopy environment model. *Atmos. Chem. Phys.* **2008**, *8*, 1329–1341. [CrossRef]
8. Hayward, S.; Muncey, R.J.; James, A.E.; Halsall, C.J.; Hewitt, C.N. Monoterpene emissions from soil in a sitka spruce forest. *Atmos. Environ.* **2001**, *35*, 4081–4087. [CrossRef]

9. Owen, S.M.; Clark, S.; Pompe, M.; Semple, K.T. Biogenic volatile organic compounds as potential carbon sources for microbial communities in soil from the rhizosphere of *Populus tremula*. *FEMS Microbiol. Lett.* **2007**, *268*, 34–39. [CrossRef] [PubMed]
10. Seubert, W. Degradation of isoprenoid compounds by micro-organisms. I. Isolation and characterization of an isoprenoid-degrading bacterium, *Pseudomonas citronellolis* n. sp. *J. Bacteriol.* **1960**, *79*, 426–434. [PubMed]
11. Cantwell, S.G.; Lau, E.P.; Watt, D.S.; Fall, R.R. Biodegradation of acyclic isoprenoids by *Pseudomonas* species. *J. Bacteriol.* **1978**, *135*, 324–433. [PubMed]
12. Förster-Fromme, K.; Jendrossek, D. Catabolism of citronellol and related acyclic terpenoids in pseudomonads. *Appl. Microbiol. Biotechnol.* **2010**, *87*, 859–869. [CrossRef] [PubMed]
13. Harder, J.; Probian, C. Microbial degradation of monoterpenes in the absence of molecular oxygen. *Appl. Environ. Microbiol.* **1995**, *61*, 3804–3808. [PubMed]
14. Foss, S.; Harder, J. *Thauera linaloolentis* sp. nov. and *Thauera terpenica* sp. nov., isolated on oxygen-containing monoterpenes (linalool, menthol, and eucalyptol) and nitrate. *Syst. Appl. Microbiol.* **1998**, *21*, 365–373. [CrossRef]
15. Foss, S.; Heyen, U.; Harder, J. *Alcaligenes defragrans* sp. nov., description of four strains isolated on alkenoic monoterpenes ((+)-menthene, alpha-pinene, 2-carene, and alpha-phellandrene) and nitrate. *Syst. Appl. Microbiol.* **1998**, *21*, 237–244. [CrossRef]
16. Kämpfer, P.; Denger, K.; Cook, A.M.; Lee, S.T.; Jackel, U.; Denner, E.B.M.; Busse, H.J. *Castellaniella* gen. nov., to accommodate the phylogenetic lineage of *Alcaligenes defragrans*, and proposal of *Castellaniella defragrans* gen. nov., comb. nov and *Castellaniella denitrificans* sp. nov. *Int. J. Syst. Evol. Micr.* **2006**, *56*, 815–819. [CrossRef] [PubMed]
17. Marmulla, R.; Harder, J. Microbial monoterpene transformations—A review. *Front. Microbiol.* **2014**, *5*. [CrossRef] [PubMed]
18. Brodkorb, D.; Gottschall, M.; Marmulla, R.; Lüddeke, F.; Harder, J. Linalool dehydratase-isomerase, a bifunctional enzyme in the anaerobic degradation of monoterpenes. *J. Biol. Chem.* **2010**, *285*, 30436–30442. [CrossRef] [PubMed]
19. Petasch, J.; Disch, E.M.; Markert, S.; Becher, D.; Schweder, T.; Hüttel, B.; Reinhardt, R.; Harder, J. The oxygen-independent metabolism of cyclic monoterpenes in *Castellaniella defragrans* 65Phen. *BMC Microbiol.* **2014**, *14*, 164. [CrossRef] [PubMed]
20. Lüddeke, F.; Wulfing, A.; Timke, M.; Germer, F.; Weber, J.; Dikfidan, A.; Rahnfeld, T.; Linder, D.; Meyerdierks, A.; Harder, J. Geraniol and geranial dehydrogenases induced in anaerobic monoterpene degradation by *Castellaniella defragrans*. *Appl. Environ. Microbiol.* **2012**, *78*, 2128–2136. [CrossRef] [PubMed]
21. Harder, J.; Marmulla, R. Catabolic pathways and enzymes involved in the anaerobic degradation of terpenes. In *Anaerobic Utilization of Hydrocarbons, Oils, and Lipids*; Boll, M., Ed.; Springer International Publishing: Cham, Switzerland, 2017; pp. 1–15. [CrossRef]
22. Weidenweber, S.; Marmulla, R.; Ermler, U.; Harder, J. X-ray structure of linalool dehydratase/isomerase from *Castellaniella defragrans* reveals enzymatic alkene synthesis. *FEBS Lett.* **2016**, *590*, 1375–1383. [CrossRef] [PubMed]
23. Lüddeke, F.; Harder, J. Enantiospecific (*S*)-(+)-linalool formation from beta-myrcene by linalool dehydratase-isomerase. *Z. Naturfr. C* **2011**, *66*, 409–412. [CrossRef]
24. Larsen, R.A.; Wilson, M.M.; Guss, A.M.; Metcalf, W.W. Genetic analysis of pigment biosynthesis in *Xanthobacter autotrophicus* Py2 using a new, highly efficient transposon mutagenesis system that is functional in a wide variety of bacteria. *Arch. Microbiol.* **2002**, *178*, 193–201. [CrossRef] [PubMed]
25. Marmulla, R.; Cala, E.P.; Markert, S.; Schweder, T.; Harder, J. The anaerobic linalool metabolism in *Thauera linaloolentis* 47Lol. *BMC Microbiol.* **2016**, *16*, 76. [CrossRef] [PubMed]
26. Yoo, S.K.; Day, D.F. Bacterial metabolism of α- and β-pinene and related monoterpenes by *Pseudomonas* sp. strain PIN. *Process. Biochem.* **2002**, *37*, 739–745. [CrossRef]
27. Traas, P.C. Advances in the chemistry of some interesting cyclic monoterpene alcohols. In *Fragrance Chemistry: The Science of the Sense of Smell*; Heimer, E.T., Ed.; Academic Press: San Diego, CA, USA, 1982; pp. 165–219.
28. Shukal, O.P.; Bhattacharyya, P.K. Microbiological transformations of terpenes: Part XI—Pathways of degradation of α-& β-pinenes in a soil pseudomonad (PL-strain). *Indian J. Biochem.* **1968**, *5*, 92–101.

29. Cheng, Z.W.; Sun, P.F.; Jiang, Y.F.; Zhang, L.L.; Chen, J.M. Kinetic analysis and bacterium metabolization of alpha-pinene by a novel identified *Pseudomonas* sp. strain. *J. Environ. Sci. (China)* **2012**, *24*, 1806–1815. [CrossRef]
30. Narushima, H.; Omori, T.; Minoda, Y. Microbial transformation of alpha-pinene. *Eur. J. Appl. Microbiol.* **1982**, *16*, 174–178. [CrossRef]
31. Lüddeke, F.; Dikfidan, A.; Harder, J. Physiology of deletion mutants in the anaerobic beta-myrcene degradation pathway in *Castellaniella defragrans*. *BMC Microbiol.* **2012**, *12*, 192. [CrossRef] [PubMed]
32. Metcalf, W.W.; Jiang, W.; Daniels, L.L.; Kim, S.K.; Haldimann, A.; Wanner, B.L. Conditionally replicative and conjugative plasmids carrying *lacZα* for cloning, mutagenesis, and allele replacement in bacteria. *Plasmid* **1996**, *35*, 1–13. [CrossRef] [PubMed]
33. Bradford, M.M. A rapid and sensitive method for the quantitation of microgram quantities of protein utilizing the principle of protein-dye binding. *Anal. Biochem.* **1976**, *72*, 248–254. [CrossRef]
34. Laemmli, U.K. Cleavage of structural proteins during the assembly of the head of bacteriophage T4. *Nature* **1970**, *227*, 680–685. [CrossRef] [PubMed]
35. Martin-Platero, A.M.; Valdivia, E.; Maqueda, M.; Martinez-Bueno, M. Fast, convenient, and economical method for isolating genomic DNA from lactic acid bacteria using a modification of the protein "salting-out" procedure. *Anal. Biochem.* **2007**, *366*, 102–104. [CrossRef] [PubMed]

Chapter III: Manuscript 2

Limonene dehydrogenase, a hydroxylating flavoenzyme in the anaerobic monocyclic monoterpene degradation

Edinson Puentes-Cala[1], Manuel Liebeke[2], Stefanie Markert[3], Jens Harder[1]*

[1]Dept. of Microbiology and [2]Dept. of Symbiosis, Max Planck Institute for Marine Microbiology, Celsiusstr. 1, D-28359 Bremen, Germany, [3]Pharmaceutical Biotechnology, University Greifswald, Felix-Hausdorff-Straße, D-17489 Greifswald, Germany

Running title: *Characterization of a limonene dehydrogenase*

*To whom correspondence should be addressed: Jens Harder, Dept. of Microbiology, Max Planck Institute for Marine Microbiology, Celsiusstr. 1, D-28359 Bremen, Germany, Tel.: ++49 421 2028-750; Fax: ++49 421 2028-790; e-mail: jharder@mpi-bremen.de

Keywords: limonene dehydrogenase, anaerobic, cyclic monoterpene, terpenoid, biodegradation, FAD, protein purification, enzyme kinetics

---

Research article submitted to The Journal of Biological Chemistry

ABSTRACT

The enzymatic functionalization of hydrocarbons is a central step in the global carbon cycle, initiating the mineralization of methane, isoprene and monoterpenes, the most abundant biologically produced hydrocarbons. A novel limonene dehydrogenase was purified from the facultative anaerobic betaproteobacterium *Castellaniella defragrans* 65Phen grown in the absence of molecular oxygen on monoterpenes under denitrifying conditions. The purified limonene:ferrocenium oxidoreductase activity was hydroxylating the methyl group of limonene (1-methyl-4-(1-methylethenyl)-cyclohexene), yielding perillyl alcohol. The enzyme showed also a dithiothreitol:perillyl alcohol oxidoreductase activity, yielding limonene. Mass spectroscopy and molecular size determinations revealed a heterodimer of CtmA and CtmB. The two proteins had recently been identified as part of the cyclic terpene metabolism (*ctm*) and annotated as FAD-dependent oxidoreductases of the protein domain family phytoene dehydrogenases and related proteins (COG1233). CtmAB is the first heterodimeric enzyme in this family. Spectroscopy revealed that flavins in the purified enzyme are oxidized by ferrocenium and are reduced by limonene. Heterologously coexpression of both CtmAB in *E. coli* yielded a weak limonene dehydrogenase activity and a lack of the flavin cofactor in CtmA. Wild-type CtmAB oxidized a wide range of monocyclic monoterpenes containing the allylic methyl group motif (1-methyl-cyclohex-1-ene). These results identified CtmAB as hydroxylating limonene dehydrogenase, the first heteromer in a family of FAD-dependent dehydrogenases acting on allylic methylene or methyl CH-bonds. We suggest a placement in EC 1.17.99.7.

INTRODUCTION

Monoterpenes constitute a large and diverse group of hydrocarbons ubiquitous in nature. Over the years around 1000 individual monoterpene structures have been identified (1-3). These ten carbon atom compounds are mainly produced by plants as major components of essential oils (4). Minor amounts are also synthesized by insects and fungi (5,6). Monoterpenes are secondary metabolites which act principally as allelochemicals. Limonene (4-isopropenyl-1-methylcyclohex-1-ene, Fig. 1) is by far the most readily available monoterpene in nature. It is found as the main component of the

essential oils of citrus plants. Between 30,000 and 50,000 tons of limonene are extracted from natural sources per year, basically as a by-product of citrus juice processing (3,7). Due to its olfactory and well-known antimicrobial properties, it is often added to food, cosmetics and house-hold products (8,9).

In the global carbon cycle, the large annual production of monoterpenes by plants is balanced by photooxidation and microbial mineralization. Aerobic bacteria use oxygenases to introduce a hydroxyl or epoxide group at different positions of limonene (10). In *Mycobacterium* sp. HXN-1500, *Pseudomonas putida* KT2440 and *Geobacillus* (ex *Bacillus*) *stearothermophilus*, a cytochrome P450 monooxygenase hydroxylates the methyl group of limonene, yielding perillyl alcohol (11-13).

Perillyl alcohol was also formed in an anaerobic bacterium as product of a limonene biotransformation. *Castellaniella defragrans* 65Phen, a denitrifying betaproteobacterium, uses a wide range of monoterpenes as sole substrate (14). Proteomic data and transposon mutants suggested a degradation pathway from limonene via perillyl alcohol and aldehyde to perillic acid. A deletion mutant in the putative perillyl aldehyde dehydrogenase revealed the co-metabolic formation of perillyl alcohol from limonene during growth on acetate. *C. defragrans´* genome contains a gene cluster named cyclic terpene metabolism (ctm) in a genetic island coding for the majority of the monoterpene metabolism genes (14). Mutants with a transposon insertion in the genes *ctmA*, *ctmB*, or *ctmE* failed to grow on limonene, yet they grew on perillyl alcohol as efficiently as the wild-type. The gene cluster *ctmABCDEFG* codes for two presumably flavin-containing oxidoreductases, CtmA (CDM25290) and CtmB (CDM25289), and an electron transfer system consisting of a 2Fe-2S ferredoxin (CtmE) and a NADH:ferredoxin oxidoreductase (CtmF). These proteins were expressed in larger quantities in α-phellandrene-grown cells, but none of the other putative proteins of unknown function (CtmCD, CtmG). CtmA and CtmB affiliate with COG1233 (phytoene dehydrogenase and related proteins), a group of flavoenzymes involved mainly in carotenoid biosynthesis. Members of this group act with electron acceptors with a positive reduction potential on the dehydrogenation of methylene groups in a diallylic motif - a hexa-1,5-diene moiety yields as oxidation product a hexa-1,3,5-triene structure - or an allylic methylene group yielding an alk-2,3-en-1-one motif. Structural information is available for

phytoene desaturase and beta-carotene ketolase (15,16). In this study, we characterized the limonene dehydrogenase enzyme activity present in *C. defragrans* 65Phen.

RESULTS

Enzyme activities in soluble extracts - The oxidation of limonene was tested with protein extracts from limonene-grown cells of *C. defragrans* 65Phen prepared in a molecular oxygen-free environment without the addition of reducing agents. The dialyzed soluble fraction catalyzed *in vitro* the formation of perillyl alcohol from limonene when the ferric iron-containing ferrocenium hexafluorophosphate (FHP) ($E° = +0.38$ V) was present as electron acceptor. The specific activity was 108 pkat (mg protein)$^{-1}$. Chiral gas chromatography of the product revealed the formation of (*S*)-(-)-perillyl alcohol from (*S*)-(-)-limonene and of (*R*)-(+)-perillyl alcohol from (*R*)-(+)-limonene with similar rates (Figures 1, Figure S1). The reverse reaction, the formation of limonene from perillyl alcohol, was detected in the presence of the reducing agent dithiothreitol (DTT) ($E° = -0.33$ V), with a lower specific activity of 0.63 pkat (mg protein)$^{-1}$.

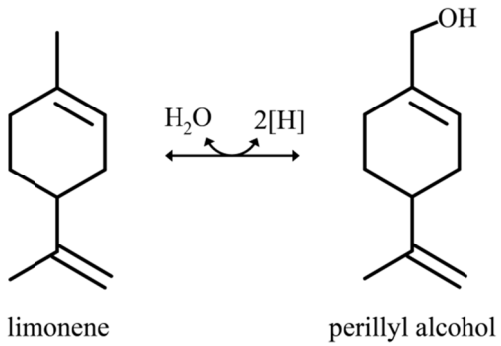

Figure 1. Reversible limonene oxidation to perillyl alcohol observed in soluble protein extracts of *C. defragrans* 65Phen.

Enzyme purification - The limonene dehydrogenase activity was purified as limonene-dependent ferrocenium reductase activity from soluble extracts of *C. defragrans* by protein chromatography in an oxygen-free chamber. During anion exchange chromatography in phosphate buffer, a total loss of activity was observed. FAD at concentrations of 20 µM restored the enzyme activity completely

during a pre-assay incubation for 4 hours at 4°C. No reactivation was observed upon incubation with FMN. Addition of FAD in the separation buffers failed to prevent enzyme inactivation during anion exchange chromatography. This finding and the small progression in purity during the anion exchange chromatography (Figure 2A) suggested as best purification method a combination of hydrophobic interaction and size exclusion chromatography on phenyl sepharose and superdex 200 columns, respectively. The purification yielded a nearly homogeneous protein (Figure 2B) and a 7 ~ 9-fold increase in specific activities of the forward and reverse reaction (Table 1 and Table 2).

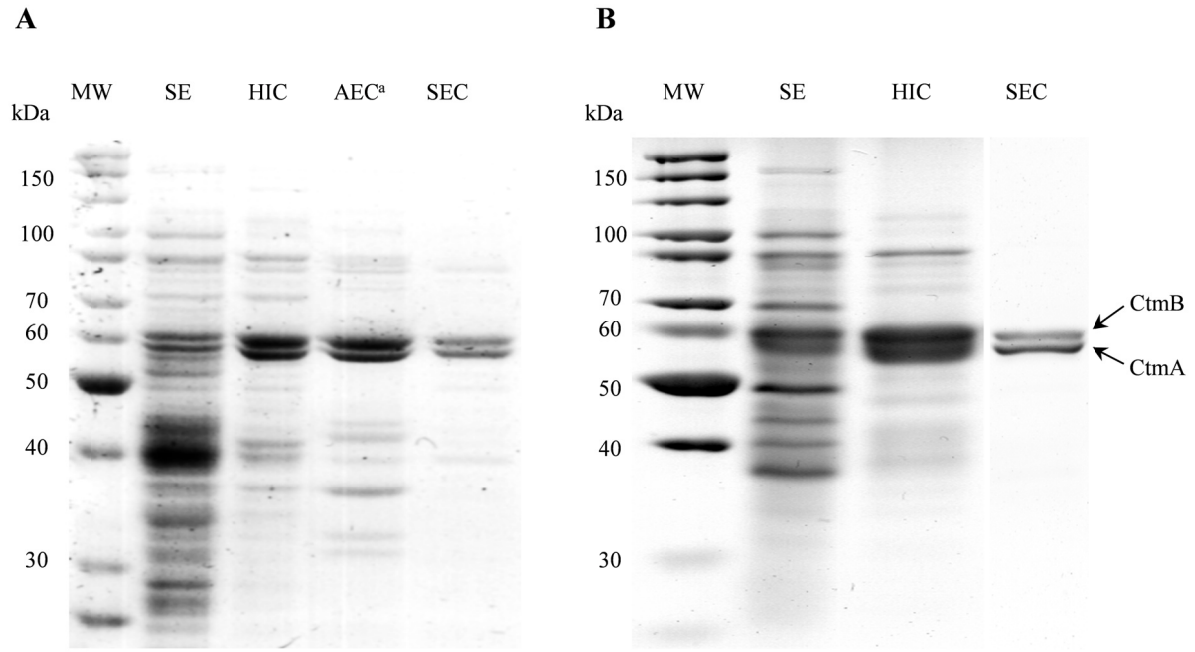

Figure 2. SDS-PAGE of active fractions of limonene dehydrogenase activity from *C. defragrans* 65Phen. (A) HIC/AEC/SEC-purification, (B) HIC/SEC purification. MW: Molecular weight marker; SE: soluble extract; active fractions after hydrophobic interaction (HIC), anion exchange (AEC) and size exclusion chromatography (SEC). [a]Activity was only detected after incubation with 20 µM FAD.

Table 1. Purification of the limonene dehydrogenase activity (detected as ferrocenium reductase activity) from soluble protein extracts of *C. defragrans* 65Phen[a].

Purification step	Total protein (mg)	Total activity (pkat)	Specific activity (pkat (mg protein)$^{-1}$)	Purification (n-fold)	Protein yield (%)
Dialyzed soluble extract	150	16200	108	1	100
HIC[b]	15.8	5799	367	3.4	10.5
SEC[c]	4.8	3605	751	6.9	3.2

[a] tested at 28°C, purification started from 1.2 g of wet biomass of *C. defragrans* 65Phen

[b] Hydrophobic interaction chromatography

[c] Size exclusion chromatography

Table 2. Purification of the perillyl alcohol reductase activity (detected as limonene formation activity) from soluble protein extracts of *C. defragrans* 65Phen.

Purification step	Total protein (mg)	Total activity (pkat)	Specific activity (pkat (mg protein)$^{-1}$)	Purification (n-fold)	Protein yield (%)
Dialyzed soluble extract	128	81	0.6	1	100
HIC[a]	18	42.5	2.4	4	14
SEC[b]	4.56	26	5.7	9.5	3.6

[a] Hydrophobic Interaction Chromatography

[b] Size Exclusion Chromatography

The active fraction had an apparent molecular weight of 152 kDa in the size exclusion chromatography. A similar result was observed via dynamic light scattering (166.2 kDa). Denaturing polyacrylamide gels revealed two dominant bands, one at 59 and another at 57 kDa (Figure 2). MALDI-ToF mass analysis identified in the larger band of the SDS-PAGE as protein CtmB

(CDM25289, gene-based predicted mass 60.7 kDa), whereas the smaller band was identified as CtmA (CDM25290, 61.7 kDa). The N-terminal peptides of CtmA were not detected in the MALDI-ToF spectra. Hence, we characterized the purified CtmA by Edman degradation of the N-terminal amino acids of the protein. The sequence confirmed the predicted open reading frame. A posttranslational cleavage was not the cause for CtmA´s apparent smaller size in denaturing acrylamide gels.

Catalytic properties of the limonene dehydrogenase – The purified native CtmAB had an optimum temperature for the photometric limonene dehydrogenase activity of 40°C (Figure S2), and at this temperature, its optimal pH ranged between 7.5 and 8.0 in potassium phosphate buffer (Figure S3). The kinetic parameters (K_M and V_{max}) were determined at the temperatures for optimal bacterial growth (28°C) and for optimal enzymatic activity (40°C) (Table 3). Limonene hydroxylation was faster than perillyl alcohol reduction. It also showed higher substrate affinity towards limonene (lower K_M) which indicates that limonene hydroxylation is CtmAB's physiologically relevant reaction.

Table 3. Catalytic features of the limonene dehydrogenase purified from *C. defragrans* 65Phen at 28°C and 40°C. All reactions contained 100 µg of purified protein. Limonene dehydrogenase activity was measured using 10 – 1000 µM limonene and with ferrocenium hexafluorophosphate (200 µM) as electron acceptor. Perillyl alcohol reduction used dithiothreitol (2 mM) as electron donor and 0.5 to 10 mM perillyl alcohol as electron acceptor. The reactions were started by the addition of the monoterpenes pre-dissolved in Tween 20-containing buffer.

Temperature	Parameter	Limonene dehydrogenase activity	Perillyl alcohol reductase activity
28°C	K_M [µM]	18 ± 2	392 ± 0
	Vmax [pkat mg^{-1}]	708 ± 31	1.7 ± 0.1
	kcat/K_M [M^{-1} s^{-1}]	(47 ± 5.6) x10^3	5.3 ± 0.3
40°C	K_M [µM]	43 ± 9	487 ± 74
	Vmax [pkat mg^{-1}]	2,260 ± 0	4.1 ± 0.1
	kcat/K_M [M^{-1} s^{-1}]	(63 ± 13) x10^3	10.3 ± 1.6

CtmAB did not used molecular oxygen as electron acceptor. The presence of molecular oxygen in the reaction cuvette caused a 40% reduction on specific activity (from 1099 ± 22 to 589 ± 50 pkat (mg protein)$^{-1}$). The reestablishment of the anoxic conditions restored the specific activity to 993 ± 9 pkat (mg protein)$^{-1}$.

Substrate spectrum – Several monoterpenes and analogous compounds were tested as substrates in the photometric limonene dehydrogenase assay (Figure 3). Monocyclic monoterpenes were oxidized with high specific activities, irrespective of the presence and position of a second double bond in the cyclohexene ring or in the isopropyl substituent. The loss of the allylic character of the methyl group correlated with inactivity of the enzyme, as demonstrated with isolimonene which does not promote growth of *C. defragrans* (17). The *p*-isopropyl group as structural element likely increases the

substrate binding as indicated by the low activity on 1-methylcyclohex-1-ene in comparison to that on monoterpenes. The substrate binding site seems to be not suitable for polar compounds (α-terpineol and terpinen-4-ol) and non-planar, spacious structures close to the allylic group (pinene, carene). The aromatic compound cymene was not oxidized.

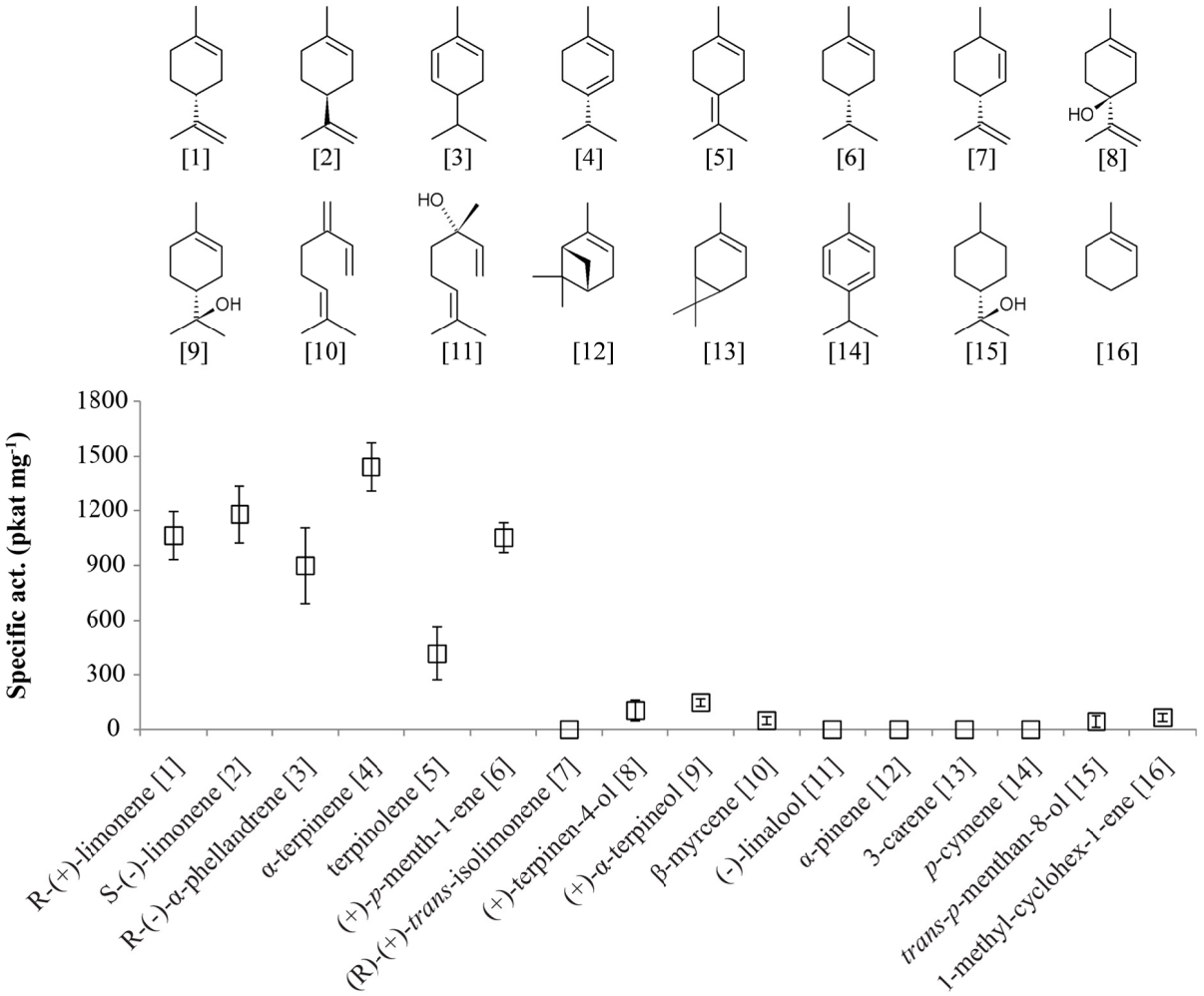

Figure 3. Substrate range for the dehydrogenase activity of limonene dehydrogenase. Reactions were carried out at 40°C and contained: 100 µg of purified protein, 200 µM ferrocenium hexafluorophosphate and 1 mM of each substrate pre-dissolved in Tween 20-containing buffer.

Heterologous expression – E. coli BL21 Star (DE3) was used to express CtmA, CtmB or CtmA and CtmB together from the plasmids pET42a(+) *ctmA*, pET42a(+) *ctmB* or pET42a(+) *ctmA ctmB*, respectively. Protein expression upon IPTG addition was observed in all three genetic constructs and CtmA, CtmB and CtmAB were visualized as ~60 kDa protein bands in denaturing gels (Figure S4A).

The identity was verified by MALDI-ToF analysis. The overexpressed protein(s) formed inclusion bodies even by induction at low temperatures, low cellular densities and low IPTG concentration (Figure S4B). Small enzyme activities were recovered in the soluble fraction after cell lysis. The forward limonene dehydrogenase activity was exclusively detected in soluble extracts containing coexpressed CtmA and CtmB (31 pkat (mg protein)$^{-1}$). The reverse reaction, the perillyl alcohol reduction, was catalyzed by all genetic constructs at similar reaction rates (coexpressed CtmA and CtmB: 330.1 ± 110 fkat (mg protein)$^{-1}$; CtmA: 303 ± 42 fkat (mg protein)$^{-1}$ and CtmB 280 ± 20 fkat (mg protein)$^{-1}$). A mixture of expressed and purified CtmA with expressed and purified CtmB did not recover the limonene dehydrogenase activity, only the perillyl alcohol reductase activity was observed. Several detergents were tested to reactivate fractions with inclusion bodies, but these experiments failed to recover detectable catalytic activity.

Spectroscopic properties and FAD content – Purified native limonene dehydrogenase had no absorption bands except the ones of aromatic amino acids (Figure 4). Upon addition of ferrocenium ions, the typical absorption spectrum of an oxidized flavin appeared with characteristic maxima at 365 and 465 nm. The peak at 620nm was also observed in solutions of ferrocenium hexafluorophosphate (100-200 μM) without enzyme addition. This corresponds to the maximum absorption wavelength for ferrocenium in the visible range of the spectrum (18). Limonene addition to the oxidized protein initiated a gradual decrease of the flavin absorbance. In this experiment, nearly 40% of CtmAB were oxidized by addition of ferrocenium ions using the model of a heterodimer CtmAB and the extinction coefficient of free FAD (ε_{450}: 11,300 M^{-1} cm^{-1} (19)).

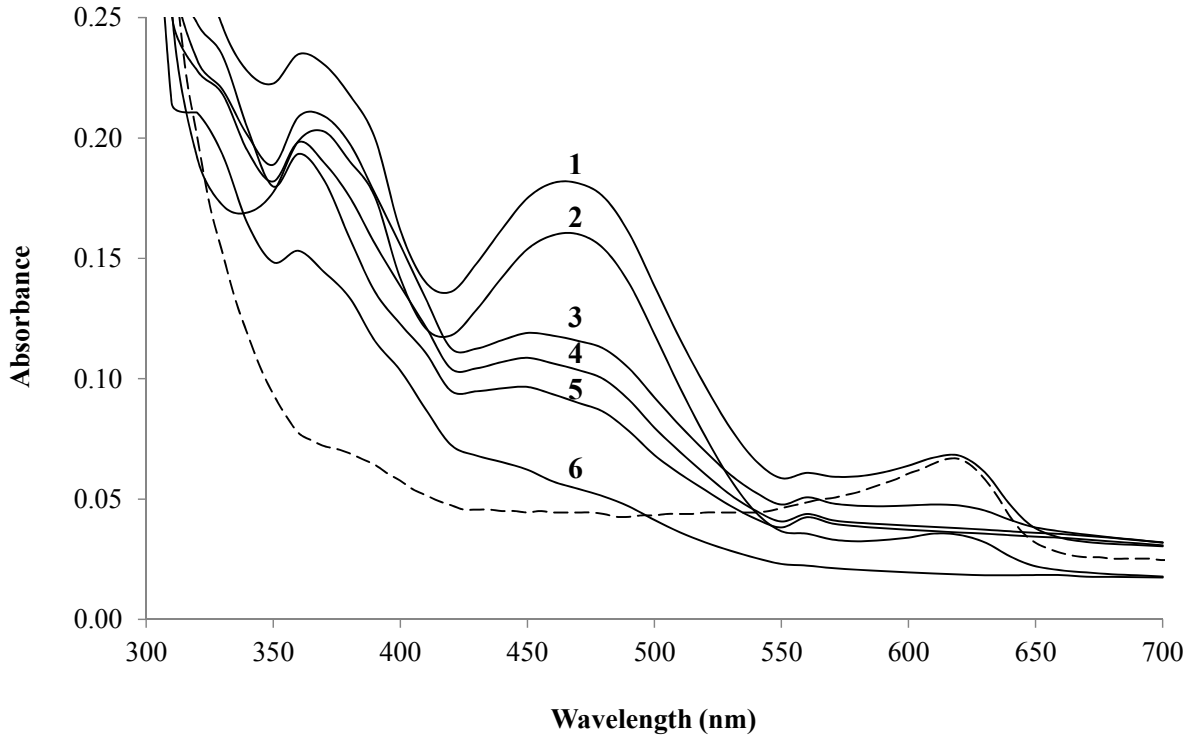

Figure 4. UV-visible spectrum of the native limonene dehydrogenase. Spectra of CtmAB purified under anaerobic conditions from *C. defragrans* (12.5 µM, (trace 6)), after oxidation with 100 µM ferrocenium hexafluorophosphate (1), followed by reduction with 50 µM limonene for 0 min (2), 2 min (3), 10 min (4) and 20 min (5). An absorption peak at 620 nm was also observed in a blank without enzyme containing 100 µM ferrocenium hexafluorophosphate in 10 mM phosphate buffer pH: 8.0 (discontinuous trace).The experiment was conducted under strict anaerobic conditions in phosphate buffer (pH: 8.0) at 21°C.

A spectrophotometric analysis of flavin released from heat-treated protein was used for quantifying the flavin content in CtmAB as described by Aliverti *et al*. (19). The native CtmAB as well as the heterologously expressed CtmAB contained 0.74 moles of flavin per heterodimer (based on a molecular mass of 122.4 kDa). The individual expression of *ctmA* and *ctmB* in *E. coli* resulted in a flavin content of 0.05 moles flavin per mol of CtmA and 0.6 moles flavin per mol of CtmB.

Flavin extraction by tricholoroacetic acid denaturation of protein resulted in a yellow precipitate and no flavin in the supernatant. This finding suggested a covalent association between the flavin cofactor and the protein and hence an underestimation of the flavin content by the aforementioned heat

treatment. The detection of flavin autofluorescence in denaturing polyacrylamide gels is widely accepted as evidence for a covalently bound flavin. Our enzyme preparation had according to the autofluorescence covalently bound flavin in both CtmA and CtmB purified from *C. defragrans* (Figure 5, Figure S5). In heterologously expressed proteins only CtmB showed flavin autofluorescence. This coincides with the flavin release from heat-treated protein and indicated that *Escherichia coli* is unable to incorporate a flavin into CtmA. Flavinylated oligopeptides were not identified by MALDI-Tof-MS or LC-ESI-MS/MS in several wild-type CtmAB preparations.

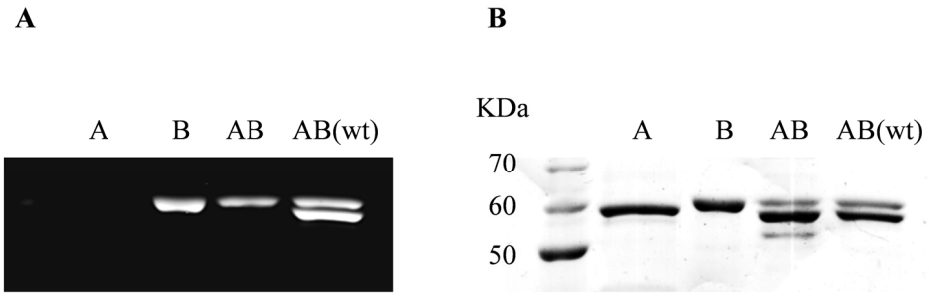

Figure 5. Fluorescence emission (A) and Coomassie staining (B) of purified native and overexpressed CtmA and CtmB proteins after SDS-PAGE. Gel loaded with 1 µg of each heterologously expressed CtmA (A) and CtmB (B), 1.5 µg of heterologously expressed CtmAB (AB) and 1.5 µg native limonene dehydrogenase (AB(wt)). The fluorescence (526 nm) was recorded using an excitation wavelength of 457 nm.

Bioinformatics analysis – Genes *ctmA* and *ctmB* encode for proteins related to the family of the phytoene dehydrogenases (COG1233) (20). CtmA and CtmB share a 27% amino acid identity and have predicted molecular masses of 61.7 and 60.7 kDa, respectively. Neither membrane-spanning regions nor signal peptides for transport beyond the cytoplasmic membrane were predicted (TMHMM (21), PSORTb (22)). Therefore, a cytoplasmic localization is expected for both proteins.

Structure predictions of CtmA and CtmB using Phyre2 (22) identified a phytoene desaturase (CrtI from *Pantoea ananatis* (PDB:4DGK) (15)) and a gamma-carotenoid desaturase (*Nd*CrtD from *Nonlabens dokdonensis* (PDB:4REP) (24)) as best homologous proteins with known structure. The structural prediction was used to manually edit a multi-sequence alignment prepared with Clustal

Omega (Figure 6) (25). In addition to CrtI and *Nd*CrtD, the alignment included the beta carotene ketolase from *Synechocystis* sp. PCC 6803 (CrtO) and the carotenoid oxidase from *Methylomonas* sp. strain 16a (CrtNb). The latter enzymes catalyze oxygen-independent ketone and aldehyde functionalization of carotenoid substrates, respectively (16,26).

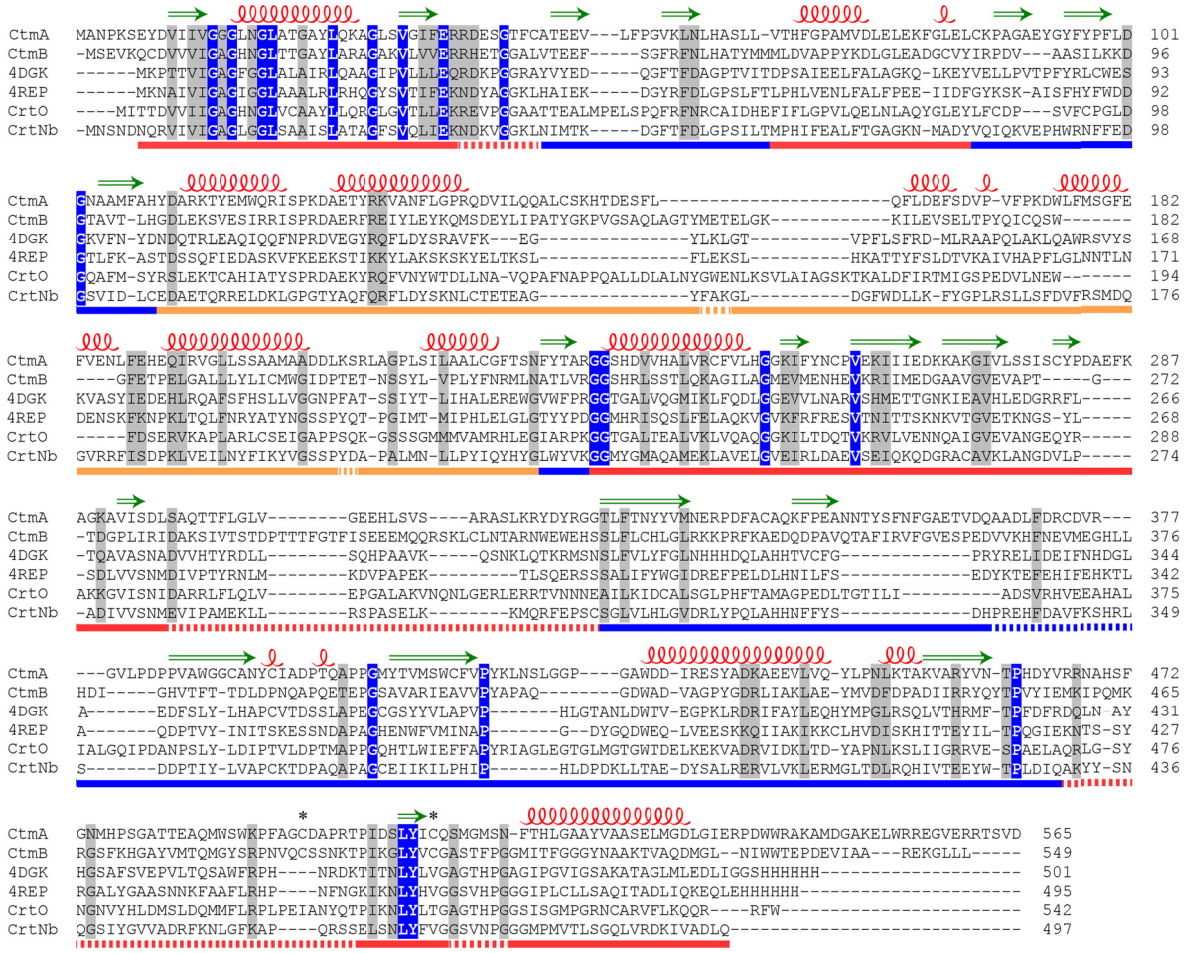

Figure 6. Alignment of CtmA and CtmB with FAD-depending oxidoreductases from the COG1233. The proteins are bacterial phytoene desaturase (CrtI) from *Pantoea ananatis* (PDB: 4DGK, (15)), 1'-OH-carotenoid 3,4-desaturase (*Nd*CrtD) from *Nonlabens dokdonensis* (PDB: 4REP, (24)), β-carotene monoketolase (CrtO) from *Synechocystis* sp. PCC 6803 (NCBI: YP_005652552, (16)), 4, 4'-diapolycopene oxidase (CrtNb) from *Methylomonas* sp. strain 16a (NCBI: AAX46185, (26)). The secondary structure elements predicted are indicated above the alignment. The colored bars underneath indicate the domain organization: the FAD-binding domain (red), the substrate-binding domain (blue), and the non-conserved helical domain (orange). Identical and highly conserved residues are highlighted in blue and grey, respectively. Two pairs of conserved cysteines between

CtmA (Cys495 and Cys508) and CtmB (Cys488 and Cys501) are indicated by an asterisk. The alignment was prepared with Clustal O (25). The structural features were predicted using Phyre2 and 3DLigandSite (23,27).

Sequence identities between the query proteins (CtmA and CtmB) and the aligned phytoene dehydrogenases ranged between 20 and 28%. Identical amino acids present in the six aligned sequences accounted for 3% (blue-shaded residues in Figure 6). Residues with similar properties accounted for another 11% (grey-shaded). Despite the low overall sequence similarity, all six proteins showed a highly conserved N-terminus. This region contains the GxGxxG motif which forms hydrogen bonds with the phosphate groups of FAD in COG1233 proteins (24,28). Three additional putative FAD-interacting regions were predicted in CtmA and CtmB (underlined red in Figure 6). Altogether these protein sections configure a hypothetical FAD-binding domain, resembling the ones present in *Nd*CrtD and CrtI (15,24). A pair of cysteines localized within the FAD-binding region near the proteins' C-terminus are not conserved in the other enzymes of COG1233, suggesting a specific role of the amino acids in the oxidation of limonene. Apart from FAD-binding domains, two additional domains were predicted: a substrate-binding domain (underlined orange in Figure 6) and a non-conserved helical domain (underlined orange).

DISCUSSION

The purification of the limonene:ferrocenium oxidoreductase activity resulted in the isolation of CtmA and CtmB. This concurs with conclusions of previous physiological studies with different transposon and deletion mutants (14). CtmA and CtmB belong to the FAD-dependent oxidoreductases related to the phytoene dehydrogenases (COG1233) (20). The latter proteins attack allylic methyl and methylene groups, CH_3- and CH_2-groups adjacent to a carbon-carbon double bond. Amongst the products of phytoene dehydrogenases are carbon-carbon double bonds, aldehydes and ketones (15,16,26). Similarly, the purified CtmAB showed dehydrogenase activity exclusively on monoterpenes carrying an allylic methyl group. In the case of R-(+)-limonene and S-(-)-limonene, such dehydrogenation resulted in the formation of the respective enantiomeric form of perillyl alcohol.

Three dimensional modeling and a multi-sequence alignment indicated that CtmA and CtmB have domain architectures typical of COG1233 proteins. Like other members of the cluster, CtmA and CtmB bear each an FAD-binding domain, a non-conserved helical domain and a putative substrate-binding domain. An atypical finding in the limonene dehydrogenase was the detection of tightly bound flavin in CtmA and CtmB from *C. defragrans*. So far, we have no molecular evidence for a covalent binding of FAD to the protein. Until now, COG1233 proteins were reported to carry an FAD that dissociated either during purification, heat-treatments or acid protein precipitations (15,20,29,30). In CtmAB, only a portion of the flavins is released by heat treatment and the detection of autofluorescence in denaturing protein gels suggest a covalent bond to the protein. A lack of flavin incorporation during heterologous expression, here CtmA, has also been observed for the phytoene desaturase of *Myxococcus xanthus*, where 0.5 mol FAD was detected per mol of protein (20). Hence, the heterologous expression of some COG1233 proteins in *E. coli* seems to be accompanied by an incomplete incorporation of FAD molecules.

The catalytic efficiency of the wild-type enzyme for limonene oxidation (Table 3) strongly suggests that the limonene dehydrogenase activity is the physiologically relevant reaction. The reverse reaction, the perillyl alcohol reductase activity was observed in apo-flavin CtmA at rates comparable to those of the overexpressed CtmB and the coexpressed CtmA and CtmB. These observations indicate that perillyl alcohol reduction is an FAD-independent reaction. With dithiothreitol as electron donor, the cysteine residues in the C-terminal FAD-binding domain may transfer the reducing equivalents. Besides the flavin binding, the heteromeric character of the limonene dehydrogenase is unusual. It is the first reported heteromer within the COG1233 enzymes, likely a heterodimer. So far only monomers or homodimers had been identified. In general, phytoene desaturases share a central non-conserved helical domain. In most cases this region is appointed as responsible for a monotopic membrane association (15,24,31); however it may also serve in CtmA and CtmB as a surface for dimer interaction.

Ferrocenium ions substitute in enzyme assays for the natural electron acceptor for the re-oxidation of the covalently bound FAD (Figure 7). We suggest that the completely oxidized FAD accepts a hydride

from limonene. This initial hydride transfer is also postulated for other COG1233 enzymes (16,24,32,33). The reaction results in the formation of an allyl cation in which the positive charge is stabilized by delocalization over the allylic moiety. The lack of activity on isolimonene demonstrates the necessity for an allylic alkene bond for this process. The stabilized carbocation is then expected to react with water accompanied by a proton transfer, yielding the corresponding alcohol. Structurally related phytoene desaturases utilize electron acceptors which like ferrocenium have positive reduction potentials, i.e. molecular oxygen or benzoquinone (15,24). In *C. defragrans*, the genes for CtmAB are clustered with genes coding for electron transfer flavoproteins (CDM25301 and CDM25302). Electron transfer flavoproteins (ETFs) are heterodimeric proteins that transfer reducing equivalents in single-electron steps to the quinone pool via a flavoprotein:ubiquinone oxidoreductase (34). Thus, single electrons may be transferred from CtmAB via ETFs to a flavoprotein:ubiquinone oxidoreductase (NCBI: CDM23589) as entrance point to the respiratory chain ending in denitrification. The oxidoreductase CDM23589 was identified by transposon mutagenesis as essential for the cyclic monoterpene degradation (14).

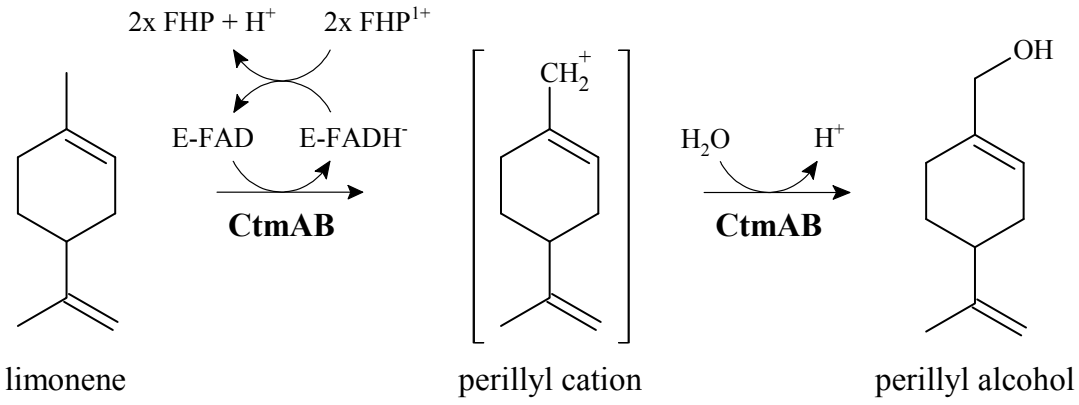

Figure 7. Proposed reaction mechanism of the limonene dehydrogenase CtmAB *in vitro*. The enzyme in its oxidized state (E-FAD) is reduced (E-FADH$^-$) by removing a hydride from limonene forming a perillyl carbocation. The cation is stabilized by water addition yielding perillyl alcohol. The enzyme is reoxidized by two molecules of the one-electron acceptor ferrocenium hexafluorophosphate (FHP).

The hydroxylating limonene dehydrogenase affiliates with the enzyme class 1.17.99, collecting all oxidoreductases acting on CH- or CH_2-groups with unknown physiological electron acceptors. This class includes other key enzymes of the anaerobic hydrocarbon metabolism which use water rather than molecular oxygen as cosubstrate for the CH-activation. Examples include the ethylbenzene and cholesterol hydrolases, two molybdenum-dependent enzymes (35-37). Another well characterized member of the group is the p-cresol methylhydroxylase, a flavocytochrome c enzyme containing one FAD and two hemes. It hydroxylates p-cresol to 4-hydroxybenzyl alcohol which is then further oxidized to 4-hydroxybenzaldehyde with phenanzine as *in vitro* electron acceptor (38,39). We propose for the limonene dehydrogenase – CtmAB - a placement in EC 1.17.99.7.

EXPERIMENTAL PROCEDURES

Cultivation - C. defragrans 65Phen was cultivated in a 10L fermenter with anaerobic artificial fresh water medium (AFW) as previously described (40). Carbonate buffer was replaced by 10 mM K_2HPO_4 (pH: 7.2). Vitamin addition was omitted and nitrogen was used as headspace gas. (*R*)-(+)-limonene (>97% purity, Sigma-Aldrich, Germany) was directly added to the medium to a final concentration of 30 mM in the aqueous phase, a virtual concentration describing the two phase system. The fermenter was inoculated with 1 liter of a freshly grown culture, incubated at 28°C and stirred at 150 rpm. After 6 to 7 days ($OD_{600nm} \approx 1.9$), the cells were harvested by centrifugation at 16000x *g* and 4°C for 40 min. The biomass was resuspended in a threefold volume of 25 mM potassium phosphate buffer, pH 8.0, prior to disruption by three passages through a French pressure cell press (SLM Aminco, Rochester, N.Y.) at 8.6 MPa. Ultracentrifugation at 230000x *g* for 30 min at 4°C yielded a soluble protein fraction.

Heterologous expression - The putative limonene dehydrogenase genes *ctmA* and *ctmB* were PCR-amplified from genomic DNA of *C. defragrans* 65Phen using the primer pairs *ctmA*_NdeI_F (TATCATATGGCAAATCCGAAAAGCGA), *ctmA*_SalI_R (AAAGTCGACTCAATCGACACTGGTCCGTCGT) and *ctmB*_NdeI_F (TAACATATGTCTGAAGTCAAACAATG), *ctmB*_SalI_R

(TAAGTCGACTCATAGGAGGAGCCCCTTTT). The amplicon *ctmAB* for the coexpression of both genes was obtained using the primer pair *ctmA*_NdeI_F and *ctmB*_SalI_R. All three amplicons were ligated into the vector pET-42a(+) (Novagen, Merck KGaA, Darmstadt, Germany), and subsequently transformed into *E. coli* BL21 Star (DE3) (Invitrogen, Karlsruhe, Germany). The correctness of the genetic constructs was verified by sequencing using the BigDye Terminator v3.1Cycle Sequencing Kit (Applied Biosystems, Life Technologies Corporation, Carlsbad, CA, USA). For protein expression, 300 mL of LB (Luria-Bertani) medium supplemented with kanamycin (30 µg/mL) were inoculated with 3 mL of an overnight culture and incubated under constant shaking (150 rpm) at 37°C until an optical density at 600 nm of 0.1 was reached. The cultures were cooled down to 18°C prior to the addition of 20 µM riboflavin (vitamin B2) and 50 µM IPTG. The cultures were further incubated for 4 h at 18°C. The biomass was harvested and disrupted as described above for *C. defragrans* 65Phen. For solubilization of inclusion bodies, pelleted fractions were anoxically incubated with 0.5% Triton X-100, 1% sodium deoxycholate or 0.2% N-lauroyl sarcosine as previously described (41).

Enzyme purification - Protein purification was performed in an ÄKTA LC system (GE Healthcare, Freiburg, Germany) installed in an anaerobic chamber at 4°C. The first purification step was a hydrophobic interaction chromatography on a phenyl-sepharose column (20 mL volume, 2.6 cm diameter). The soluble extract received concentrated salt solutions to final concentrations of 75 mM potassium phosphate, 60 mM ammonium sulfate and 20 mM potassium chloride, pH 8.0. This was also the starting buffer. This optimized buffer composition guaranteed protein stability and column binding. The protein eluted using 10 mM potassium phosphate, pH 8.0. The active fractions were concentrated with a centrifugation filter (Amicon Ultra 15 mL, 10 kDa, Merck Millipore, Darmstadt, Germany) and further purified on a Superdex 200 column (120 mL volume, 1.6 cm diameter) equilibrated with 10 mM potassium phosphate, pH 8.0. The fractions with limonene dehydrogenase activity were pooled and used for enzymatic activity measurements.

Enzyme activity - Continuous and end-point analyses were used for measuring the reversible oxidation of limonene in protein extracts. All assays were prepared inside an anaerobic chamber at 4°C. To facilitate monoterpene availability in the aqueous phase, these were dissolved in 10 mM

K_2HPO_4, pH 8.0, containing 2.5% v/v Tween 20. The final content of Tween 20 in the assays was 0.5% v/v.

Limonene oxidation (forward reaction) was assayed spectrophotometrically in 1 mL quartz cuvettes. A typical reaction contained in a 1mL-volume 100 - 200 µg protein, 200 µM ferrocenium hexafluorophosphate and limonene (10 µM – 1000 µM) in 10 mM phosphate buffer, pH 8.0. The reaction was started with the addition of the monoterpene-containing buffer and proceeded at either 28°C or 40°C. The absorption decrease of the ferrocenium ion was followed at 290 nm ($\Delta\varepsilon$ = 7,100 M^{-1} cm^{-1}). The molar extinction coefficient of ferrocenium was calculated from a calibration curve prepared in phosphate buffer 10 mM, pH 8.0 (y=0.0071x; R^2=0.9916). Limonene consumption and perillyl alcohol formation were monitored by gas chromatography. For this, 200 µL of n-hexane were added to each sample and vortexed for 30 seconds. After 10 minutes shaking at 60 rpm, the samples were centrifuged at 13000x *g* for 10 min for complete phase separation. 1 µL of the organic phase was analyzed in a gas chromatography coupled to a flame ionization detector (Perkin Elmer Auto System XL, Überlingen, Germany). Analyte separation was performed on an Optima-5 column (50 m x 0.32 mm x 0.25 µm; Macherey-Nagel, Düren, Germany) with an injection port temperature of 250°C, a detection temperature of 350°C, and the following column program: an initial column temperature of 40°C for 2 min, increasing to 100°C with a rate at 4°C min^{-1}, staying constant for 0.1 min, further increasing to 320 °C at 45°C min^{-1} and finally a constant temperature for 3 min. The split ratio was 1:9. All concentrations refer to the aqueous phase. For analyte quantification, calibration curves with authentic standards were prepared. For stereospecific GC analysis, 1 µL of sample was separated on a Hydrodex-β-6TBDM column (25 m x 0.25 mm; Macherey-Nagel, Düren, Germany) by the program: injection temperature of 200°C; flame ionization detection temperature of 230°C, the column temperature was 80°C for 1 min, increasing to 130°C at a rate of 5 °C min^{-1}, after 0.5 min further increasing to 230°C at 20°C min^{-1} and stationary for 2 min.

Perillyl alcohol reductase activity, the physiologically reverse reaction, was tested in 1 mL reactions containing 100 – 200 µg protein, 2 mM dithiothreithol (DTT) and perillyl alcohol (0.5 - 10 mM). Reactions were performed in 3 mL glass vials closed with a butyl rubber septum. Incubation took

place at 28 and 40°C for 4h. Limonene formation was extracted with hexane and quantified by gas chromatography as described above.

Optimal conditions such as protein concentration, temperature, incubation time and pH were determined for forward and reverse reactions. The pH optimum was tested using several buffers with pH values adjusted near their specific pK_a at 37°C in a range of 4 to 10 (50 mM sodium citrate pH 4 - 6; 25 mM potassium phosphate pH 6 - 8; 25 mM Tris pH 7.5 - 8.5; 50 mM glycine/HCl pH 9 - 10).

Analytical methods - Proteins were quantified according to Bradford (42) with bovine serum albumin as standard and visualized in 10-12% v/v acrylamide SDS-PAGE stained with Coomassie blue (43). For protein analysis by mass spectroscopy, bands from SDS-PAGE were excised, in-gel-digested with trypsin and analyzed on a 4800 MALDI-TOF/TOF Analyzer (Applied Biosystems, Darmstadt, Germany). Additionally, CtmAB purified from *C. defragrans* was subjected to in-solution tryptic digestion, separated in a reversed phase C18 column on a nano ACQUITY-UPLC (Waters Corporation, Milford, MA, USA) and analyzed on a LTQ-Orbitrap Classic mass spectrometer equipped with an ESI ion source (Thermo Fisher Scientific Inc., Waltham, MA, USA). For protein identification the mass spectra were analyzed against a protein database from *Castellaniella defragrans* using the Mascot search engine ver. 2.4.0 (Matrix Science Ltd. London, UK). For posttranslational modifications the spectra were searched against the parent amino acid sequences of proteins CtmA and CtmB allowing FMN- and FAD-flavinylation in all amino acid residues using Sequest ver.27, rev. 11 (Thermo Fisher Scientific Inc.). The N terminus of native CtmA was sequenced by Edman degradation (Proteome Factory AG, Berlin, Germany) after one dimensional separation by SDS-PAGE and a semi-dry blotting onto a polyvinylidene difluoride (PVDF) membrane. In-gel fluorescence was recorded prior to Coomassie blue staining. The denaturing-polyacrylimide gels were immersed in 10% acetic acid for 10 min. Fluorescence was recorded on a Typhoon 9400 (GE Healthcare, Freiburg, Germany) with an excitation at 457 nm and emission at 526 nm. Protein absorption spectra were recorded using a DU 600 UV/VIS spectrophotometer (Beckman Coulter, Krefeld, Germany). FAD was extracted and quantified as described by Aliverti *et al.* (18). The molecular mass of the enzyme was estimated on a Superdex 200 column (120 mL, 1.6 cm

diameter) using thyroglobulin (669 kDa), ferritin (440 kDa), catalase (232 kDa), aldolase (158 kDa), albumin (66.3 kDa), ovalbumin (46 kDa), chymotrypsinogen A (25 kDa) and ribonuclease A (13,7 kDa) as standards. An additional molecular mass determination was conducted by dynamic light scattering on a DynaPro Plate Reader II (Wyatt Technology Corp., Santa Barbara, CA) at 21°C as indicated by the manufacturer.

All results in this contribution are reported as the average of triplicate measurements plus minus the standard deviation of the mean.

Bioinformatics analyses -Nucleotide and amino acid database searches were carried out with NCBI BLAST (44). Three dimensional protein modeling was conducted with Phyre2 (23) and 3DLigandSite (27). The amino acid sequence alignment was prepared with Clustal Omega (25). Subcellular localization of the proteins was predicted using TMHMM Server v. 2.0 and PSORTb v3.0.2 (21,22).

ACKNOWLEDGEMENT

We thank Jan Petasch for the construction of the expression plasmids and initial experiments. This study was financed by the Max Planck Society. E.P.C. was supported by a grant from the DAAD in Germany and from the Corporación para la Investigación de la Corrosión and COLCIENCIAS in Colombia.

CONFLICT OF INTEREST

The authors declare that they have no conflicts of interest with the contents of this article.

AUTHOR CONTRIBUTIONS

J.H. conceived and coordinated the study. E.P.C. performed the experiments reported in this study. M.L. and S.M. contributed MS analyses. E.P.C. and J.H. analyzed the data and wrote the manuscript.

REFERENCES

1. Erman, W. F. (1985) *Chemistry of the Monoterpenes. An Encyclopedic Handbook.*, Marcel Dekker, New York

2. Holstein, S. A., and Hohl, R. J. (2004) Isoprenoids: remarkable diversity of form and function. *Lipids* **39**, 293-309

3. Jongedijk, E., Cankar, K., Ranzijn, J., van der Krol, S., Bouwmeester, H., and Beekwilder, J. (2015) Capturing of the monoterpene olefin limonene produced in *Saccharomyces cerevisiae*. *Yeast* **32**, 159-171

4. Tholl, D. (2015) Biosynthesis and biological functions of terpenoids in plants. *Adv. Biochem. Eng. Biotechnol.* **148**, 63-106

5. Boronat, A., and Rodriguez-Concepcion, M. (2015) Terpenoid biosynthesis in prokaryotes. *Adv. Biochem. Eng. Biotechnol.* **148**, 3-18

6. Schmidt-Dannert, C. (2015) Biosynthesis of terpenoid natural products in fungi. *Adv. Biochem. Eng. Biotechnol.* **148**, 19-61

7. Schwab, W., Fuchs, C., and Huang, F. C. (2013) Transformation of terpenes into fine chemicals. *Eur. J. Lipid Sci. Technol.* **115**, 3-8

8. Zhang, Z. J., Vriesekoop, F., Yuan, Q. P., and Liang, H. (2014) Effects of nisin on the antimicrobial activity of D-limonene and its nanoemulsion. *Food Chem.* **150**, 307-312

9. Brennan, T. C., Kromer, J. O., and Nielsen, L. K. (2013) Physiological and transcriptional responses of *Saccharomyces cerevisiae* to D-limonene show changes to the cell wall but not to the plasma membrane. *Appl. Environ. Microbiol.* **79**, 3590-3600

10. Marostica, M. R., and Pastore, G. M. (2007) Biotransformation of limonene: A review of the main metabolic pathways. *Quim. Nova* **30**, 382-387

11. van Beilen, J. B., Holtackers, R., Luscher, D., Bauer, U., Witholt, B., and Duetz, W. A. (2005) Biocatalytic production of perillyl alcohol from limonene by using a novel *Mycobacterium* sp. cytochrome P450 alkane hydroxylase expressed in *Pseudomonas putida*. *Appl. Environ. Microbiol.* **71**, 1737-1744

12. Cornelissen, S., Julsing, M. K., Volmer, J., Riechert, O., Schmid, A., and Buhler, B. (2013) Whole-cell-based CYP153A6-catalyzed (*S*)-limonene hydroxylation efficiency depends on host background and profits from monoterpene uptake via AlkL. *Biotechnol. Bioeng.* **110**, 1282-1292

13. Cheong, T. K., and Oriel, P. J. (2000) Cloning and expression of the limonene hydroxylase of *Bacillus stearothermophilus* BR388 and utilization in two-phase limonene conversions. *Appl. Biochem. Biotechnol.* **84-86**, 903-915

14. Petasch, J., Disch, E. M., Markert, S., Becher, D., Schweder, T., Huttel, B., Reinhardt, R., and Harder, J. (2014) The oxygen-independent metabolism of cyclic monoterpenes in *Castellaniella defragrans* 65Phen. *BMC Microbiol.* **14**, 164-176

15. Schaub, P., Yu, Q. J., Gemmecker, S., Poussin-Courmontagne, P., Mailliot, J., McEwen, A. G., Ghisla, S., Al-Babili, S., Cavarelli, J., and Beyer, P. (2012) On the structure and function of the phytoene desaturase CRTI from *Pantoea ananatis*, a membrane-peripheral and FAD-dependent oxidase/isomerase. *PLoS ONE* **7**, e39550

16. Breitenbach, J., Gerjets, T., and Sandmann, G. (2013) Catalytic properties and reaction mechanism of the CrtO carotenoid ketolase from the cyanobacterium *Synechocystis* sp. PCC 6803. *Arch. Biochem. Biophys.* **529**, 86-91

17. Heyen, U., and Harder, J. (1998) Cometabolic isoterpinolene formation from isolimonene by denitrifying *Alcaligenes defragrans*. *Fems Microbiol. Lett.* **169**, 67-71

18. Singh, A., Chowdhury, D. R., and Paul, A. (2014) A kinetic study of ferrocenium cation decomposition utilizing an integrated electrochemical methodology composed of cyclic voltammetry and amperometry. *Analyst* **139**, 5747-5754

19. Aliverti, A., Curti, B., and Vanoni, M. A. (1999) Identifying and quantitating FAD and FMN in simple and in iron-sulfur-containing flavoproteins. *Methods Mol. Biol.* **131**, 9-23

20. Dailey, T. A., and Dailey, H. A. (1998) Identification of an FAD superfamily containing protoporphyrinogen oxidases, monoamine oxidases, and phytoene desaturase. Expression and characterization of phytoene desaturase of *Myxococcus xanthus*. *J. Biol. Chem.* **273**, 13658-13662

21. Krogh, A., Larsson, B., von Heijne, G., and Sonnhammer, E. L. (2001) Predicting transmembrane protein topology with a hidden Markov model: application to complete genomes. *J. Mol. Biol.* **305**, 567-580

22. Yu, N. Y., Laird, M. R., Spencer, C., and Brinkman, F. S. (2011) PSORTdb - an expanded, auto-updated, user-friendly protein subcellular localization database for *Bacteria* and *Archaea*. *Nucleic Acids Res.* **39**, D241-244

23. Kelley, L. A., Mezulis, S., Yates, C. M., Wass, M. N., and Sternberg, M. J. (2015) The Phyre2 web portal for protein modeling, prediction and analysis. *Nat. Protoc.* **10**, 845-858

24. Ahn, J.-W., and Kim, K.-J. (2015) Crystal structure of 1′-OH-carotenoid 3,4-desaturase from *Nonlabens dokdonensis* DSW-6. *Enzyme Microb. Technol.* **77**, 29-37

25. Sievers, F., Wilm, A., Dineen, D., Gibson, T. J., Karplus, K., Li, W. Z., Lopez, R., McWilliam, H., Remmert, M., Soding, J., Thompson, J. D., and Higgins, D. G. (2011) Fast, scalable generation of high-quality protein multiple sequence alignments using Clustal Omega. *Mol. Syst. Biol.* **7**, 539-544

26. Tao, L., Schenzle, A., Odom, J. M., and Cheng, Q. (2005) Novel carotenoid oxidase involved in biosynthesis of 4,4 '-diapolycopene dialdehyde. *Appl. Environ. Microbiol.* **71**, 3294-3301

27. Wass, M. N., Kelley, L. A., and Sternberg, M. J. (2010) 3DLigandSite: predicting ligand-binding sites using similar structures. *Nucleic Acids Res.* **38**, W469-473

28. Dym, O., and Eisenberg, D. (2001) Sequence-structure analysis of FAD-containing proteins. *Protein Sci.* **10**, 1712-1728

29. Gemmecker, S., Schaub, P., Koschmieder, J., Brausemann, A., Drepper, F., Rodriguez-Franco, M., Ghisla, S., Warscheid, B., Einsle, O., and Beyer, P. (2015) Phytoene desaturase from *Oryza sativa*: oligomeric assembly, membrane association and preliminary 3D-analysis. *Plos One* **10**, e0131717

30. Al Babili, S., von Lintig, J., Haubruck, H., and Beyer, P. (1996) A novel, soluble form of phytoene desaturase from *Narcissus pseudonarcissus* chromoplasts is Hsp70-complexed and competent for flavinylation, membrane association and enzymatic activation. *Plant J* **9**, 601-612

31. Kloer, D. P., Ruch, S., Al-Babili, S., Beyer, P., and Schulz, G. E. (2005) The structure of a retinal-forming carotenoid oxygenase. *Science* **308**, 267-269

32. Sandmann, G. (2009) Evolution of carotene desaturation: The complication of a simple pathway. *Arch. Biochem. Biophys.* **483**, 169-174

33. Steiger, S., Perez-Fons, L., Cutting, S. M., Fraser, P. D., and Sandmann, G. (2015) Annotation and functional assignment of the genes for the C-30 carotenoid pathways from the genomes of two bacteria: *Bacillus indicus* and *Bacillus firmus*. *Microbiol-Sgm* **161**, 194-202

34. Costas, A. M. G., Poudel, S., Miller, A. F., Schut, G. J., Ledbetter, R. N., Fixen, K. R., Seefeldt, L. C., Adams, M. W. W., Harwood, C. S., Boyd, E. S., and Peters, J. W. (2017) Defining electron bifurcation in the electron-transferring flavoprotein family. *J. Bacteriol.* **199**, e00440-17

35. Chiang, Y. R., Ismail, W., Muller, M., and Fuchs, G. (2007) Initial steps in the anoxic metabolism of cholesterol by the denitrifying *Sterolibacterium denitrificans*. *J. Biol. Chem.* **282**, 13240-13249

36. Heider, J., Szaleniec, M., Sunwoldt, K., and Boll, M. (2016) Ethylbenzene dehydrogenase and related molybdenum enzymes involved in oxygen-independent alkyl chain hydroxylation. *J. Mol. Microbiol. Biotechnol.* **26**, 45-62

37. Strijkstra, A., Trautwein, K., Jarling, R., Wohlbrand, L., Dorries, M., Reinhardt, R., Drozdowska, M., Golding, B. T., Wilkes, H., and Rabus, R. (2014) Anaerobic activation of *p*-cymene in denitrifying betaproteobacteria: methyl group hydroxylation versus addition to fumarate. *Appl. Environ. Microbiol.* **80**, 7592-7603

38. Cunane, L. M., Chen, Z. W., McIntire, W. S., and Mathews, F. S. (2005) *p*-cresol methylhydroxylase: Alteration of the structure of the flavoprotein subunit upon its binding to the cytochrome subunit. *Biochemistry (Mosc.)* **44**, 2963-2973

39. Boll, M., and Heider, J. (2010) Anaerobic degradation of hydrocarbons: mechanisms of C–H-bond activation in the absence of oxygen. in *Handbook of Hydrocarbon and Lipid Microbiology* (Timmis, K. N. ed.), Springer Berlin Heidelberg, Berlin, Heidelberg. pp 1011-1024

40. Heyen, U., and Harder, J. (2000) Geranic acid formation, an initial reaction of anaerobic monoterpene metabolism in denitrifying *Alcaligenes defragrans*. *Appl. Environ. Microbiol.* **66**, 3004-3009

41. Jevsevar, S., Gaberc-Porekar, V., Fonda, I., Podobnik, B., Grdadolnik, J., and Menart, V. (2005) Production of nonclassical inclusion bodies from which correctly folded protein can be extracted. *Biotechnol. Progr.* **21**, 632-639

42. Bradford, M. M. (1976) Rapid and sensitive method for quantitation of microgram quantities of protein utilizing principle of protein-dye binding. *Anal. Biochem.* **72**, 248-254

43. Laemmli, U. K. (1970) Cleavage of structural proteins during assembly of head of bacteriophage T4. *Nature* **227**, 680-685

44. Altschul, S. F., Gish, W., Miller, W., Myers, E. W., and Lipman, D. J. (1990) Basic local alignment search tool. *J. Mol. Biol.* **215**, 403-410

Supplementary material

Limonene dehydrogenase, a hydroxylating flavoenzyme in the anaerobic monocyclic monoterpene degradation

Edinson Puentes-Cala[1], Manuel Liebeke[2], Stefanie Markert[3], Jens Harder[1]*

[1]Dept. of Microbiology and [2]Dept. of Symbiosis, Max Planck Institute for Marine Microbiology, Celsiusstr. 1, D-28359 Bremen, Germany, [3]Pharmaceutical Biotechnology, University Greifswald, Felix-Hausdorff-Straße, D-17489 Greifswald, Germany

*To whom correspondence should be addressed: Jens Harder, Dept. of Microbiology, Max Planck Institute for Marine Microbiology, Celsiusstr. 1, D-28359 Bremen, Germany, Tel.: ++49 421 2028-750; Fax: ++49 421 2028-790; E-mail: jharder@mpi-bremen.de

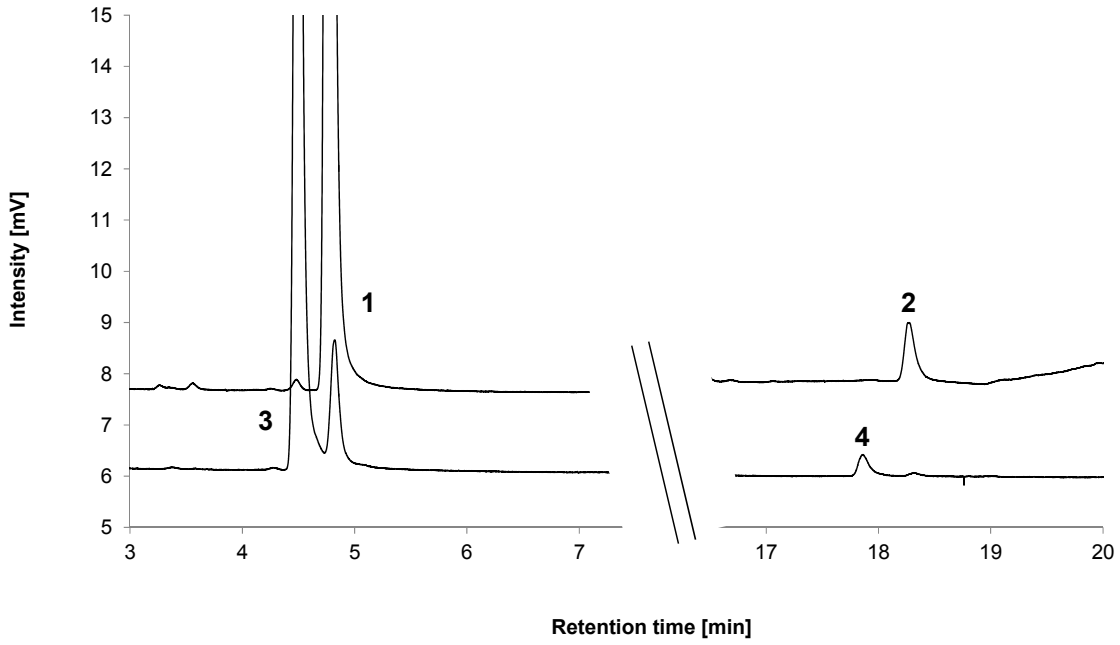

Figure S1. Enantiomeric gas chromatography of monoterpenes extracted after incubation with 0.8µM limonene dehydrogenase. Reactions were carried out at 40°C and contained: 100 µg of purified protein, 200 µM ferrocenium hexafluorophosphate and 1 mM of R-(+)-limonene (peak 1) and S-(-)-limonene (peak 3) pre-dissolved in Tween 20-containing buffer. Peak 2 corresponds to R-(+)-perillyl alcohol. Peak 4 corresponds to S-(-)-perillyl alcohol.

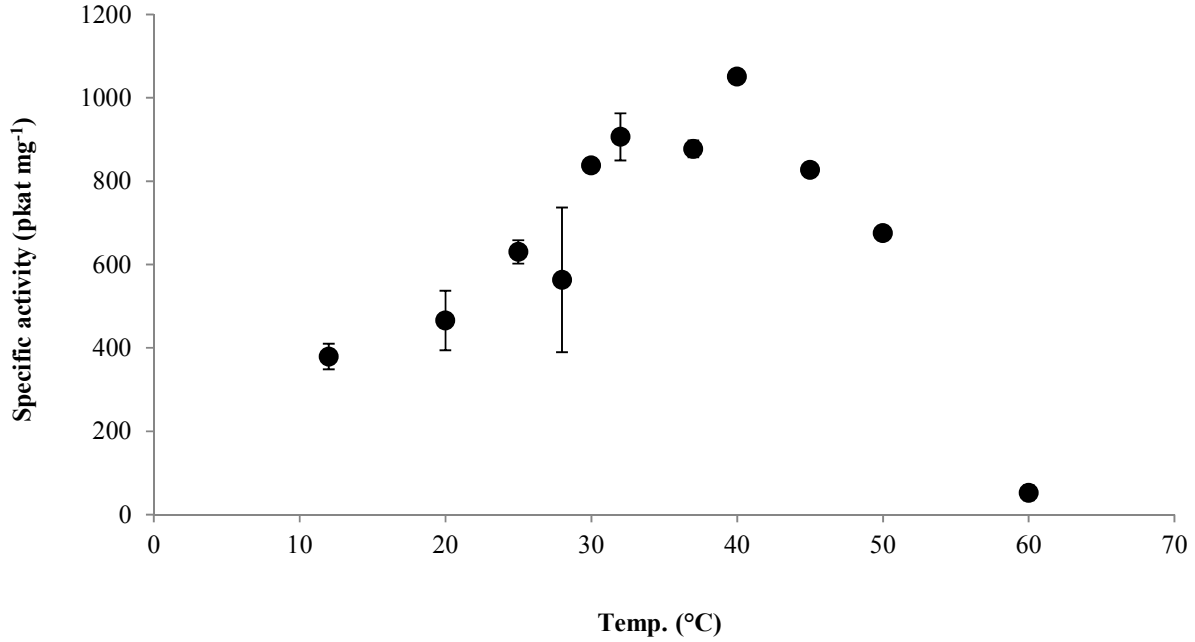

Figure S2. Limonene dehydrogenase activity as function of temperature. The reactions contained 100 µg of purified protein, 100 µM limonene and 200 µM ferrocenium hexafluorophosphate.

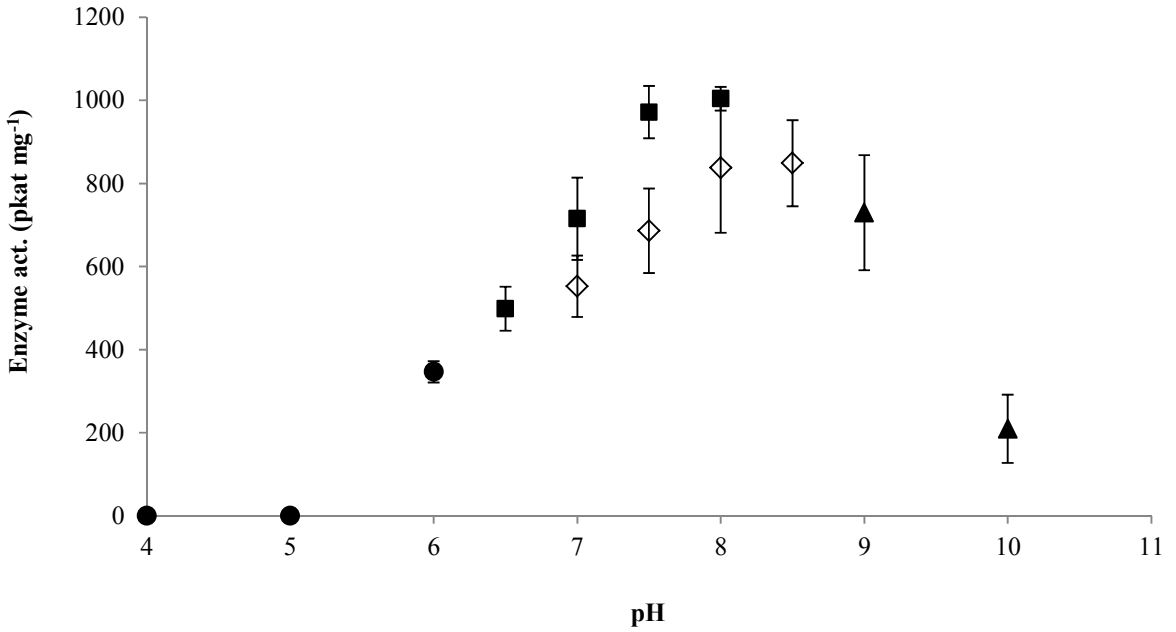

Figure S3. Limonene dehydrogenase activity as function of pH at 40°C. The reactions contained 100 µg of purified protein, 100 µM limonene and 200 µM ferrocenium hexafluorophosphate. The following buffers were used: ●, sodium citrate (50 mM; pH 4 – 6); ■, potassium phosphate (25 mM, pH 6.5 – 8); ◊, Tris-Cl (25 mM, pH 7 – 8.5); ▲, glycine/HCl (50 mM, pH 9 – 10).

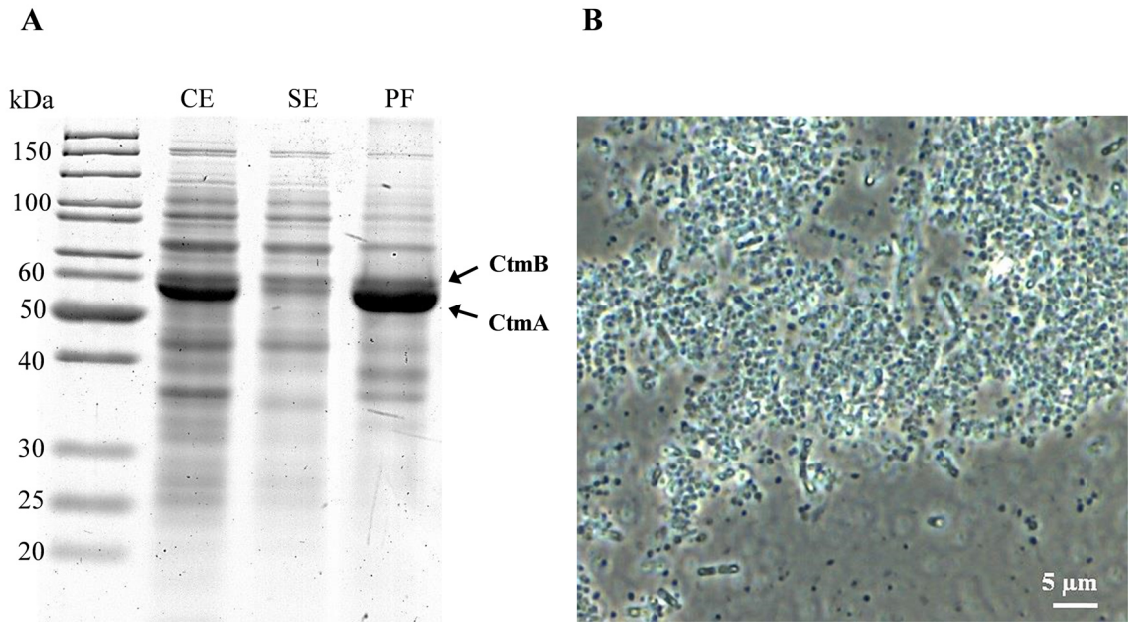

Figure S4. Heterologously expressed CtmAB. A. SDS-PAGE of overexpressed CtmAB upon cellular disruption. MW: molecular weight marker; CE: crude extract; SE: soluble extract; PF: pelleted fraction after ultracentrifugation. Identity of the individual proteins according to MALDI-ToF analysis is indicated with arrows. **B.** Microscopic inspection of the pelleted fraction denoting the presence of inclusion bodies.

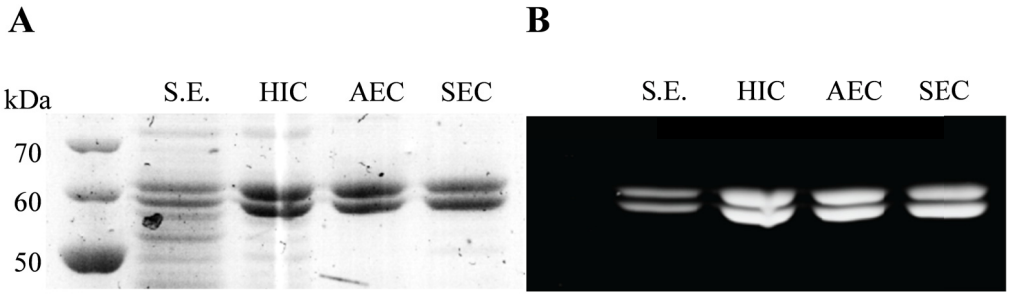

Figure S5. SDS-PAGE Coomassie staining (A) and in-gel flavin fluorescence emission (B) of protein fractions from *C. defragrans* with limonene dehydrogenase activity after protein chromatography. S.E.: soluble extract; active fractions after hydrophobic interaction (HIC), anion exchange (AEC) and size exclusion chromatography (SEC). Fluorescence (526 nm) recorded using an excitation wavelength of 452 nm.

Chapter IV: Manuscript 3

Initial purification of novel monoterpene synthases from *Castellaniella defragrans*

Edinson Puentes-Cala[1], Elizabeth Engler-Hüsch[1], Manuel Liebeke[2], Jens Harder[1]*

[1]Dept. of Microbiology and [2]Dept. of Symbiosis, Max Planck Institute for Marine Microbiology, Celsiusstr. 1, D-28359 Bremen, Germany

*To whom correspondence should be addressed: Jens Harder, Dept. of Microbiology, Max Planck Institute for Marine Microbiology, Celsiusstr. 1, D-28359 Bremen, Germany, Tel.: +49 421 2028-750; Fax: +49 421 2028-790; e-mail: jharder@mpi-bremen.de

Manuscript in preparation.

Abstract

Castellaniella defragrans utilizes several monoterpenes as sole carbon and energy source under denitrifying conditions. The oxidation of the acyclic monoterpene alcohol linalool to geranic acid is catalyzed by linalool dehydratase/isomerase, and geraniol and geranial dehydrogenases. However, recent studies suggested an alternative pathway for the complete linalool mineralization, involving an ATP-dependent cyclization reaction yielding monocyclic dienes as products. In this study, we report the partial purification of a novel linalool-dependent monoterpene cyclase. In addition, an alcohol dehydratase activity acting on α-terpineol and terpinen-4-ol and producing monocyclic dienes was observed and partially purified. All three biotransformations required magnesium ions and ATP. The advantage for *C. defragrans* is twofold: non-functionalized monoterpenes are less toxic than the monoterpene alcohols, and the transformation products are intermediates of the monoterpene degradation pathway.

Introduction

The betaproteobacterium *Castellaniella* (ex-*Alcaligenes*) *defragrans* 65Phen mineralizes several monoterpenes under anaerobic denitrifying conditions (Foss *et al*. 1998). Monoterpene alcohols such as the acyclic linalool and the monocyclic α-terpineol, terpinene-4-ol and perillyl alcohol all support *C. defragrans*'s growth using nitrate as electron acceptor. The enzymes linalool dehydratase/isomerase (Ldi) (EC 5.4.4.4, EC 4.2.1.127) and the geraniol and geranial dehydrogenases catalyze the successive oxidation of linalool over geranial to geranic acid (Brodkorb *et al*. 2010; Lüddeke *et al*. 2012a; Lüddeke and Harder 2011). The latter two enzymes also catalyze the biotransformation of perillyl alcohol over perillyl aldehyde to perillic acid (Harder and Marmulla 2017; Petasch *et al*. 2014). A mutant of *C. defragrans* lacking the *ldi* gene showed growth on linalool, but not on geraniol or geranic acid suggesting the existence of an alternative pathway for linalool degradation (Lüddeke *et al*. 2012a). More recently, an ATP-dependent biotransformation of linalool into monocyclic monoterpenes was observed in cell lysates of *C. defragrans* 65Phen Δ*ldi* (Marmulla 2015), denoting a link between the acyclic and monocyclic monoterpene degradation.

Up to date, the biochemistry of the utilization of α-terpineol and terpinen-4-ol has not been investigated in *C. defragrans*. As it is the case for other monoterpenes, the biotransformation of monoterpene alcohols has mainly been reported in aerobic organisms in which mono- and di-oxygenases are involved (Ilc *et al*. 2016; Marmulla and Harder 2014; Misra *et al*. 1996). The dehydration of α-terpineol to terpinolene has been proposed to occur in cultures of *Pseudomonas aeruginosa* and *Thauera terpenica* (Hylemon and Harder 1998; Tadasa *et al*. 1976), however without further follow-up research. In this study, we report the discovery of the anaerobic dehydration of α-terpineol and terpinen-4-ol in *C. defragrans* yielding monocyclic monoterpene dienes as products. We attempted the purification and identification of this newly discovered catalytic activity and that of the linalool-depending monoterpene synthase. The characterization of these novel biocatalysts is crucial to fully understand the anaerobic monoterpene degradation in *C. defragrans* as well as for future biotechnological applications.

Materials and methods

Cultivation conditions and preparation of protein extracts

C. defragrans 65Phen and a *C. defragrans* 65Phen Δ*ldi* mutant were cultivated in anaerobic artificial fresh water medium as described previously (Petasch *et al*. 2014). For biomass production cultivation in a 10L fermenter (Biostat Bplus 10LMO, Sartorius AG, Göttingen, Germany) was conducted as described (Heyen and Harder 2000). Cultivation of the wild-type strain had a liquid hydrophobic phase of (*R*)-(+)-limonene (>97% purity, Sigma-Aldrich, Germany) corresponding to a theoretical concentration of 30 mM in the aqueous phase. Cultures of *C. defragrans* Δ*ldi* were grown on linalool (>97% purity, Sigma-Aldrich, Germany) as carbon source. To circumvent linalool toxicity, the fermenter was supplied every two days with 0.5 – 1 mM of the monoterpene. Once the cultures reached late exponential phase (OD_{600} for limonene-grown ~2; linalool-grown ~0.7), the biomass was harvested by centrifugation (16000x *g* for 40 min at 4°C). The pelleted biomass was shock-frozen in liquid nitrogen and stored at -80°C. For protein extraction, the biomass was resuspended in a two-fold volume of 25 mM Tris-Cl buffer, pH 7.5, allowed to thaw at room temperature and disrupted by three passages on either a French pressure cell press (SLM Aminco, Rochester, N.Y.) at 8.6 MPa or a One-

Shot cell disrupter (Constant Systems Ltd., Daventry, GB) set at 1.5 kbar. A soluble protein extract was prepared by ultracentrifugation of the crude lysate at 230,000x *g* for 30 min at 4°C.

Protein purification

Protein purification was performed with an ÄKTA LC system (GE Healthcare, Freiburg, Germany) at 4°C. All buffers were prepared and pH-adjusted at room temperature. When needed, salinity of protein solutions was adjusted to the chromatography buffer. Eluting proteins were collected in 1 mL fractions and directly used for enzyme assays or frozen in liquid nitrogen. Protein purity was followed by SDS-PAGE. For size exclusion chromatography, soluble proteins were loaded onto a Superdex 200-pg column (120 mL volume, 1.6 cm diameter) equilibrated with 25 mM Tris-Cl, 100 mM KCl, pH 7.5. Protein fractionation took place at a constant flow of 0.5 mL min^{-1}. The apparent molecular size of active proteins was calculated from calibration curves prepared with commercial gel filtration standards (Bio-Rad Laboratories GmbH, Munich, Germany). Anion exchange chromatography (AEC) was carried out on a diethylaminoethyl sepharose column (1.6 x 7 cm; column volume (CV): 14 mL) equilibrated with 25 mM Tris-Cl, pH 7.5. Unbound proteins were collected in the flow-through and tested for activity as a single fraction. Column-bound proteins were separated over a KCl gradient increasing from 0 to 300 mM. For the linalool-dependent activity such gradient was applied over a volume of 70 mL (5 CV), while the α-terpineol/terpinene-4-ol-dependent activity was fractionated over 300 mL (21 CV). Tightly-bound proteins, which eluted after increasing KCl from 300 mM to 1000 mM in a single step, were collected as a single fraction and tested for enzyme activity. For hydrophobic interaction chromatography (HIC) a butyl sepharose column (HiScreen Butyl FF, CV: 4.7 mL) was used. The column was equilibrated with 1 M $NH_4(SO_4)_2$ in 25 mM Tris-Cl, pH 7.5. Proteins were fractionated over a 94 mL (20 CV) gradient of ammonium sulfate from 1000 – 0 mM.

Enzyme activity assays

Enzyme assays were performed in 1.5 mL glass vials (WICOM Germany GmbH, Heppenheim, Germany) closed with a lid and a Teflon-coated septum. Standard assays contained 10 mM ATP, 15 mM Mg^{2+}, 2 mM dithiothreitol (DTT) dissolved in 25 mM Tris-Cl, pH 7.5 in a final volume of 500 µL. Whole protein assays (cell lysates, resuspended pellets or soluble protein extracts) contained 2.5

mg protein. Assays with partially purified proteins contained between 0.1 and 0.3 mg protein. The reactions were started by the addition of 5 mM of monoterpene substrate dissolved in 25 mM Tris-Cl, pH: 7.5 containing 0.5% v/v Tween-20. Final concentration of Tween-20 in the assays was 0.1%. The assays were conducted in anoxic conditions and incubated at 28°C for 2 – 3 hours. After incubation, 200 µL of n-hexane were added to each assay, vortexed for 30 seconds and further incubated under constant shaking at 60 rpm for 10 minutes. Then the samples were centrifuged at 13,000x *g* for 10 min for phase separation. 1 µL of the organic phase was analyzed by gas chromatography with flame ionization detection (Perkin Elmer Auto System XL, Überlingen, Germany) on an Optima-5 column (50 m x 0.32 mm inner diameter, 0.25 µm film thickness; Macherey-Nagel, Düren, Germany). The temperature program comprised: injection port at 250°C, initial column temperature of 80°C for 2 min, increasing to 120°C with a rate at 4°C min^{-1}, 120°C for 0.1 min, increasing to 320 °C at 45°C min^{-1}, 320°C for 2.9 min. The detector was set at 350°C. The split ratio was set to 1:9. All reported concentrations refer to the aqueous phase. Analyte concentrations were calculated from calibration curves prepared with authentic standards.

Analytical methods

Proteins were quantified using the Bradford method (Bradford 1976) with bovine serum albumin as standard and visualized by SDS-PAGE (10% v/v acrylamide) stained with Coomassie blue (Laemmli 1970). For protein mass spectroscopy, either bands excised from SDS-PAGE or liquid protein fractions were trypsin-digested and analyzed on a Q Exactive Plus Hybrid Quadrupole-Orbitrap mass spectrometer (Thermo Fisher Scientific, Bremen, Germany). Mass spectra of digested peptides were analyzed with Proteome Discoverer v2.1 (Thermo Fisher Scientific).

Results

Partial purification of a novel linalool-dependent monoterpene cyclase

A novel catalytic activity acting on the acyclic monoterpene linalool was recently observed in protein extracts of *C. defragrans* 65Phen Δ*ldi* (Marmulla 2015). This ATP-dependent biotransformation resulted in the formation of the monocyclic monoterpenes α-terpinene and terpinolene under anoxic conditions. To further characterize this monoterpene synthase-like activity, soluble protein extracts of

linalool-grown *C. defragrans* Δ*ldi* were prepared by cell disruption and ultracentrifugation. In enzyme assays, soluble extracts exhibited a linalool-dependent α-terpinene-synthase activity of 10 pkat mg^{-1} and a terpinolene-synthase activity of 10.4 pkat mg^{-1} using Mg^{2+} and ATP as co-substrates (Table 1). Catalytic activity was also observed in resuspended ultracentrifugation pellets, which transformed linalool exclusively into α-terpinene (9.1 pkat mg^{-1}). In order to purify the enzymatic activity, soluble protein extracts were subjected to protein liquid chromatography. Attempts of purification with butyl and phenyl sepharose columns resulted in total loss of activity, while with a weak anion exchanger (AEC) only terpinolene synthase activity was recovered (data not shown). The use of size exclusion chromatography (SEC) as first purification step allowed the recovery of both monoterpene synthase activities (α-terpinene- and terpinolene-forming), although they overlapped almost completely over several fractions of the gel filtration (Figure S1). The fractions with the highest activity for α-terpinene and terpinolene production were combined into two separate pools (P1 and P2, respectively). The elution volume from the SEC column for P1 corresponds to a molecular size of 314 kDa and of 172 kDa for P2. Both pools were tested for catalytic activity. P1 showed an increase both in α-terpinene and in terpinolene synthase activity with respect to the soluble extract (Table 1). P2 showed increase only in terpinolene synthesis and no detectable α-terpinene production (Table S1). Both pools were independently loaded onto an AEC column and fractionated over a KCl gradient (Figure S2, Figure S3). AEC fractions of P1 showed overlapping α-terpinene and terpinolene synthesis from protein eluting between 150 and 200 mM of KCl. In these the specific activity showed a higher increase in the production of terpinolene than of α-terpinene (Table 1). For subsample P2, a significant enrichment in terpinolene synthase activity was observed after conducting AEC (Table S1). The catalytic proteins from P2 eluted from the AEC column within the same KCl concentration range as the active fractions of P1 (Figure S3).

Table 1. Partial purification of linalool-dependent α-terpinene and terpinolene synthase activities using protein extracts from *C. defragrans* 65Phen Δ*ldi* grown on linalool.

Purification level	Protein [mg]	α-terpinene synthase			terpinolene synthase			Protein yield [%]
		Total activity [pkat]	Specific activity [pkat mg^{-1}]	Relative specific activity	Total activity [pkat]	Specific activity [pkat mg^{-1}]	Relative specific activity	
SE	227	2269	10	1	2365	10.4	1	100
SEC								
Pool 1 [P1]	43.5	650	14.9	1.49	699	16.1	1.54	19.2
AEC [KCl $_{mM}$]								
128	0.24	0	0	0	3.86	16.1	1.55	0.11
145	0.37	4.86	13.2	1.32	25.7	70.0	6.72	0.16
163	0.45	3.95	8.77	0.88	11.4	25.4	2.44	0.20
180	0.53	5.8	10.92	1.09	7.48	14.1	1.35	0.23
196	0.83	5.43	6.51	0.65	7.3	8.76	0.84	0.37
214	1.68	3.82	2.27	0.23	6.51	3.87	0.37	0.74
231	2.15	0	0	0	3.2	1.49	0.14	0.95

The partial purification of α-terpinene- and terpinolene-synthesizing activities from P1 and P2 showed similar protein patterns in denaturing protein gels (Figure 1). Protein bands common to the active fractions in both samples were observed at 55, 35 and 27 kDa. The fractions from the AEC with the highest catalytic activity in P1 (145 mM KCl) and P2 (161 mM KCl) were trypsin-digested and analyzed by LC-ESI-MS/MS. Out of the 78 proteins identified, 40 were detected in both P1 and P2 fractions (Table 2). 13 additional proteins were detected solely in P1, whereas 25 were exclusive to P2.

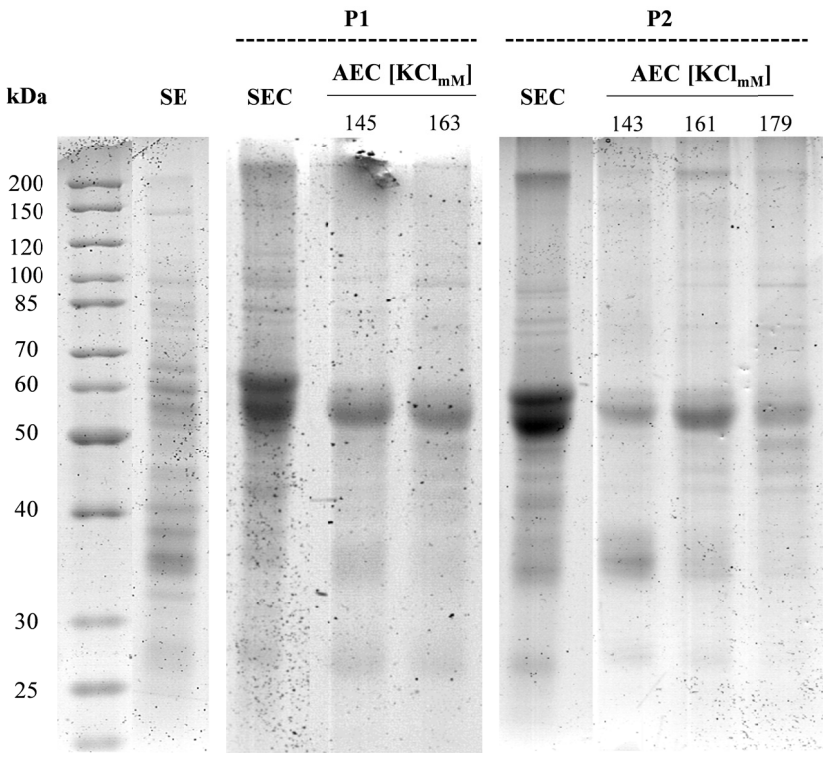

Figure 1. Protein fractions with linalool-dependent α-terpinene (P1) and terpinolene (P2) synthase activities. Molecular size marker (kDa); soluble protein extracts (SE) were fractionated using size exclusion (SEC) and anion exchange chromatography (AEC) columns. KCl concentrations in eluted AEC fractions are shown [KCl_{mM}].

Table 2. Proteins detected in fractions from anion exchange chromatography with linalool-dependent α-terpinene (P1) and terpinolene (P2) synthase activities.

Protein_id	P1 [145 mM][a]	P2 [161 mM]	Description	MW [kDa]	Coverage (%)[b]
CDM22544	●	●	Glutamate synthase [NADPH] small chain	53.8	26.9
CDM22556	●	●	Imidazole glycerol-phosphate dehydratase	21.4	53.8
CDM22584	●	-	LSU ribosomal protein L24p	11.1	34.0
CDM22608	●	-	SSU ribosomal protein S10p	11.8	23.3
CDM22636	●	-	LSU ribosomal protein L10p	18.5	66.7
CDM22637	●	-	LSU ribosomal protein L1p	23.7	30.3
CDM22646	●	-	Cold shock protein CspG	7.3	69.1
CDM22649	●	●	Universal stress protein, UspA family	15.9	30.2
CDM22659	●	●	DNA gyrase subunit B	90.1	35.3
CDM22660	●	●	DNA polymerase III beta-subunit	41.2	53.0
CDM22669	●	-	Putative restriction endonuclease	36.0	53.2
CDM22691	●	●	Pyruvate kinase	50.6	25.3
CDM22890	●	●	Hypothetical protein	20.9	35.3
CDM22976	●	●	Homogentisate 1,2-dioxygenase	47.7	42.8
CDM22977	●	●	Homogentisate 1,2-dioxygenase	43.3	28.7
CDM22987	●	●	Acetyl-CoA acetyltransferase	42.5	39.6
CDM23097	●	●	Glutamate synthase large chain	172.8	23.4
CDM23141	●	-	Carboxyl-terminal protease	54.6	20.2
CDM23151	●	●	HPr kinase/phosphorylase	34.2	30.1
CDM23364	-	●	Phosphoglucosamine mutase	47.2	20.6
CDM23395	-	●	4-carboxymuconolactone decarboxylase	17.4	27.7

CDM23408	-	●	Sulfite reductase beta-subunit	63.4	35.8
CDM23494	●	●	Glucose-6-phosphate 1-dehydrogenase	54.2	24.6
CDM23540	-	●	Ribonuclease E	113.3	27.1
CDM23573	-	●	LysR-family regulator CbI	35.4	38.4
CDM23590	●	-	Transcriptional regulator, TetR family	28.1	21.2
CDM23619	●	●	Gamma-glutamyl phosphate reductase	45.0	26.8
CDM23622	-	●	Leucyl-tRNA synthetase	98.6	33.4
CDM23789	●	●	Ferric uptake regulation protein	16.0	48.2
CDM23800	●	●	Putative zinc protease	102.0	36.8
CDM23801	●	●	Omega-amino acid-pyruvate aminotransferase	49.0	34.1
CDM23832	●	●	Isocitrate dehydrogenase	45.9	22.2
CDM23883	-	●	Alkylhydroperoxidase AhpD	12.1	27.8
CDM23944	●	-	Copper-containing nitrite reductase	49.9	23.1
CDM24086	●	●	Transcription termination factor Rho	47.2	71.1
CDM24108	-	●	Allantoicase	37.9	40.5
CDM24117	●	-	Sulfurtransferase	33.0	22.8
CDM24130	●	●	Valyl-tRNA synthetase	105.7	47.0
CDM24332	-	●	Hypothetical protein	87.6	37.9
CDM24369	-	●	Inorganic pyrophosphatase	19.5	24.3
CDM24437	-	●	Translation elongation factor Ts	30.8	45.0
CDM24511	-	●	Hypothetical protein	30.4	38.0
CDM24539	●	●	Branched-chain amino acid ABC transporter, amino acid-binding protein	38.8	26.3
CDM24540	-	●	Non-specific DNA-binding protein Dps	19.2	45.1

CDM24610	-	●	Glucose-1-phosphate cytidylyltransferase	28.7	43.2
CDM24623	●	●	Hypothetical protein	32.0	28.5
CDM24665	-	●	Probable hydrolase	31.6	27.6
CDM24698	●	●	ATP-dependent protease La Type I	89.9	28.0
CDM24735	●	●	Phosphopantothenoylcysteine decarboxylase	41.7	29.9
CDM24736	-	●	Deoxyuridine 5'-triphosphate nucleotidohydrolase	16.1	52.3
CDM24902	●	●	Pyruvate kinase	51.8	49.0
CDM25054	-	●	Adenosylmethionine-8-amino-7-oxononanoate aminotransferase	49.1	20.3
CDM25079	●	-	Malate dehydrogenase	35.2	21.0
CDM25094	●	●	Acyl-CoA dehydrogenase	59.6	51.4
CDM25099	-	●	Nitrous-oxide reductase	70.7	50.4
CDM25257	-	●	Citrate lyase	30.7	75.3
CDM25292	●	-	Transcriptional regulator, MarR family	21.0	45.7
CDM25300	-	●	Acyl coenzyme A hydrolase/transferase	44.6	20.5
CDM25304	-	●	3-hydroxyisobutyryl-CoA hydrolase	42.2	31.7
CDM25337	●	●	Molybdopterin-binding protein	31.5	45.5
CDM25340	●	●	Branched-chain amino acid aminotransferase	34.0	40.8
CDM25357	●	●	Phosphoribosyl aminoimidazole carboxamide formyltransferase	45.6	35.6
CDM25383	●	-	Probable signal peptide protein	20.8	27.4
CDM25422	●	●	Hypothetical protein	40.5	35.7
CDM25495	●	●	Methionyl-tRNA synthetase	76.4	53.4
CDM25575	●	●	Molybdenum cofactor biosynthesis	18.8	38.3

			protein MoaB		
CDM25670	●	●	Aldehyde dehydrogenase B	57.0	43.6
CDM25701	●	●	LSU ribosomal protein L25p	21.5	42.3
CDM25729	-	●	Succinate-semialdehyde dehydrogenase	51.6	45.2
CDM25802	●	●	Catalase	53.8	52.5
CDM25843	-	●	Heat shock protein 60 family co-chaperone GroES	10.2	29.5
CDM25923	●	●	Enoyl-CoA hydratase	27.9	29.8
CDM25962	-	●	N-acetyl-gamma-glutamyl-phosphate reductase	38.3	68.6
CDM26021	●	●	Aspartyl-tRNA amidotransferase subunit C	11.1	36.3
CDM26022	●	●	Aspartyl-tRNA amidotransferase subunit A	53.5	64.9
CDM26023	●	●	Aspartyl-tRNA amidotransferase subunit B	53.1	46.0
CDM26026	●	●	Exodeoxyribonuclease III	29.8	27.8
CDM26082	-	●	Heat shock protein Hsp20	16.6	48.7

[a]Concentration of KCl in analyzed fractions; Proteins detected (●) and no detected (-) by LC-ESI-MS/MS.

[b]Percentage of the protein sequence covered by the detected peptides

Partial purification of a cyclic monoterpene alcohol dehydratase

The cyclic monoterpene alcohols α-terpineol and terpinen-4-ol are known to support growth of *C. defragrans* (Foss *et al*. 1998); however, their degradation has thus far not been investigated. In this study cell suspensions and protein extracts from limonene-grown biomass were tested for activity on these monoterpene alcohols with and without the addition of several co-substrates. The dehydroxylation of both alcohols was observed in soluble protein extracts supplemented with ATP, divalent cations and dithiothreitol. Catalytic activity on α-terpineol resulted in the formation of the monoterpene hydrocarbons α-terpinene (2.4 ± 0.2 pkat mg^{-1}) and terpinolene (9.7 ± 0.4 pkat mg^{-1}).

With terpinen-4-ol as substrate, similar results were observed (3.9 ± 0.1 pkat mg^{-1} and 8 ± 1 pkat mg^{-1} for α-terpinene and terpinolene formation, respectively). Soluble protein extracts showing catalytic activity were fractionated over a salinity gradient using anion exchange chromatography (AEC). The alcohol dehydratase activity was recovered solely as terpinolene synthase in fractions eluting between 210 and 260 mM KCl. Such fractions showed identical specific activity for α-terpineol and terpinen-4-ol dehydroxylation (Figure S4). Hence, terpinen-4-ol was adopted as substrate for further activity assays. The partially purified protein, active on monocyclic monoterpene alcohols, exhibited an apparent molecular size of 133 kDa on the gel filtration and did not show catalytic activity on the acyclic linalool (data not shown). Fractions from AEC with dehydratase activity on terpinene-4-ol were injected onto a hydrophobic interaction chromatography (HIC) column, resulting in a 15-fold net increase in specific enzyme activity (Table 3) and the enrichment of protein bands of 42 and 38 kDa in denaturing gels (Figure 2).

Table 3. Purification of terpinen-4-ol dehydratase activity from soluble protein extracts of *C. defragrans* 65Phen grown on limonene.

Purification step	Total protein [mg]	Total activity [pkat]	Specific activity [pkat mg^{-1}]	Relative specific activity	Protein yield (%)
SE	500	5005	10 ± 0.2	1	100
AEC [KCl_{mM}]					
210 - 260	8	486	61 ± 7	6	1.6
HIC [$NH_4(SO_4)_{2\ mM}$]					
150- 140	0.26	38	147 ± 15	15	0.05

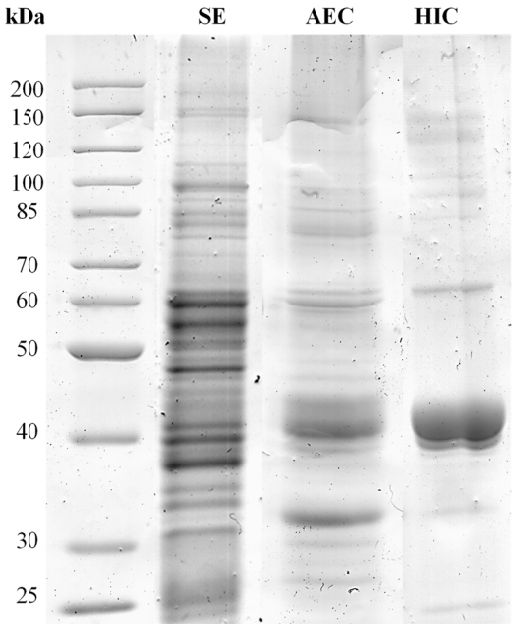

Figure 2. SDS-PAGE of fractions with terpinen-4-ol dehydratase activity from protein extracts of *C. defragrans* 65Phen. Molecular size marker (kDa), soluble protein extract (SE), active fractions from anion exchange chromatography (AEC), and hydrophobic interaction chromatography (HIC).

Several proteins were detected in the bands excised (at 62, 42, 38, 33 and 25 kDa) from denaturing gels with active fractions from AEC and HIC (Figure 2, Table 4). The identified proteins are involved in several metabolic processes such as amino acid (CDM22780 and CDM25869) and fatty acid metabolism (CDM23550, CDM25241, CDM25258 and CDM25291), glycolysis (CDM23611), one hypothetical protein (CDM25297) and two miscellaneous proteins (CDM22609 and CDM25844). Protein CDM25241 was detected in two bands of the analyzed gels i.e. at 42-38 kDa and 25 kDa. Its presence in the 25 kDa region is most likely a result of protein degradation given its theoretical molecular size of 44.5 kDa.

Table 4. Proteins detected in fractions with terpinen-4-ol dehydratase activity.

Apparent size of excised band (kDa)[a]	Protein_id	Protein annotation	Theoretical molecular size (kDa)	Coverage (%)[b]
62	CDM25844	Heat shock protein 60 family chaperone GroEL	57.4	34.3
42 and 38	CDM22609	Translation elongation factor Tu	42.8	31.6
	CDM22780	Isovaleryl-CoA dehydrogenase	42.6	47.7
	CDM23466	NADH:ubiquinone oxidoreductase chain F	49.8	33.4
	CDM23611	Enolase	45.6	46.0
	CDM25241	Acyl-CoA dehydrogenase protein	44.5	50.5
	CDM25258	Acyl-CoA dehydrogenase	42.5	42.3
	CDM25291	Acyl-CoA acetyltransferase	41.0	66.8
	CDM25297	hypothetical protein	37.6	55.6
	CDM25869	O-acetylhomoserine sulfhydrylase / O-succinylhomoserine sulfhydrylase	45.8	78.6
33	CDM23550	3-oxoacyl-[acyl-carrier-protein] synthase, KASIII	33.9	21.6
25	CDM25241	Acyl-CoA dehydrogenase protein	44.5	18.2

[a]Protein bands cut from SDS-PAGE preparations were analyzed by LC-ESI-MS/MS.

[b]Percentage of the protein sequence covered by the detected peptides.

Discussion

C. defragrans 65Phen mineralizes several monoterpenes, including alcohols, in anoxic denitrifying medium. In this study, we report a novel monoterpene alcohol dehydratase and the partial purification of two catalytic activities acting on acyclic and monocyclic monoterpene alcohols. The fate of linalool in *C. defragrans* was originally inferred from the description of the enzymes that catalyze its oxidation to geranic acid (Brodkorb *et al*. 2010; Heyen and Harder 2000; Lüddeke *et al*. 2012b). However, the existence of an alternative pathway has been suggested due to the absence of a degradation pathway for geranic acid and the observations made on growth experiments with deletion mutants (Lüddeke *et al*. 2012a). The discovery of a linalool-dependent monoterpene cyclase producing cyclic dienes confirms such hypothesis (Marmulla 2015). The products of linalool dehydroxylation and cyclization are α-terpinene and terpinolene. The formation of both products is catalyzed by soluble protein extracts at similar reaction rates; however protein purification favored the enrichment of terpinolene production (Table 1). With our purification protocol, it was not possible to isolate the synthesis of α-terpinene from that of terpinolene. In fact, α-terpinene synthesis stagnated while terpinolene production was further enriched in sample P1 (Table 1, Figure S2), suggesting that the synthesis of both monoterpene products may be catalyzed by the same enzyme. Most known monoterpene cyclases synthetize several monoterpene products simultaneously (Fahnrich *et al*. 2011), while the mechanisms regulating the fate of the reactions are not fully understood (Degenhardt *et al*. 2009). Interestingly, the molecular size of fractions exhibiting α-terpinene synthesis in the gel filtration was nearly two times the size of those with maximum terpinolene production (Figure S1). Thus, the production of each monoterpene product could be associated to the level of enzymes' quaternary organization. P1 and P2 shared similar protein compositions, however due to the high number of proteins detected no candidate protein could be associated to the catalytic activity.

Interestingly, another ATP-dependent synthesis of α-terpinene and terpinolene was detected in soluble protein extracts using α-terpineol and terpinen-4-ol as substrates. As for the linalool-dependent reaction, liquid chromatography led to the enrichment of terpinolene synthase activity only. The molecular size of the active fraction in the gel filtration was 133 kDa. The partially purified protein

showed identical catalytic activity on both cyclic monoterpene alcohols, but not on the acyclic linalool. The combination of AEC and HIC led to the enrichment of several proteins with an equally diverse set of predicted biological functions (Figure 2, Table 4). Among them four proteins encoded within the genomic island specialized in monoterpene degradation were detected (Petasch *et al*. 2014). Proteins CDM25241, CDM25258 and CDM25291 are annotated as involved in acyl-CoA metabolism and were found up-regulated in the proteome of monoterpene-grown *C. defragrans* (Petasch *et al*. 2014). The fourth protein detected in terpinolene-synthesizing fractions, CDM25297, has not predicted function. Remarkably, CDM25241 belongs to the acyl-CoA dehydrogenases (ACAD) subfamily 10. This cluster of mainly uncharacterized proteins bear typical ACAD domains at the N- and C-termini and a central ATP-binding domain unique for ACAD10 and ACAD11 (He *et al*. 2011; Swigonova *et al*. 2009). A single representative of the ACAD10 subfamily has to some extend been characterized *in vitro* (He *et al*. 2011). The enzyme subcloned from human brain tissue showed minimal activity on two branched-chain substrates (*R*- and *S*-2 methyl-C15-CoA), without any apparent involvement of its ATP-binding domain. Thus, its physiological role is still considered as unknown. The presence of an ATP-binding domain in CDM25241 and its strategic localization among genes involved in monoterpene metabolism make of this protein a candidate to be considered in future research.

The synthesis of monocyclic monoterpene hydrocarbons from linalool, α-terpineol and terpinen-4-ol is pivotal to explain the versatility of *C. defragrans* towards monoterpenes. By centralizing the degradation of its monoterpene substrates, *C. defragrans* avoids genetic and metabolic redundancy which represents an evolutionary advantage in the environment. Terpinolene and α-terpinene are substrates to the recently described limonene dehydrogenase (Puentes-Cala *et al*. submitted), which channels their degradation into the monocyclic monoterpene degradation pathway (Petasch *et al*. 2014).

Acknowledgements

We thank M.Sc. Dolma Michellod for her support on protein MS determinations. E.P.C. was supported by a grant from the DAAD in Germany and from the Corporación para la Investigación de la Corrosión and COLCIENCIAS in Colombia. This study was funded by the Max Planck-Society.

References

Bradford MM (1976) Rapid and sensitive method for quantitation of microgram quantities of protein utilizing principle of protein-dye binding. Anal Biochem 72:248-254

Brodkorb D, Gottschall M, Marmulla R, Lüddeke F, Harder J (2010) Linalool dehydratase-isomerase, a bifunctional enzyme in the anaerobic degradation of monoterpenes. J Biol Chem 285:30436-30442

Degenhardt J, Kollner TG, Gershenzon J (2009) Monoterpene and sesquiterpene synthases and the origin of terpene skeletal diversity in plants. Phytochemistry 70:1621-1637

Fahnrich A, Krause K, Piechulla B (2011) Product variability of the 'cineole cassette' monoterpene synthases of related *Nicotiana species*. Mol Plant 4:965-984

Foss S, Heyen U, Harder J (1998) *Alcaligenes defragrans* sp. nov., description of four strains isolated on alkenoic monoterpenes ((+)-menthene, α-pinene, 2-carene, and α-phellandrene) and nitrate. Syst Appl Microbiol 21:237-244

Harder J, Marmulla R (2017) Catabolic pathways and enzymes involved in the anaerobic degradation of terpenes. In: Boll M (ed) Anaerobic utilization of hydrocarbons, oils, and lipids. Springer International Publishing, Cham, pp 1-15

He M, Pei Z, Mohsen AW, Watkins P, Murdoch G, van Veldhoven PP, Ensenauer R, Vockley J (2011) Identification and characterization of new long chain acyl-CoA dehydrogenases Mol Genet Metab 102:418-429

Heyen U, Harder J (2000) Geranic acid formation, an initial reaction of anaerobic monoterpene metabolism in denitrifying *Alcaligenes defragrans*. Appl Environ Microbiol 66:3004-3009

Hylemon PB, Harder J (1998) Biotransformation of monoterpenes, bile acids, and other isoprenoids in anaerobic ecosystems. Fems Microbiol Rev 22:475-488

Ilc T, Parage C, Boachon B, Navrot N, Werck-Reichhart D (2016) Monoterpenol oxidative metabolism: role in plant adaptation and potential applications. Front Plant Sci 7:509-524

Laemmli UK (1970) Cleavage of structural proteins during assembly of head of bacteriophage T4. Nature 227:680-685

Lüddeke F, Dikfidan A, Harder J (2012a) Physiology of deletion mutants in the anaerobic beta-myrcene degradation pathway in *Castellaniella defragrans*. BMC Microbiol 12:192-202

Lüddeke F, Harder J (2011) Enantiospecific (S)-(+)-linalool formation from beta-myrcene by linalool dehydratase-isomerase. Z Naturforsch C 66:409-412

Lüddeke F *et al*. (2012b) Geraniol and geranial dehydrogenases induced in anaerobic monoterpene degradation by *Castellaniella defragrans*. Appl Environ Microbiol 78:2128-2136

Marmulla R (2015) The anaerobic linalool metabolism in the betaproteobacteria *Castellaniella defragrans* 65Phen and *Thauera linaloolentis* 47Lol. Dissertation. University Bremen

Marmulla R, Harder J (2014) Microbial monoterpene transformations-a review. Front Microbiol 5:346-359

Misra G, Pavlostathis SG, Perdue EM, Araujo R (1996) Aerobic biodegradation of selected monoterpenes. Appl Microbiol Biotechnol 45:831-838

Petasch J *et al*. (2014) The oxygen-independent metabolism of cyclic monoterpenes in *Castellaniella defragrans* 65Phen. BMC Microbiol 14:164-176

Puentes-Cala E, Manuel Liebeke M, Markert S, Harder J (submitted) Limonene dehydrogenase, a hydroxylating flavoenzyme in the anaerobic monocyclic monoterpene degradation. J Biol Chem

Swigonova Z, Mohsen AW, Vockley J (2009) Acyl-CoA dehydrogenases: dynamic history of protein family evolution. J Mol Evol 69:176-193

Tadasa K, Fukazawa S, Kunimatsu M, Hayashi T (1976) Microbiological conversion of α-terpineol (2) Agr Biol Chem 40:1069-1073

Supplementary material

Initial purification of novel monoterpene synthases from *Castellaniella defragrans*

Edinson Puentes-Cala[1], Elizabeth Engler-Hüsch[1], Manuel Liebeke[2], Jens Harder[1]*

[1]Dept. of Microbiology and [2]Dept. of Symbiosis, Max Planck Institute for Marine Microbiology, Celsiusstr. 1, D-28359 Bremen, Germany

*To whom correspondence should be addressed: Jens Harder, Dept. of Microbiology, Max Planck Institute for Marine Microbiology, Celsiusstr. 1, D-28359 Bremen, Germany, Tel.: +49 421 2028-750; Fax: +49 421 2028-790; E-mail: jharder@mpi-bremen.de

Table S1. Partial purification of terpinolene synthase activity from linalool using protein extracts from *C. defragrans* 65Phen Δ*ldi*.

Purification step	**Protein [mg]**	**Total activity [pkat]**	**Specific act. [pkat mg^{-1}]**	**Relative specific activity**	**Protein yield [%]**
SE	227	2365	10.4	1	100
SEC					
Pool 2	32	1024	32	3.1	14
AEC [KCl$_{mM}$]					
143	0.42	9.4	22.3	2.1	0.2
161	0.45	69.7	155	15	0.2
179	0.4	31.1	79	7.6	0.2
196	0.41	10.8	26.3	2.5	0.2
212	0.7	6.4	9.1	0.9	0.3
229	1.37	3	2	0.2	0.6

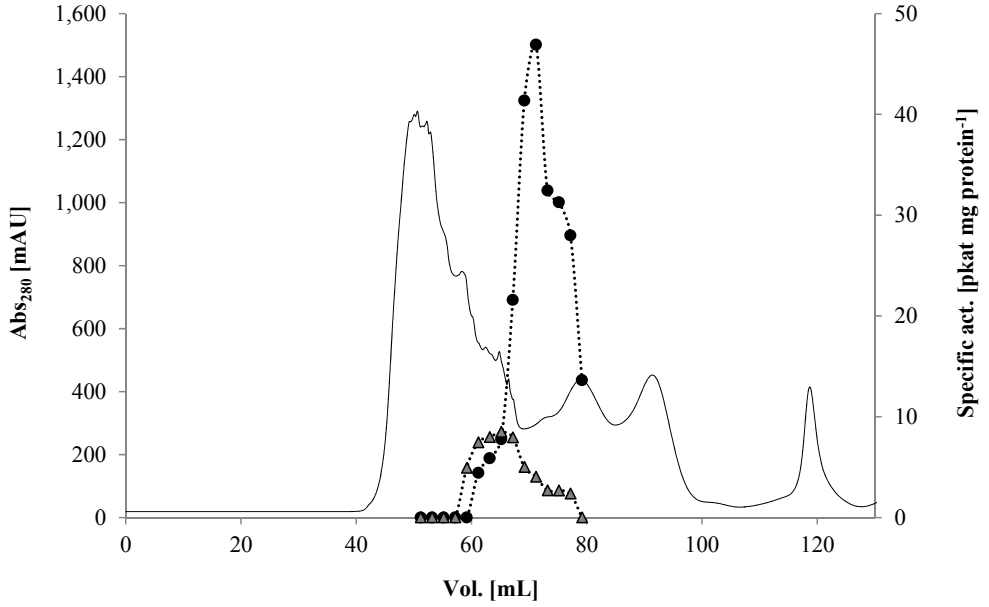

Figure S1. Linalool-dependent terpinolene (●) and α-terpinene (▲) synthase activity in size exclusion chromatography fractions.

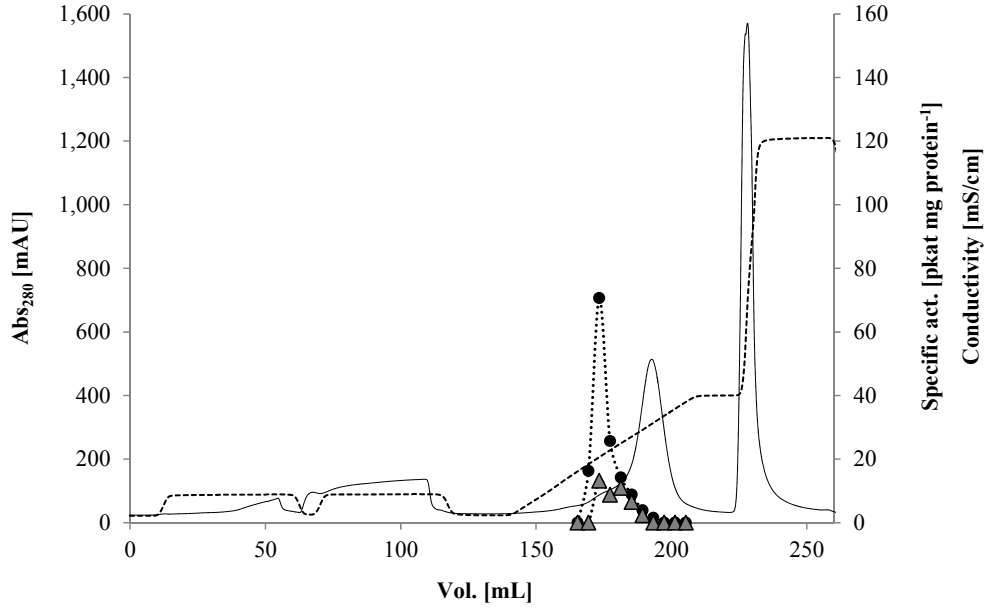

Figure S2. Linalool-dependent terpinolene (●) and α-terpinene (▲) synthase activity from sample P1 after anion exchange chromatography.

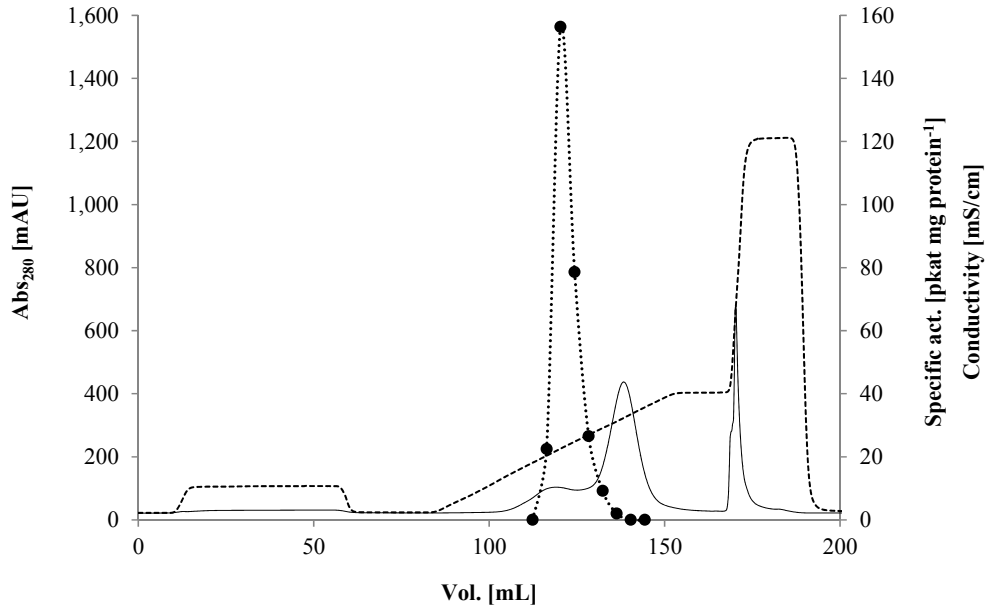

Figure S3. Linalool-dependent terpinolene (●) synthase activity from sample P2 after anion exchange chromatography.

A

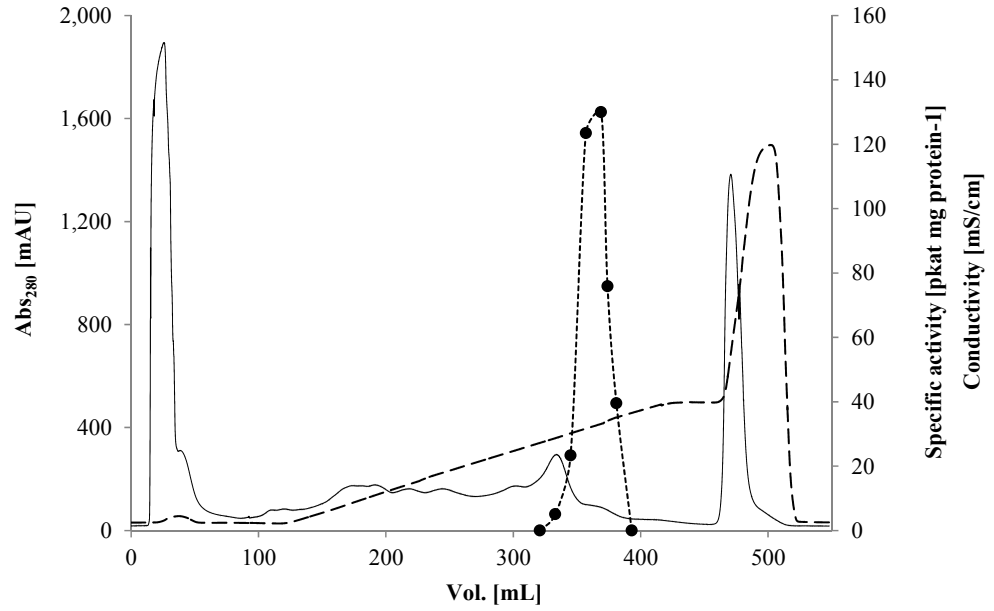

B

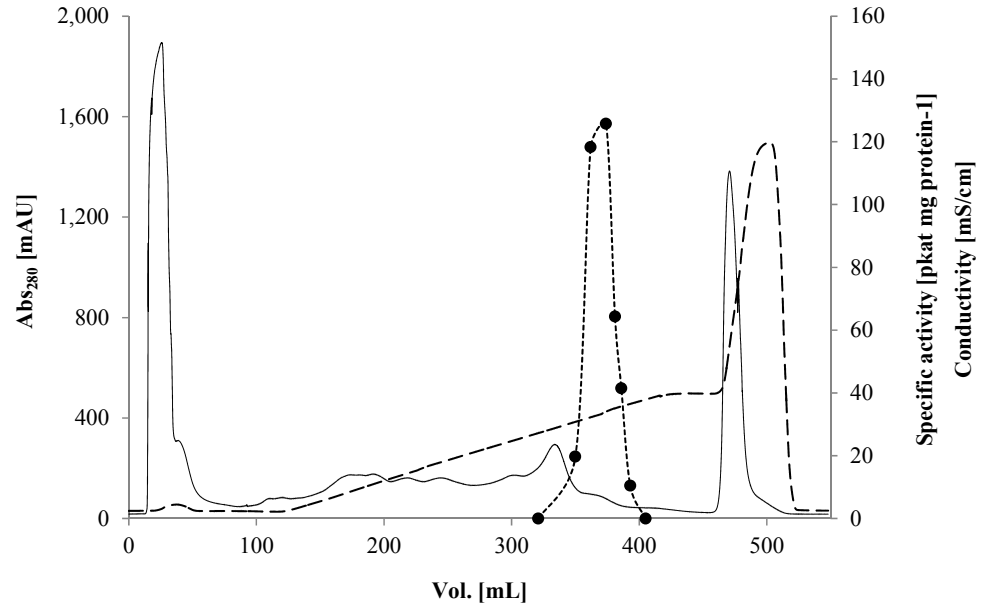

Figure S4. Terpinen-4-ol (A) and α-terpineol (B) dehydratase activity [terpinolene-forming (●)] of protein fractions obtained after anion exchange chromatography.

Chapter V: Manuscript 4

An RND transporter in the monoterpene metabolism of *Castellaniella defragrans*

Edinson Puentes-Cala, Jens Harder*

Dept. of Microbiology, Max Planck Institute for Marine Microbiology, Bremen

*To whom correspondence should be addressed: Jens Harder, Dept. of Microbiology, Max Planck Institute for Marine Microbiology, Celsiusstr. 1, D-28359 Bremen, Germany, Tel.: +49 421 2028-750; Fax: +49 421 2028-790; e-mail: jharder@mpi-bremen.de

Manuscript in preparation.

Abstract

The betaproteobacterium *Castellaniella defragrans* 65Phen grows on monoterpenes at concentrations toxic to many bacteria. Tolerance mechanisms include modifications of the membrane fatty acid composition and the mineralization of monoterpenes. In this study, we characterized a novel efflux transporter associated to the monoterpene metabolism. The inner-membrane transporter AmeD (apolar monoterpene efflux) affiliated to the HAE3 (hydrophobe/amphiphile efflux) family of Resistance-Nodulation-Division (RND) superfamily, known for transporting substrates into the periplasm. AmeD is co-expressed with the outer membrane protein AmeA and the periplasmic proteins AmeB and AmeC, suggesting an export channel into the environment similar to HAE1-type RND exporters. Proteins AmeABCD are encoded within a genetic island involved in the metabolism of acyclic and cyclic monoterpenes. The deletion of *ameABCD* translated into decreased monoterpene tolerance in liquid cultures. Interestingly, with acetate as cosubstrate the bacteria are more tolerant to monoterpenes. The uptake of Nile Red depended on an inhibition with the protonophore carbonyl cyanide *m*-chlorophenylhydrazone (CCCP). Cells lacking AmeABCD accumulated more Nile Red, suggesting an export function of the proteins. Our observations demonstrated a participation of the tetrapartite RND transporter AmeABCD in monoterpene detoxification in *C. defragrans*.

Keywords: RND efflux pump, monoterpene, toxicity, anaerobic metabolism, *Castellaniella defragrans*.

Introduction

Monoterpenes are a diverse group of volatile biogenic hydrocarbons found mainly in the essential oils of plants. Produced as secondary metabolites, these compounds exhibit a myriad of biological functions such as pollinator attraction, plant-plant communication and as antimicrobials (Mahmoud and Croteau 2002). Due to their hydrophobic nature, monoterpenes tend to accumulate in cellular membranes altering the proton gradient, the electron transport and the stability of membrane proteins (Abrahim *et al*. 2003; Brennan *et al*. 2012; Griffin *et al*. 1999). Microorganisms using monoterpenes as carbon and energy sources have evolved mechanisms to circumvent this toxicity. Changes in

membrane fluidity, monoterpene biotransformation and active secretion count among such adaptations (Bicas *et al*. 2008; Ramos *et al*. 2002; Ultee *et al*. 2000). Numerous efflux pumps of the Resistance-Nodulation-Division (RND) superfamily are reported to confer tolerance towards monoterpenes and other hydrocarbons (Kieboom *et al*. 1998; Segura *et al*. 2012). The RND efflux transporters MexAB-OprM and MexCD-OprJ have shown to be essential for growth of *Pseudomonas aeruginosa* exposed to monoterpene constituents of the tea-tree oil (Papadopoulos *et al*. 2008). Similarly, the complex AcrAB-TolC and several mutants thereof increased tolerance and enhanced monoterpene production in engineered *E. coli* strains (Dunlop *et al*. 2011; Foo and Leong 2013). Typically, RND efflux transporters active on organic solvents belong to the hydrophobe/amphiphile efflux-1 (HAE1) family (Eswaran *et al*. 2004; Garcia *et al*. 2010; Nikaido 2011; Tseng *et al*. 1999). Members of this family are mostly tripartite consisting of an inner membrane substrate/proton antiporter, an outer membrane pore and a periplasmic membrane fusion protein (MFP). The latter links the inner and outer membrane components and facilitates substrate transport across the periplasm straight into the extracellular environment. Substrate specificity is determined by the inner membrane RND pump which recruits substrates from the periplasm or from the outer leaflet of the inner membrane.

The betaproteobacterium *Castellaniella* (ex *Alcaligenes*) *defragrans* 65Phen mineralizes several monoterpenes under denitrifying conditions (Foss *et al*. 1998) and tolerates concentrations of α-phellandrene up to 30% v/v in a two-phase system (Heyen 1999). The proteome of *C. defragrans* grown on α-phellandrene revealed the increased expression of the putative RND transporter AmeD, as well as AmeABC, whose genes (*ameABC*) are encoded directly upstream of *ameD* (Petasch *et al*. 2014). In the same study, a transposon insertion in *ameB* resulted in defective growth on several monoterpenes. The gene cassette *ameABCD* is co-located with several genes associated to monoterpene metabolism (Fig. 1). In this study, we characterized the AmeABCD system conducting transport and growth studies with *Castellaniella defragrans* 65Phen and a deletion mutant lacking the genes *ameABCD*.

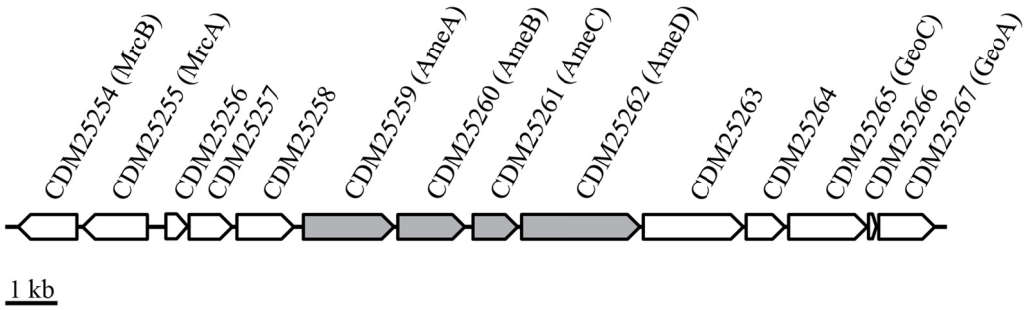

Fig. 1. Gene cluster of the putative RND transporter AmeABCD (grey) and its genetic neighbors within the genomic island specialized in monoterpene metabolism: upstream the monoterpene ring cleavage operon *mrcABCDEFGH* and downstream parts of the cyclic monoterpene metabolism (*geoA* and *geoC*).

Materials and methods

Bacterial strains and culture conditions

An in-frame deletion mutant lacking the gene cassette *ameABCD* (*C. defragrans* 65Phen Δ*ameABCD*) was prepared from *Castellaniella defragrans* 65Phen Rif^R as previously described (Lüddeke *et al*. 2012), and kindly provided by Jan Petasch (Max Planck Institute for Marine Microbiology, Bremen). The construct for *ameABCD* deletion was prepared using the primer pairs Ameup_XbaI_F (ATCGATCTAGATGGCGCGAGGTGGTGTTGTC) and Ameup_SpeI_R (CCGACGACTAGTGGCAAGACCCGCAACCTGTG), and Amedown_SpeI_F (AAGCTAACTAGTCATGTGTGTCTCCTCTGTGGTT) and Amedown_HindIII_R (ACTCAAAGCTTCTACTGAAAAACAGGAACGCAG). The deletion mutant and the rifampicin-resistant *C. defragrans* 65Phen (in the text referred to as wild-type) were cultivated in liquid Artificial Fresh Water medium (AFW) under anoxic denitrifying conditions as described elsewhere (Petasch *et al*. 2014). When indicated, between 10 and 20 mM sodium acetate was added as carbon source. Monoterpenes (>90% purity, Sigma-Aldrich, Germany) were supplied either in the carrier phase 2,2,4,4,6,8,8-heptamethylnonane (HMN) or dissolved in dimethyl sulfoxide (DMSO). Cultures were

incubated at 28°C under constant agitation (60 rpm). Microbial growth was monitored by measuring the optical density at 600 nm.

Fluorometric assays

As a proof of concept, Nile Red accumulation and extrusion was tested in *C. defragrans* cells by modifying previously described protocols (Bohnert *et al*. 2010; Bohnert *et al*. 2011). Briefly, cells of wild-type *C. defragrans* and Δ*ameABCD* were grown to late exponential phase in AFW medium containing both limonene (3 mM in HMN) and acetate (10 mM) as carbon sources. Cells were harvested at 5000x *g* for 30 min at 20°C and washed two times with AFW medium without any organic carbon source. After centrifugation, cells were resuspended in the same carbon-deprived medium to OD_{600} 0.5 and, when indicated, carbonyl cyanide *m*-chlorophenylhydrazone (CCCP) and phe-arg β-naphthylamide (PAβN) were added to final concentrations of 2 µM and 20 µg mL^{-1} (38.5 µM), respectively (from stock solutions in DMSO of 200 µM CCCP and 2 mM PAβN). The handling and preparation of microbial suspensions and chemical solutions was performed in an anaerobic chamber at 4°C. For influx assays, 198 µL of each cell suspension was transferred to a black 96-well plate (Fluotrac, Greiner Bio-One GmbH, Frickenhausen, Germany). Fifteen minutes after CCCP addition, Nile Red was added to a concentration of 2 µM (from a 200 µM stock solution in DMSO) and homogenized by repeated pipetting. The plate was covered with a sealing-film (thickness 50 µm, Carl Roth GmbH, Karlsruhe, Germany) to minimize exposition to oxygen during fluorescence monitoring. Fluorescence intensity was measured at room temperature with an Infinite M200 PRO (Tecan Austria GmbH, Grödig, Austria) with excitation at 552 nm and emission at 636 nm. Prior to each measurement, the plate was automatically shaken at 691 rpm for 30 seconds at amplitude of 1.5 mm. To measure efflux of Nile Red, cells were incubated anaerobically under constant shaking (60 rpm) with 2 µM of Nile Red and 2 µM of CCCP for 2 h at room temperature. Cells were washed two times by centrifugation at 5000x *g* for 15 min at 20°C and resuspended in AFW medium deprived of carbon sources. When indicated, PAβN (38.5 µM) was added to cell suspensions. 190 µL of the cell suspension were transferred to a 96-well plate and reenergized with 50 mM of sodium acetate. The

plate was covered with sealing film, rapidly taken out of the anaerobic chamber and fluorescence was measured.

Bioinformatics analysis

NCBI, UniProt and RAST (Overbeek *et al*. 2014) were used to retrieve the protein sequences for AmeABCD and related proteins, and to perform similarity and identity searches (Altschul *et al*. 1990) and conserved domain architecture analysis (Marchler-Bauer *et al*. 2017). AmeABCD sequences were analyzed for signal peptides, transmembrane helices and subcellular localization prediction using SignalP v4.1 (Nielsen 2017), TMHHM v2.0 (Krogh *et al*. 2001) and PSORTb v3.0.2 (Yu *et al*. 2010), respectively. The results obtained were validated by comparison with the results from InterPro (Finn *et al*. 2017). Visualization of transmembrane regions was generated with TMRPres2D (Spyropoulos *et al*. 2004). Three dimensional protein modeling was conducted with Phyre2 (Kelley *et al*. 2015). For the phylogenetic analysis of AmeD, sequences from the RND families HAE1, HAE2 and HAE3 were extracted from the TCDB database (Saier *et al*. 2016) and aligned with MAFFT v7.0 (Katoh *et al*. 2017). A maximum likelihood tree based on the JTT matrix model was calculated using MEGA v7.0 (Kumar *et al*. 2016) performing 1000 bootstrap replicates. The tree were visualized with Archaeopteryx v0.9921 beta (Han and Zmasek 2009).

Results and discussion

Growth on monoterpenes

The transposon insertion mutant *C. defragrans* 65Phen *ameB*::Tn5 revealed reduced growth on monoterpenes (Petasch *et al*. 2014). To assess the role of the RND transporter during monoterpene utilization, the wild-type strain and the deletion mutant 65Phen Δ*ameABCD* were compared in growth experiments (Fig. 2). Both strains exhibited similar growth when fed with acetate as sole carbon source and while growing cometabolically on both acetate and limonene (Fig. 2a-b). Apparently, in the latter cultures acetate was the preferred as substrate over limonene, while the cytotoxic effects of the monoterpene were not observed (Fig. 2b). The more soluble monoterpenoids perillyl alcohol, perillyl aldehyde and perillic acid did not show cytotoxicity either. In fact, these were utilized as sole

carbon sources by the deletion strain Δ*ameABCD* nearly as efficiently as the wild type (Fig. 2c, Fig. S1a-b). The physiological consequences of *ameABCD* deletion became observable during growth on limonene, α-terpinene and other non-functionalized monoterpenes (Fig. 2d, Fig. S1c-f). In these cultures, the deletion mutant grew only poorly on the monoterpene hydrocarbons. Apparently, despite limonene's low water solubility (100-150 μM) (Brennan *et al*. 2012; Fichan *et al*. 1999) and the presence of an organic carrier phase (HMN) that reduces mass transfer, limonene diffusion into Δ*ameABCD* cells exceeded its biotransformation to perillyl alcohol and other products. Instead, limonene most likely accumulated in membranes, impairing proton gradient formation and in consequence hindering energy conservation (Segura *et al*. 2012).

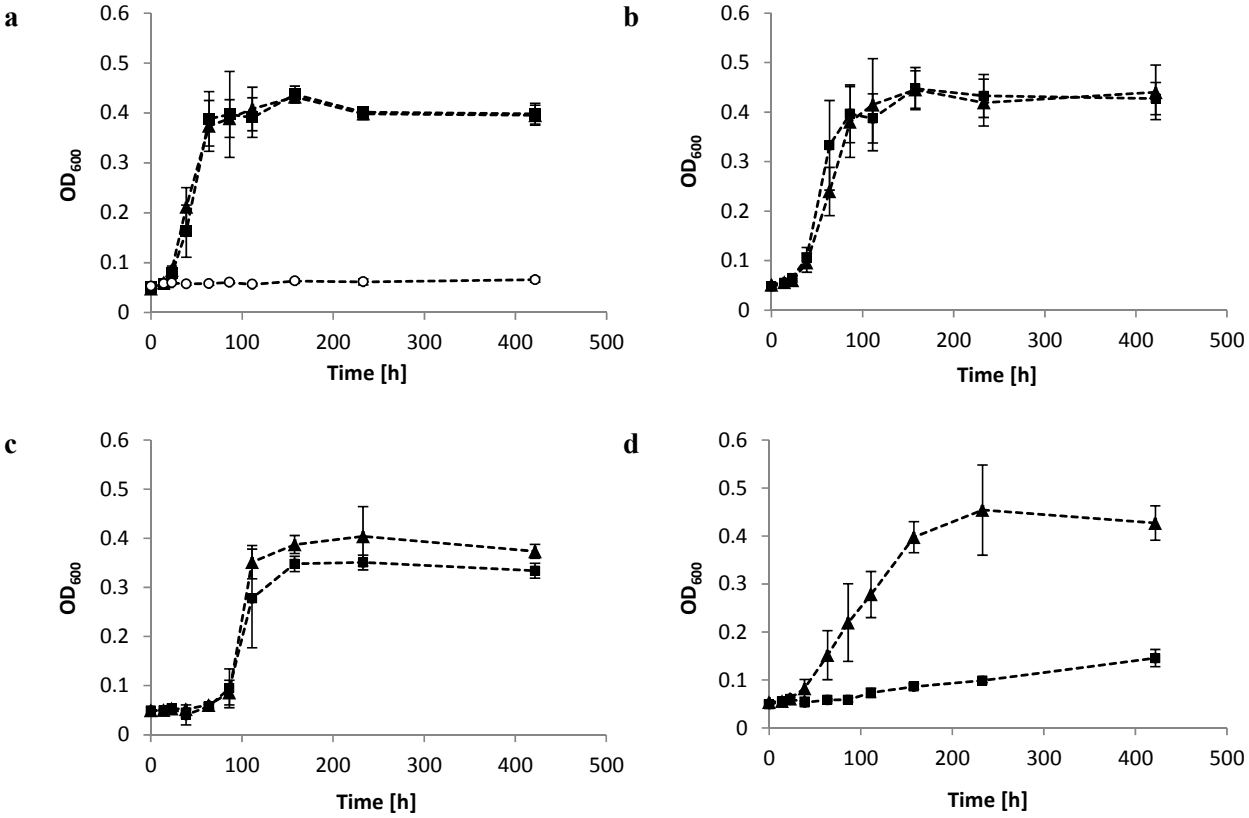

Fig. 2. Bacterial growth of wild-type [▲] and Δ*ameABCD* [■] strains of *C. defragrans* 65Phen on acetate (a), acetate and limonene (b), perillyl alcohol (c), and limonene (d) monitored at OD_{600}.

In order to further characterize growth of Δ*ameABCD* cells in media with both acetate and limonene as carbon sources, we replaced the carrier phase HMN by dimethyl sulfoxide (DMSO). DMSO facilitated limonene dissolution in the medium and allowed to test higher monoterpene concentrations.

In these cultures, the deletion mutant strain showed biomass yields comparable to those of the wild-type strain at concentrations of limonene up to 5 mM (Fig. 3, Fig. S2). At concentrations over 10 mM of homogenously dissolved limonene, the growth yield of Δ*ameABCD* cells was significantly reduced with respect to wild-type cells. These observations suggested that similar to previous cytotoxicity studies the addition of an second energy source, namely acetate, translates into a significant increase in monoterpene tolerance (Abrahim *et al*. 2003; Segura *et al*. 2012; Sikkema *et al*. 1995; Uribe *et al*. 1984). The energy generated from acetate and similar compounds is likely used to provide a proton gradient as energy source for a cellular detoxification. Unlike the mutant Δ*ameABCD*, the wild-type strain showed growth in all limonene concentrations tested (Fig. 3, Fig. S2), suggesting that proteins AmeABCD constitute yet another line of defense against monoterpene toxicity in *C. defragrans* complementing already described mechanisms such as the adaptational changes in membrane composition and the metabolic biotransformation of monoterpene substrates (Foss and Harder 1998; Harder and Marmulla 2017).

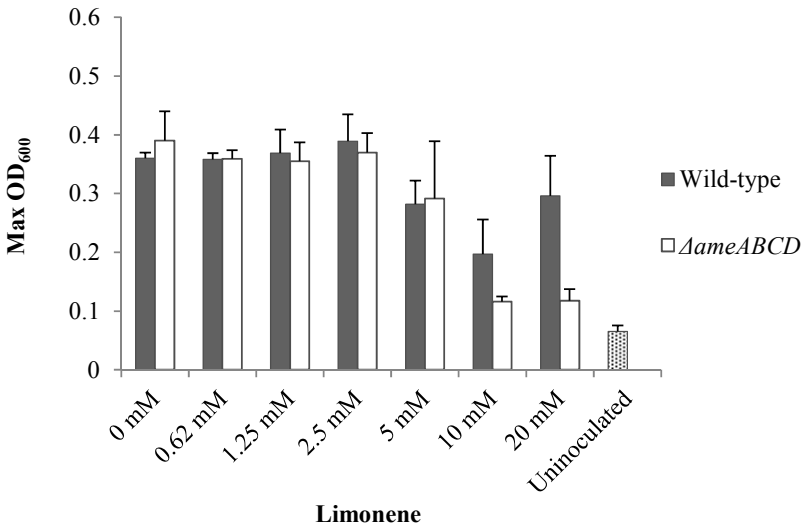

Fig. 3. Maximum optical densities of wild-type and Δ*ameABCD C. defragrans* 65Phen in acetate (10 mM) cultures containing limonene at various concentrations. Limonene was dissolved in DMSO prior to addition to the medium to facilitate mass transfer. The error bars indicate the standard deviation of the means for three independent experiments.

Influx and efflux of Nile Red

A set of fluorometric assays were conducted to monitor the *in vivo* accumulation and export of Nile Red in *C. defragrans* wild-type and Δ*ameABCD*. The cells were grown in AFW medium with 10 mM acetate and 3 mM limonene dissolved in HMN. Given its lipophilic nature, Nile Red accumulates in cell membranes which results in a significant increase in its fluorescent quantum yield (Blair and Piddock 2016). Assays with Nile Red and other environment-sensitive dyes are routinely used as a proxy to show the contribution of efflux pumps in bacterial resistance to xenobiotics (Blair and Piddock 2016; Paulsen *et al*. 1996; Soto 2013). Nile Red accumulated in *C. defragrans* cells treated with the protonophore carbonyl cyanide *m*-chlorophenyl hydrazine (CCCP), but not in untreated cells (Fig. 4). The lack of fluorescence signal in the untreated controls (Fig. 4a) indicates that Nile Red is indeed a suitable substrate for efflux pumps present in physiologically active cells of both wild-type and Δ*ameABCD C. defragrans*. When de-energized with CCCP, the mutant Δ*ameABCD* exhibited a slightly higher Nile Red accumulation than the wild-type (Fig. 4b), suggesting a contribution of AmeABCD to a residual export of Nile Red in the presence of the protonophore. An inhibitor of RND transporters is phenylalanine-arginine β-naphthylamide (PAβN). Its presence increased the accumulation of Nile Red in the wild-type strain and thus confirmed that the residual export activity was caused by RND efflux pumps (Fig. 4c).

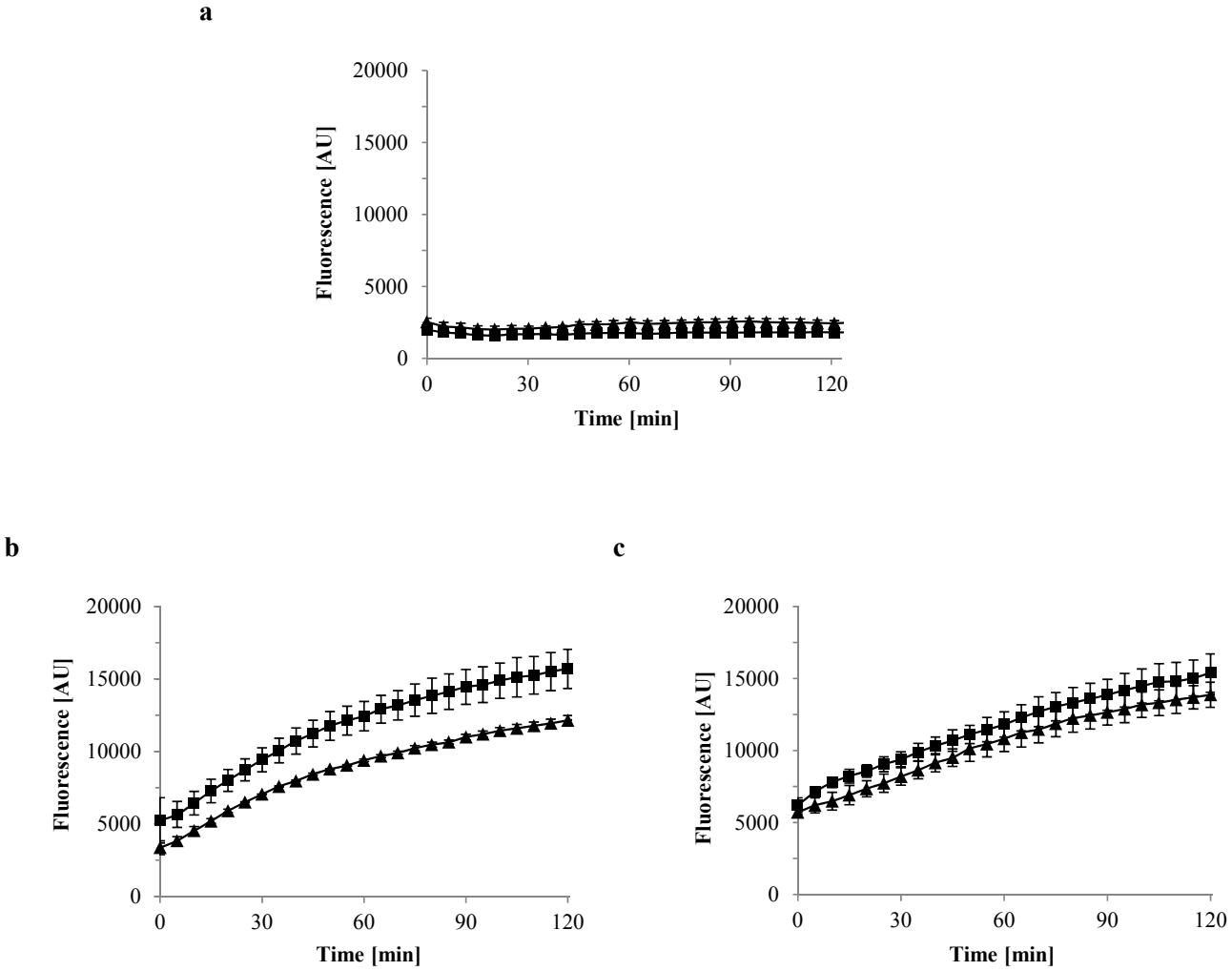

Fig. 4. Influx of Nile Red in cells of *C. defragrans* 65Phen grown on acetate (10 mM) in cometabolism with limonene (3 mM) (wild-type: ▲; Δ*ameABCD*: ■). Nile Red (2 µM) was added directly to the cells (a) or together with 2 µM of the proton-gradient uncoupling agent carbonyl-cyanide *m*-chlorophenylhydrazone (CCCP) (b). The combined effect of CCCP and the RND pump inhibitor phe-arg β-naphthylamide (PAβN, 38.5 µM) is also shown (c). The influx of Nile Red was followed by measuring fluorescence intensity (excitation: 552 nm; emission 636 nm).

Real-time efflux experiments typically require the re-energization of CCCP-treated cells loaded with Nile Red using a readily fermentable substrate such as glucose (Bohnert *et al*. 2010; Paixao *et al*. 2009). In non-fermenting bacteria dye efflux is generally inferred from measuring intracellular dye accumulation rather than from online efflux measurements (Morita *et al*. 2001; Richmond *et al*. 2013). Nevertheless, as a proof of concept a real-time Nile Red efflux assay was conducted with Nile Red-

preloaded *C. defragrans* wild-type and Δ*ameABCD*. After Nile Red loading and two washing steps, acetate (50 mM) was added to reenergize the cells. The efflux of Nile Red showed almost identical apparent kinetics in both strains (Fig. 5a). Acetate addition had no effect, as similar efflux curves were observed in cells to which no acetate was added (data not shown). The decrease in fluorescence may be caused by passive diffusion of Nile Red to the outside of the cells or by reactivation of transporters after the removal of the protonophore. We used the addition of PAβN to wild-type and Δ*ameABCD* cells to verify the involvement of active exporter. The Nile Red efflux was reduced (Fig. 5b), suggesting the involvement of RND pumps in the diffusion process. The obligate-respiring *C. defragrans* react slowly in comparison to fermenting bacteria which restore active dye efflux within seconds after glucose addition resulting in the loss of the fluorescent signal within the first 5 minutes of incubation (Blair and Piddock 2016; Bohnert *et al*. 2011; Iyer *et al*. 2015).

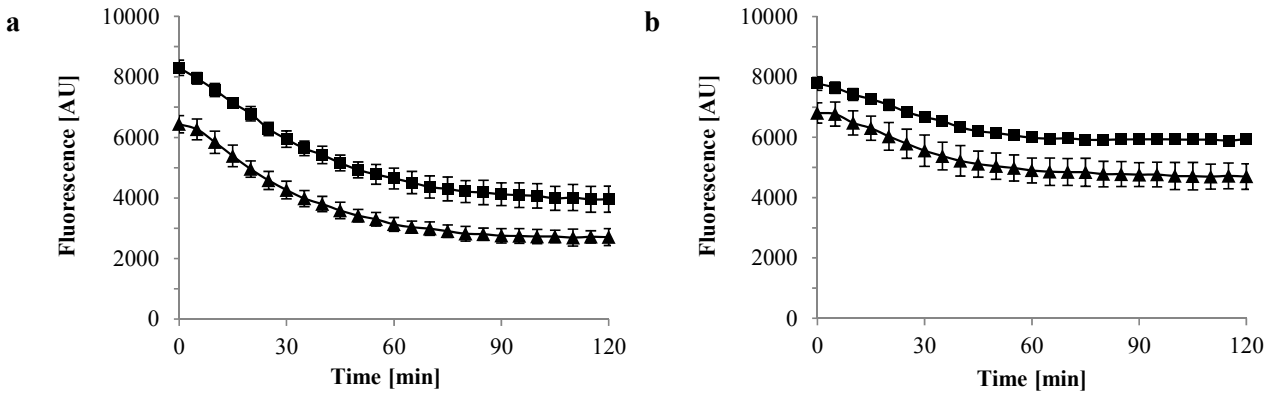

Fig. 5. Nile Red efflux by wild-type (▲) and Δ*ameABCD* (■) strains of *C. defragrans* 65Phen. Bacterial cells were preloaded with 2 µM Nile Red in the presence of CCCP (2 µM) at 28°C under constant shaking (120 rpm) for 2 hours. After two washing steps, the cells were reenergized with 50 mM acetate and fluorescence was recorded (a). The effect of 38.5 µM of PAβN on reenergized cells was tested (b).

In silico analysis of RND efflux transporters in C. defragrans.

The genome of *C. defragrans* contains 9 putative RND pumps. Seven of them (CDM22941, CDM23198, CDM23199, CDM24125, CDM24282, CDM24412 and CDM25333) affiliate to the HAE1 family, the most studied group of RND transporters. HAE1 transporters associate with

periplasmic and outer membrane proteins and mostly confer tolerance to xenobiotics in clinical and environmental isolates (Blanco *et al*. 2016; Tseng *et al*. 1999).

Another transporter found in *C. defragrans* (CDM25549) belongs to the SecDF family, a group of chaperon transporters that participate in the export of proteins across the inner membrane (Tsukazaki and Nureki 2011). The ninth protein, AmeD (CDM25262), affiliates with the HAE3 family, a family of mainly uncharacterized transporters.

This putative transporter and its accompanying proteins (AmeABC) were up-regulated in the proteome of α-phellandrene-grown *C. defragrans* (Petasch *et al*. 2014) and therefore subjected to identity and similarity searches. The closest homologs for the cluster AmeABCD were the hypothetical proteins EPZ15054, EPZ15055, EPZ15056 and EPZ15057 from *Thauera terpenica* 58Eu^T with sequence identities ranging between 61 and 80%. Similar to *C. defragrans*, *T. terpenica* 58Eu^T is able to anaerobically mineralize a wide range of monocyclic and bicyclic monoterpenes (Foss and Harder 1998).

AmeA (CDM25259) is a protein of 605 amino acid residues. It consists of an N-terminal signal peptide and a large conserved domain of unknown function (DUF1302). Its predicted localization as an outer membrane protein concurs with its structural homology with the adhesin/invasin OpcA (PDB: 2VDF). OpcA is an integral outer membrane protein which acts as virulence factor in *Neisseria meningitidis* by promoting bacterial adhesion to endothelial cells (Cherezov *et al*. 2008; Moore *et al*. 2005). The second up-regulated protein -AmeB- (CDM25260, 451 aa) was predicted as periplasmic and affiliated to the LolA superfamily (DUF1329). Although the crystal structure of several proteins within this superfamily has been resolved (e.g. PDB: 4Z48, 3BK5 and 3BUU), their function in the periplasm remains unknown. Nonetheless, DUF1329 proteins share structural features with the periplasmic chaperone LolA which shuttles the translocation of lipoproteins from the inner to the outer membrane in Gram-negative bacteria (Takeda *et al*. 2003). Protein AmeB has been shown to be essential for growth on monoterpenes since a transposon insertion within *ameB* resulted in reduced growth on limonene, myrcene and perillic acid (Petasch *et al*. 2014). Protein AmeC (CDM25261, 316 aa) affiliates to the COG4447, a group of proteins related to stability and assembly factors of the photosystem II in plants. AmeC is also predicted as a periplasmic protein and hence is likely involved

in the assembly of the RND transporter complex. Lastly, protein AmeD (CDM25262, 787 aa) belongs to the RND efflux transporter superfamily and affiliates with the hydrophobe/amphiphile efflux-3 family (HAE3) (COG1033). The 12 transmembrane-spanning regions (TMS) and 2 periplasmic loops (located between TMS 1 and 2 and between TMS 7 and 8) conserved among all RND efflux pumps were predicted from the amino acid sequence (Fig. S3) (Paulsen *et al*. 1996; Tseng *et al*. 1999). In a phylogenetic reconstruction with sequences from RND transporter families HAE1, HAE2 and HAE3, AmeD and its closest homologs clustered in a distinct lineage within the HAE3 branch (Fig. 6). To date, the only characterized representatives from HAE3 are two closely related hopanoid transporters (HpnN) from *Rhodopseudomonas palustris* TIE-1 and *Burkholderia multivorans* (Fig. 6) (Doughty *et al*. 2011; Kumar *et al*. 2017). In both organisms, HpnN catalyzes the translocation of hopanoids from the inner membrane to the periplasm without the need for association or co-transcription with periplasmic proteins or outer membrane channels. Conversely, all members in the AmeD lineage are encoded within gene cassettes containing outer- and inner-membrane proteins homologous to AmeA and AmeD, respectively, and two periplasmic proteins homologous to AmeB and AmeC. This predicted subunit composition and architecture resembles some of the RND transporters of the HAE1 family thus far described in Gram-negative bacteria (Daury *et al*. 2016).

Although most HAE1 transporter complexes are composed of three proteins, a few examples for the requirement of a fourth protein are known. The transporter systems CusCFBA and TriABC-OpmH both require two periplasmic proteins to catalyze the efflux of heavy metals (i.e. Cu^{+} and Ag^{+}) and the antimicrobial triclosan, respectively (Delmar *et al*. 2014; Mima *et al*. 2007). The role of the forth protein is rather diverse: while CusF acts as a soluble periplasmic metal-binding protein in *E. coli* (Delmar *et al*. 2015), both TriA and TriB act as a membrane fusion proteins (MFP) coupling the RND pump TriC to the outer channel protein OpmH in *Pseudomonas aeruginosa* (Ntreh *et al*. 2016; Weeks *et al*. 2015). Additional systems such as the MuxABC-OpmB and AcrABZ-TolC also require a forth protein which locates in the inner membrane and in the cytoplasm, respectively (Mima *et al*. 2009; Wang *et al*. 2017). In our case, the roles of AmeB and AmeC cannot be predicted unequivocally. Nonetheless, the affiliation of both proteins with periplasmic chaperons suggests their participation in the assembly and stability of the RND complex and hence both may act as MFP.

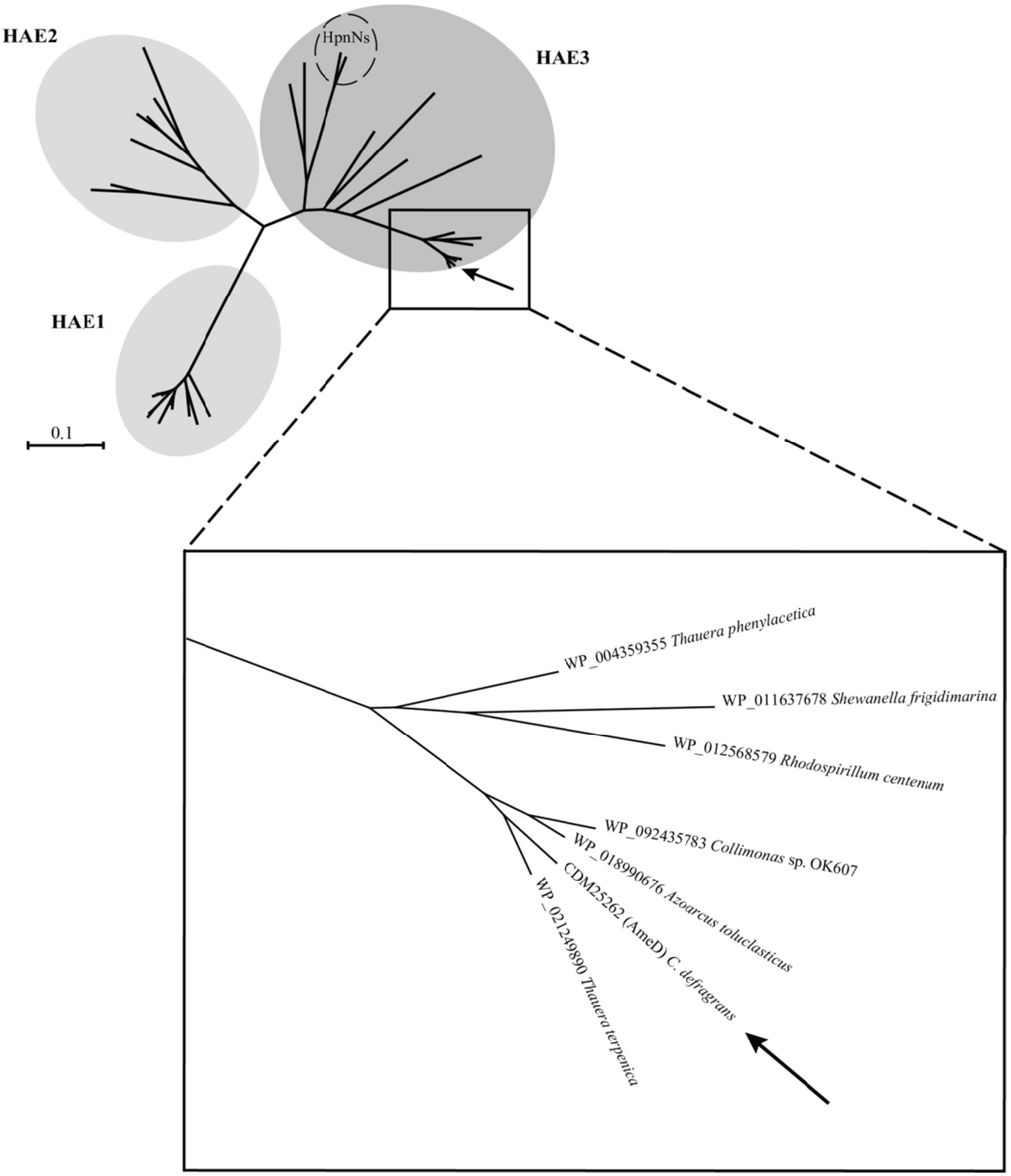

Fig. 6. Unrooted phylogenetic tree of representatives from the RND families HAE1, HAE2 and HAE3. AmeD (arrow) and its closest homologs clustered in a distinct branch within HAE3 (square). RND hopanoid transporters (HpnN) from *Rhodopseudomonas palustris* TIE-1 and *Burkholderia multivorans* are indicated within the dashed circle. Enlarged area displays the sequences most closely related to AmeD within the HAE3 family. Proteins sequences of each HAE family were aligned using MAFFT (Katoh *et al*. 2017). A maximum likelihood tree was calculated with MEGA 7 (Kumar *et al*. 2016) and visualized with Archaeopteryx 0.9921 beta (Han and Zmasek 2009).

Conclusion

In this study, the role of the putative RND transporter complex AmeABCD in monoterpene growth of *Castellaniella defragrans* was investigated. The results showed reduced biomass yield in an *ameABCD* deletion mutant growing on non-functionalized monoterpenes as sole carbon sources. The addition of acetate as cometabolic substrate increased significantly the tolerance of the deletion mutant towards limonene. Deletion of *ameABCD* resulted also in higher net influx of Nile Red into CCCP-treated *C. defragrans*, suggesting the participation of the RND transporter in dye efflux in the wild-type cells. AmeD is affiliated to a lineage of RND transporters within the HAE3 family that unlike other HAE3 members associate with two periplasmic proteins and one outer membrane channel to export to the extracellular space analogous to RND transporters of the HAE1 family. It is still unclear whether AmeB and AmeC act both as periplasmic membrane fusion proteins. Their homology to chaperones and assembly factors grant both proteins with potential for facilitating protein-protein interactions and the assembly of the RND complex. The inducible proteins AmeABCD provide *C. defragrans* with tolerance against the toxic monoterpene substrates that it naturally uses as carbon and energy sources.

Conflict of Interest

The authors declare that they have no conflict of interest.

Acknowledgements

We thank Jan Petasch for the construction of deletion mutant. E.P.C. was supported by a grant from the DAAD in Germany and from the Corporación para la Investigación de la Corrosión and COLCIENCIAS in Colombia. This study was funded by the Max Planck-Society.

References

Abrahim D, Francischini AC, Pergo EM, Kelmer-Bracht AM, Ishii-Iwamoto EL (2003) Effects of α-pinene on the mitochondrial respiration of maize seedlings. Plant Physiol Bioch 41:985-991

Altschul SF, Gish W, Miller W, Myers EW, Lipman DJ (1990) Basic local alignment search tool. J Mol Biol 215:403-410

Bicas JL, Fontanille P, Pastore GM, Larroche C (2008) Characterization of monoterpene biotransformation in two pseudomonads. J Appl Microbiol 105:1991-2001

Blair JMA, Piddock LJV (2016) How to measure export via bacterial multidrug resistance efflux pumps. MBio 7: e00840-16

Blanco P *et al*. (2016) Bacterial multidrug efflux pumps: much more than antibiotic resistance determinants. Microorganisms 4:14-32

Bohnert JA, Karamian B, Nikaido H (2010) Optimized Nile Red efflux assay of AcrAB-TolC multidrug efflux system shows competition between substrates. Antimicrob Agents Chemother 54:3770-3775

Bohnert JA, Schuster S, Szymaniak-Vits M, Kern WV (2011) Determination of real-time efflux phenotypes in *Escherichia coli* AcrB binding pocket phenylalanine mutants using a 1,2'-dinaphthylamine efflux assay. Plos One 6:e21196

Brennan TCR, Turner CD, Kromer JO, Nielsen LK (2012) Alleviating monoterpene toxicity using a two-phase extractive fermentation for the bioproduction of jet fuel mixtures in *Saccharomyces cerevisiae*. Biotechnol Bioeng 109:2513-2522

Cherezov V, Liu W, Derrick JP, Luan B, Aksimentiev A, Katritch V, Caffrey M (2008) *In meso* crystal structure and docking simulations suggest an alternative proteoglycan binding site in the OpcA outer membrane adhesin. Proteins 71:24-34

Daury L, Orange F, Taveau JC, Verchère A, Monlezun L, Gounou C, Marreddy RK, Picard M, Broutin I, Pos KM, Lambert O (2016) Tripartite assembly of RND multidrug efflux pumps. Nat Commun 7:10731-10738

Delmar JA, Su CC, Yu EW (2014) Bacterial multidrug efflux transporters. Annu Rev Biophys 43:93-117

Delmar JA, Su CC, Yu EW (2015) Heavy metal transport by the CusCFBA efflux system. Protein Sci 24:1720-1736

Doughty DM, Coleman ML, Hunter RC, Sessions AL, Summons RE, Newman DK (2011) The RND-family transporter, HpnN, is required for hopanoid localization to the outer membrane of *Rhodopseudomonas palustris* TIE-1. Proc Natl Acad Sci USA 108:1045-1051

Dunlop MJ *et al*. (2011) Engineering microbial biofuel tolerance and export using efflux pumps. Mol Syst Biol 7:487-493

Eswaran J, Koronakis E, Higgins MK, Hughes C, Koronakis V (2004) Three's company: component structures bring a closer view of tripartite drug efflux pumps. Curr Opin Struct Biol 14:741-747

Fichan I, Larroche C, Gros JB (1999) Water solubility, vapor pressure, and activity coefficients of terpenes and terpenoids. J Chem Eng Data 44:56-62

Finn RD, Attwood TK, Babbitt TC, Bateman A, Bork P, Bridge AJ, Chang H, Dosztányi Z, El-Gebali S, Fraser M, Gough J, Haft D, Holliday GL, Huang H, Huang X, Letunic I, Lopez R, Lu S, Marchler-Bauer A, Mi H, Mistry J, Natale DA, Necci M, Nuka G, Orengo CA, Park Y, Pesseat S, Piovesan D, Potter SC, Rawlings ND, Redaschi N, Richardson L, Rivoire C, Sangrador-Vegas A, Sigrist C, Sillitoe I, Smithers B, Squizzato S, Sutton G, Thanki N, Thomas PD, Tosatto SC, Wu CH, Xenarios I, Yeh LS, Young SY, Mitchell AL (2017) InterPro in 2017-beyond protein family and domain annotations. Nucleic Acids Res 45:190-199

Foo JL, Leong SS (2013) Directed evolution of an *E. coli* inner membrane transporter for improved efflux of biofuel molecules. Biotechnol Biofuels 6:81-92

Foss S, Harder J (1998) *Thauera linaloolentis* sp. nov. and *Thauera terpenica* sp. nov., isolated on oxygen-containing monoterpenes (linalool, menthol, and eucalyptol) and nitrate. Syst Appl Microbiol 21:365-373

Foss S, Heyen U, Harder J (1998) *Alcaligenes defragrans* sp. nov., description of four strains isolated on alkenoic monoterpenes ((+)-menthene, alpha-pinene, 2-carene, and alpha-phellandrene) and nitrate. Syst Appl Microbiol 21:237-244

Garcia V, Godoy P, Daniels C, Hurtado A, Ramos JL, Segura A (2010) Functional analysis of new transporters involved in stress tolerance in *Pseudomonas putida* DOT-T1E. Environ Microbiol Rep 2:389-395

Griffin S, Wyllie SG, Markham J (1999) Determination of octanol-water partition coefficient for terpenoids using reversed-phase high-performance liquid chromatography. J Chromatogr A 864:221-228

Han MV, Zmasek CM (2009) phyloXML: XML for evolutionary biology and comparative genomics. BMC Bioinformatics 10:356-361

Harder J, Marmulla R (2017) Catabolic pathways and enzymes involved in the anaerobic degradation of terpenes. In: Boll M (ed) Anaerobic utilization of hydrocarbons, oils, and lipids. Springer International Publishing, Cham, pp 1-15

Heyen U (1999) Der anaerobe Abbau von Monoterpenen durch das Betaproteobakterium *Alcaligenes defragrans*. Dissertation. University Bremen.

Iyer R, Ferrari A, Rijnbrand R, Erwin AL (2015) A fluorescent microplate assay quantifies bacterial efflux and demonstrates two distinct compound binding sites in AcrB. Antimicrob Agents Chemother 59:2388-2397

Katoh K, Rozewicki J, Yamada KD (2017) MAFFT online service: multiple sequence alignment, interactive sequence choice and visualization. Brief Bioinform bbx108

Kelley LA, Mezulis S, Yates CM, Wass MN, Sternberg MJ (2015) The Phyre2 web portal for protein modeling, prediction and analysis. Nat Protoc 10:845-858

Kieboom J, Dennis JJ, de Bont JA, Zylstra GJ (1998) Identification and molecular characterization of an efflux pump involved in *Pseudomonas putida* S12 solvent tolerance. J Biol Chem 273:85-91

Krogh A, Larsson B, von Heijne G, Sonnhammer EL (2001) Predicting transmembrane protein topology with a hidden Markov model: application to complete genomes. J Mol Biol 305:567-580

Kumar N, Su CC, Chou TH, Radhakrishnan A, Delmar JA, Rajashankar KR, Yu EW (2017) Crystal structures of the *Burkholderia multivorans* hopanoid transporter HpnN. Proc Natl Acad Sci USA 114:6557-6562

Kumar S, Stecher G, Tamura K (2016) MEGA7: Molecular evolutionary genetics analysis version 7.0 for bigger datasets. Mol Biol Evol 33:1870-1874

Lüddeke F, Dikfidan A, Harder J (2012) Physiology of deletion mutants in the anaerobic beta-myrcene degradation pathway in *Castellaniella defragrans*. BMC Microbiol 12:192-202

Mahmoud SS, Croteau RB (2002) Strategies for transgenic manipulation of monoterpene biosynthesis in plants. Trends Plant Sci 7:366-373

Marchler-Bauer A *et al*. (2017) CDD/SPARCLE: functional classification of proteins via subfamily domain architectures. Nucleic Acids Res 45:200-203

Mima T, Joshi S, Gomez-Escalada M, Schweizer HP (2007) Identification and characterization of TriABC-OpmH, a triclosan efflux pump of *Pseudomonas aeruginosa* requiring two membrane fusion proteins. J Bacteriol 189:7600-7609

Mima T, Kohira N, Li Y, Sekiya H, Ogawa W, Kuroda T, Tsuchiya T (2009) Gene cloning and characteristics of the RND-type multidrug efflux pump MuxABC-OpmB possessing two RND components in *Pseudomonas aeruginosa*. Microbiol 155:3509-3517

Moore J, Bailey SES, Benmechernene Z, Tzitzilonis C, Griffiths NJE, Virji M, Derrick JP (2005) Recognition of saccharides by the OpcA, OpaD, and OpaB outer membrane proteins from *Neisseria meningitidis*. J Biol Chem 280:31489-31497

Morita Y, Komori Y, Mima T, Kuroda T, Mizushima T, Tsuchiya T (2001) Construction of a series of mutants lacking all of the four major *mex* operons for multidrug efflux pumps or possessing each one of the operons from *Pseudomonas aeruginosa* PAO1: MexCD-OprJ is an inducible pump. FEMS Microbiol Lett 202:139-143

Nielsen H (2017) Predicting Secretory Proteins with SignalP. Methods Mol Biol 1611:59-73

Nikaido H (2011) Structure and mechanism of RND-type multidrug efflux pumps. Adv Enzymol Relat Areas Mol Biol 77:1-60

Ntreh AT, Weeks JW, Nickels LM, Zgurskaya HI (2016) Opening the channel: the two functional interfaces of *Pseudomonas aeruginosa* OpmH with the triclosan efflux pump TriABC. J Bacteriol 198:3176-3185

Overbeek R, Olson R, Pusch GD, Olsen GJ, Davis JJ, Disz T, Edwards RA, Gerdes S, Parrello B, Shukla M, Vonstein V, Wattam AR, Xia F, Stevens R (2014) The SEED and the Rapid Annotation of microbial genomes using Subsystems Technology (RAST): Nucleic Acids Res 42:206-214

Paixao L; Rodrigues L, Couto I, Martins M, Fernandes P, de Carvalho CC, Monteiro GA, Sansonetty F, Amaral L, Viveiros M (2009) Fluorometric determination of ethidium bromide efflux kinetics in *Escherichia coli*. J Biol Eng 3:18-30

Papadopoulos CJ, Carson CF, Chang BJ, Riley TV (2008) Role of the MexAB-OprM efflux pump of *Pseudomonas aeruginosa* in tolerance to tea tree (*Melaleuca altenifolia*) oil and its monoterpene components terpinen-4-ol, 1,8-cineole, and alpha-terpineol. Appl Environ Microbiol 74:1932-1935

Paulsen IT, Brown MH, Skurray RA (1996) Proton-dependent multidrug efflux systems. Microbiol Rev 60:575-608

Petasch J, Disch EM, Markert S, Becher D, Schweder T, Hüttel B, Reinhardt R, Harder J (2014) The oxygen-independent metabolism of cyclic monoterpenes in *Castellaniella defragrans* 65Phen BMC microbiology 14:164-176

Ramos JL, Duque E, Gallegos MT, Godoy P, Ramos-Gonzalez MI, Rojas A, Teran W, Segura A (2002) Mechanisms of solvent tolerance in Gram-negative bacteria. Annu Rev Microbiol 56:743-768

Richmond GE, Chua KL, Piddock LJV (2013) Efflux in *Acinetobacter baumannii* can be determined by measuring accumulation of H33342 (bis-benzamide). J Antimicrob Chemoth 68:1594-1600

Saier MH, Jr., Reddy VS, Tsu BV, Ahmed MS, Li C, Moreno-Hagelsieb G (2016) The Transporter Classification Database (TCDB): recent advances. Nucleic Acids Res 44:372-379

Segura A, Molina L, Fillet S, Krell T, Bernal P, Munoz-Rojas J, Ramos JL (2012) Solvent tolerance in Gram-negative bacteria. Curr Opin Biotechnol 23:415-421

Sikkema J, Debont JAM, Poolman B (1995) Mechanisms of membrane toxicity of hydrocarbons. Microbiol Rev 59:201-222

Sonnhammer EL, von Heijne G, Krogh A (1998) A hidden Markov model for predicting transmembrane helices in protein sequences. Proc Int Conf Intel Sys Mol Biol 6:175-182

Soto SM (2013) Role of efflux pumps in the antibiotic resistance of bacteria embedded in a biofilm. Virulence 4:223-229

Spyropoulos IC, Liakopoulos TD, Bagos PG, Hamodrakas SJ (2004) TMRPres2D: high quality visual representation of transmembrane protein models. Bioinformatics 20:3258-3260

Takeda K, Miyatake H, Yokota N, Matsuyama S, Tokuda H, Miki K (2003) Crystal structures of bacterial lipoprotein localization factors, LolA and LolB. EMBO J 22:3199-3209

Tseng TT, Gratwick KS, Kollman J, Park D, Nies DH, Goffeau A, Saier MH, Jr. (1999) The RND permease superfamily: an ancient, ubiquitous and diverse family that includes human disease and development proteins. J Mol Microbiol Biotechnol 1:107-125

Tsukazaki T, Nureki O (2011) The mechanism of protein export enhancement by the SecDF membrane component. Biophysics 7:129-133

Ultee A, Kets EPW, Alberda M, Hoekstra FA, Smid EJ (2000) Adaptation of the food-borne pathogen *Bacillus cereus* to carvacrol. Arch Microbiol 174:233-238

Uribe S, Alvarez R, Pena A (1984) Effects of beta-pinene, a nonsubstituted monoterpene, on rat-liver mitochondria pestic. Biochem Phys 22:43-50

Wang Z , Fan G, Hryc CF, Blaza JN, Serysheva II, Schmid MF, Chiu W, Luisi BF, Du D (2017) An allosteric transport mechanism for the AcrAB-TolC multidrug efflux pump. eLife 6:e24905

Weeks JW, Nickels LM, Ntreh AT, Zgurskaya HI (2015) Non-equivalent roles of two periplasmic subunits in the function and assembly of triclosan pump TriABC from *Pseudomonas aeruginosa*. Mol Microbiol 98:343-356

Yu NY, Wagner JR, Laird MR, Melli G, Rey S, Lo R, Dao P, Sahinalp SC, Ester M, Foster LJ, Brinkman FS (2010) PSORTb 3.0: improved protein subcellular localization prediction with refined localization subcategories and predictive capabilities for all prokaryotes. Bioinformatics 26:1608-1615.

Supplementary material

An RND transporter in the monoterpene metabolism of *Castellaniella defragrans*

Edinson Puentes-Cala, Jens Harder*

Dept. of Microbiology, Max Planck Institute for Marine Microbiology, Bremen

*To whom correspondence should be addressed: Jens Harder, Dept. of Microbiology, Max Planck Institute for Marine Microbiology, Celsiusstr. 1, D-28359 Bremen, Germany, Tel.: +49 421 2028-750; Fax: +49 421 2028-790; e-mail: jharder@mpi-bremen.de

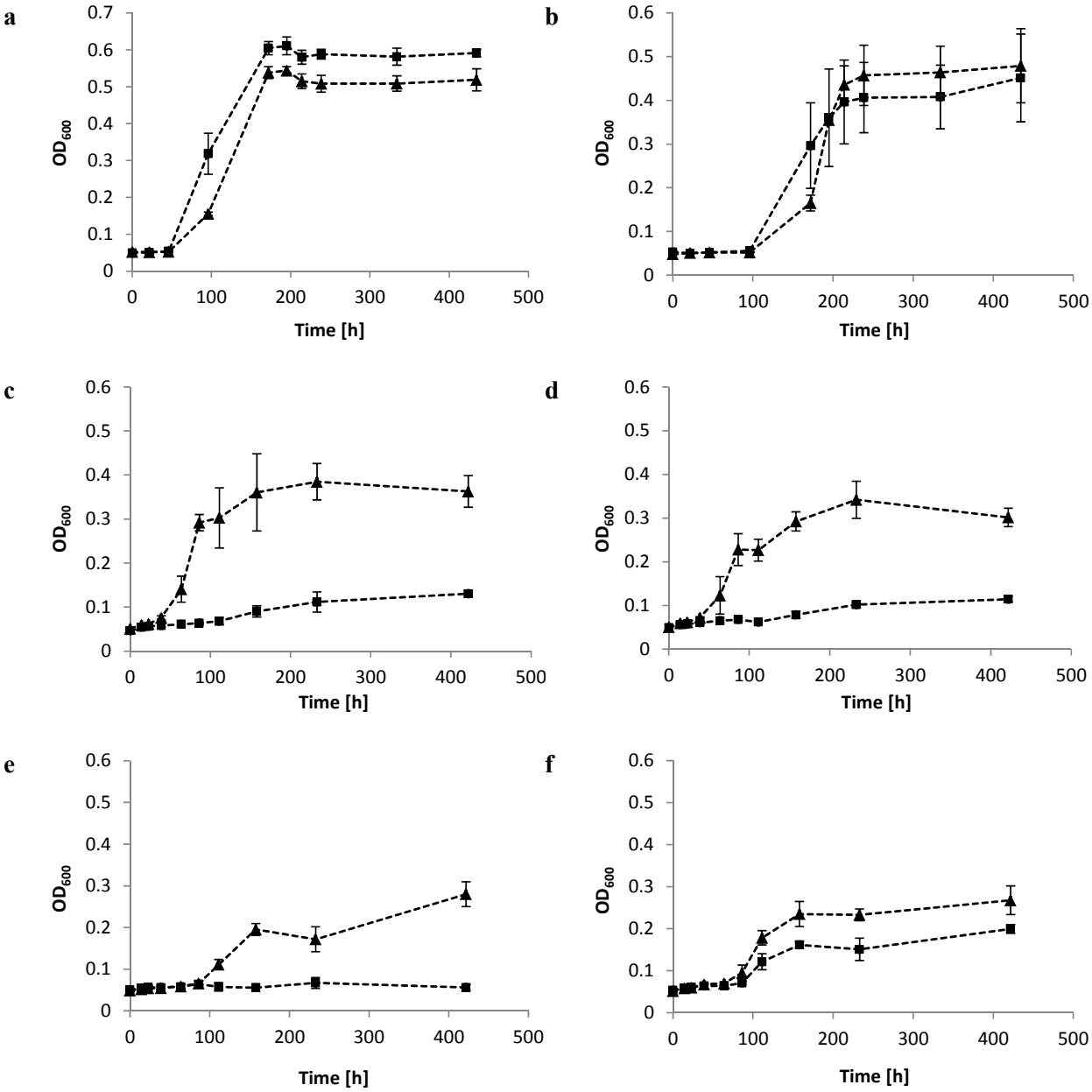

Fig. S1. Bacterial growth of wild-type (▲) and Δ*ameABCD* (■) strains of *C. defragrans* 65Phen on perillyl aldehyde (a), perillic acid (b), α-terpinene (c), terpinolene (d), sabinene (e) and myrcene (f). Acetate was added to a concentration of 20 mM. Monoterpenes were added in a carrier phase (HMN) to a final concentration of 3 mM.

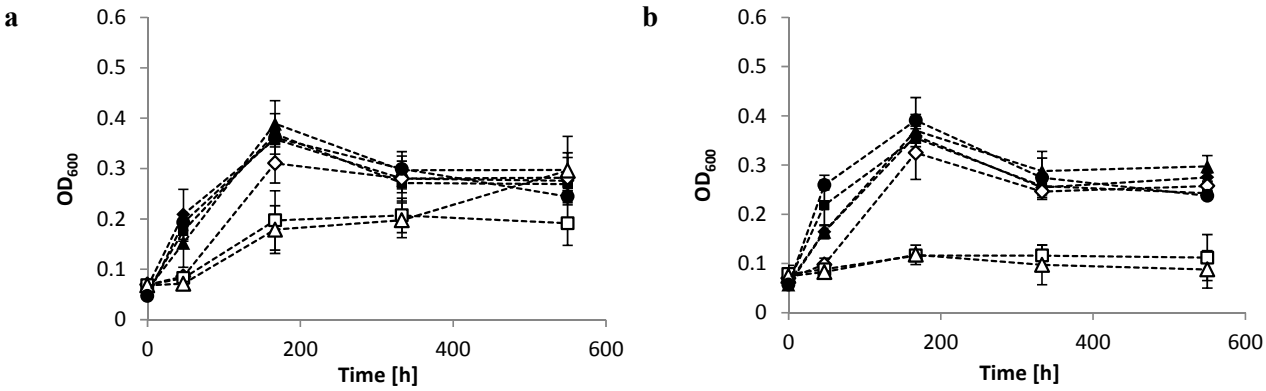

Fig. S2. Growth of wild-type (a) and Δ*ameABCD* (b) *C. defragrans* 65Phen in acetate in cometabolism with various concentrations of limonene: 0 mM [●], 0.62 mM [♦], 1.25 mM [■], 2.5 mM [▲], 5 mM [◊], 10 mM [□], 20 mM [Δ]. To enhance mass transfer limonene was predissolved in DMSO.

a

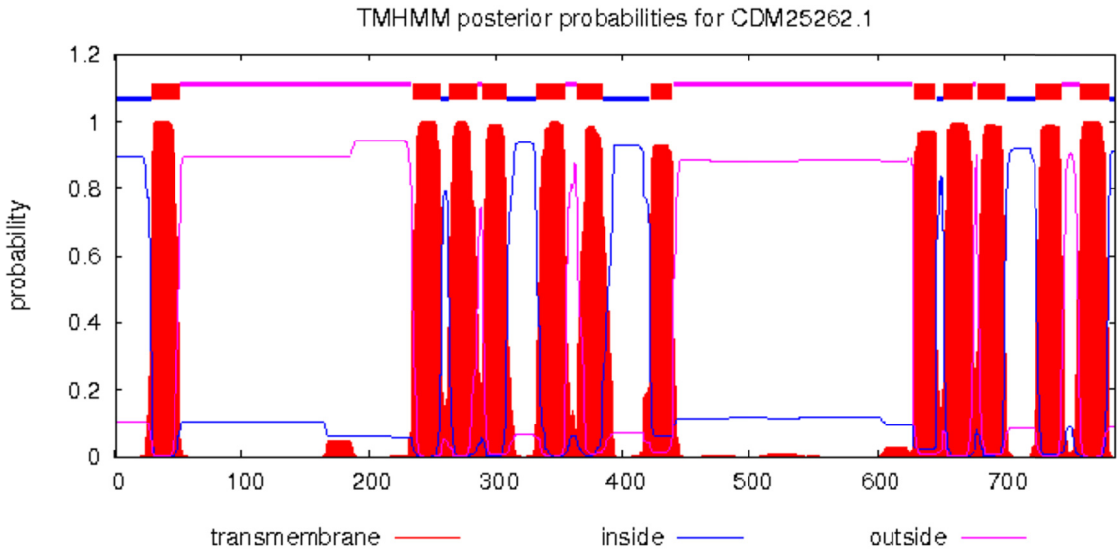

b

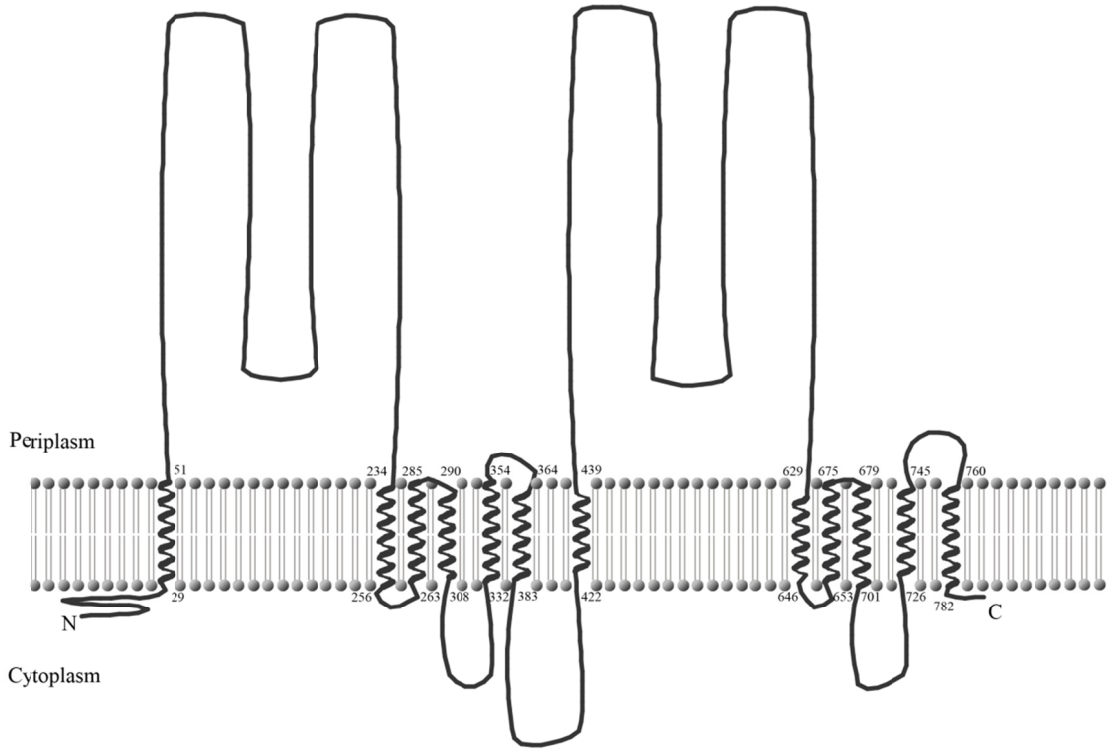

Fig. S3. Transmembrane-spanning regions predicted in AmeD using TMHHM ver. 2.0 (Sonnhammer *et al.* 1998) (a) and visualized by TMRPres2D ver 0.93 (Spyropoulos *et al.* 2004) (b).

Chapter VI: Discussion and outlook

Castellaniella defragrans 65Phen mineralizes more than a dozen monoterpene compounds under anaerobic denitrifying conditions (Foss *et al*. 1998). For this reason *C. defragrans* has become a model organism to study anaerobic monoterpene degradation. During the course of this doctoral thesis I searched for novel degradation pathways that explain *C. defragrans'* metabolic versatility towards monoterpenes. Additionally, I studied what seems to be a major mechanism that allows *C. defragrans* to evade monoterpene toxicity.

6.1 Novel pathways in anaerobic monoterpene degradation

6.1.1 Bicyclic monoterpene metabolism

The evidence presented in **Chapter II** showed that the degradation of the bicyclic monoterpenes α-pinene, 3-carene and sabinene proceeds via the formation of monocyclic intermediates in *C. defragrans* (Puentes-Cala *et al*. 2018). All the intermediates I detected in cultures and enzyme assays support growth of *C. defragrans* (Foss *et al*. 1998). Strikingly, with the exception of α-terpineol and terpinen-4-ol, these monocyclic monoterpene intermediates are all substrates of the limonene dehydrogenase CtmAB, the enzyme characterized in **Chapter III**. The latter explains why the deletion of the *ctmAB* genes prompted the accumulation of monocyclic metabolites in cultures grown cometabolically on acetate and bicyclic monoterpenes (Puentes-Cala *et al*. 2018). The apparent link between the bicyclic and the monocyclic monoterpene metabolism was further confirmed by proteomics analysis and by the phenotype of transposon insertion mutants which showed the need for the monocyclic monoterpene degradation pathway for growth on bicyclic monoterpenes.

The decyclization reactions required for chemically synthesizing monocyclic compounds from bicyclic monoterpenes requires the transformation of a ring equivalent into an alkene bond or a

functional group. These processes almost invariably involve the formation of transient carbocation intermediates (Traas 1982; Yoo and Day 2002). Typically, electrophilic reagents attack the allylic double bond present in the bicyclic monoterpene. The nascent cationic charge may migrate within the cyclohexane ring or undergo Wagner–Meerwein rearrangements forming monocyclic products or new bicyclic derivatives, respectively (Arbuzov and Isaeva 1976; Banthorpe and Whittaker 1966; Traas 1982). The type of carbocations and products formed relies heavily on the reaction conditions and on the electrophiles and nucleophiles, e.g. water, available for carbocation formation and stabilization, respectively (Gainsford *et al*. 2001). Examples for the chemical modification of bicyclic monoterpenes include the industrial production of valuable alcohols, such as menthol, α- and γ-terpineol and isoborneol from the readily available α- and β-pinene. In biological systems the conditions of such decyclization reactions are controlled at the active sites of specialized enzymes which determine the formation and fate of reaction intermediates. In *Castellaniella defragrans* the products of bicyclic monoterpene decyclization were limited to α- and γ-terpinene, limonene, terpinolene, α-terpineol and terpinen-4-ol, which all act as substrates for bacterial growth.

We observed that the *in vitro* biotransformation of bicyclic monoterpenes was ATP-stimulated and irreversibly lost upon separation into soluble and membrane fractions by ultracentrifugation. The latter suggests that the enzyme may be a complex between soluble and membrane-bound proteins which were separated by the centrifugal forces. Thus, its purification will require a careful standardization in order to preserve the enzyme's quaternary architecture. The extraction of membrane proteins from the lipid bilayer and the stabilization of hydrophobic regions are commonly carried out with amphiphilic compounds such as Triton X-100 and Tween20, alkyl sugars (e.g. *n*-decyl-β-D-maltoside) and zwitterionic detergents (e.g. lauryldimethylamine-N-oxide) (Arachea *et al*. 2012; Prive 2007). The stabilization in solution of the membrane-bound component of this novel monoterpene decyclase may allow the purification of the complex via protein chromatography. Nevertheless, protein denaturation is not uncommon when using even mild detergents. An alternative approach I propose involves the enrichment of the enzymatic activity by rate-zonal density gradient ultracentrifugation followed by the characterization of the zones with the highest catalytic activity

(Fernandez-Martinez *et al*. 2016; Marmulla 2015). A similar approach has recently been used to enrich a linalool isomerase from *Thauera linaloolentis* 47Lol (Marmulla *et al*. 2016b).

6.1.2 Monoterpene alcohol dehydratases

Systematic studies on the anaerobic monoterpene metabolism of *C. defragrans* led to description of a pathway for the utilization of the acyclic monoterpenes β-myrcene and linalool. The reactions of this pathway are catalyzed by the enzymes linalool dehydratase/isomerase (Ldi) and the geraniol (GeoA) and geranial (GeoB) dehydrogenases (Brodkorb *et al*. 2010; Lüddeke *et al*. 2012b) yielding geranic acid as product (Figure 1). The further degradation of geranic acid was hypothesized to occur via β-oxidation-like reactions in analogy to the acyclic terpene utilization (Atu) pathway of *Pseudomonas* (Förster-Fromme and Jendrossek 2006; Förster-Fromme and Jendrossek 2010). However, such a pathway has not been found in the genome of *C. defragrans* (Petasch *et al*. 2014). Instead, in light of new evidence the formation of geranic acid from linalool seems to be the result of a combination of a detoxification mechanism and unspecific oxidation reactions. The transformation of geraniol into linalool and then into myrcene is catalyzed by Ldi with reaction rates that are three orders of magnitude faster than in the opposite direction (Figure 1) (Brodkorb *et al*. 2010). Hence, it is likely that the thermodynamically favored reactions of the Ldi are envisioned to reduce alcohol concentrations below toxicity levels by producing the less toxic β-myrcene. Alternatively, geraniol concentrations can also be reduced by oxidation to geranial and geranic acid by GeoA and GeoB, respectively (Harder and Marmulla 2017; Lüddeke *et al*. 2012b). These two enzymes have a wide substrate spectrum and have shown to be essential for growth on several monocyclic monoterpenes (Petasch *et al*. 2014). In fact, GeoA showed higher catalytic efficiency for the monocyclic perillyl alcohol than for geraniol (Lüddeke *et al*. 2012b), while in another experiment a *geoB* deletion inhibited growth of *C. defragrans* on perillyl aldehyde (Petasch *et al*. 2014). Interestingly, the Ldi is required for growth of *C. defragrans* on both myrcene and geraniol, but not for growth on linalool (Lüddeke *et al*. 2012a). This suggests the existence of a pathway for linalool metabolism independent of geraniol formation and oxidation.

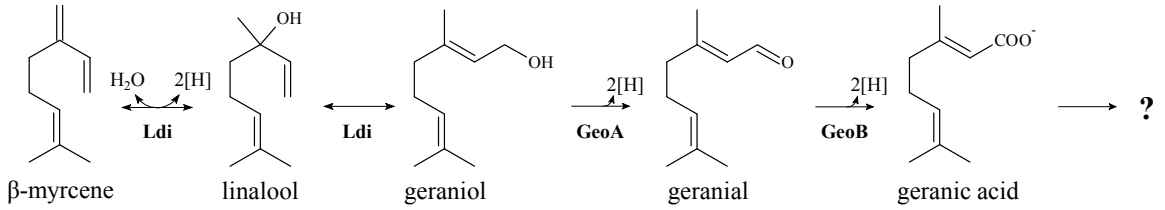

Figure 1. Proposed pathway for β-myrcene degradation in *C. defragrans* 65Phen.

On the other hand, up until now the fate of the monocyclic monoterpene alcohols α-terpineol and terpinen-4-ol in *C. defragrans* had not been investigated. The dehydration of α-terpineol to form terpinolene has been proposed in *Thauera terpenica* and *Pseudomonas aeruginosa* (Hylemon and Harder 1998; Tadasa *et al*. 1976), however, without any supporting biochemical evidence. This motivated us to study the initial transformation on monocyclic monoterpene alcohols in *C. defragrans*.

ATP-dependent biotransformations producing monocyclic monoterpene dienes from linalool, α-terpineol and terpinen-4-ol were observed in soluble protein extracts of *C. defragrans* 65Phen [**Chapter IV**]. The partial purification of the catalytic activities revealed that the fractions active on α-terpineol were also active on terpinen-4-ol but not on linalool. Likewise, the fractions active on linalool were not active on either of the monocyclic alcohols. These observations suggest the discovery of two novel monoterpene alcohol dehydratases in *C. defragrans*. In all cases the reactions yielded α-terpinene and terpinolene as products. These monocyclic monoterpene dienes are substrates of the limonene dehydrogenase CtmAB [**Chapter III**]. This suggests that the mineralization of linalool, α-terpineol and terpinen-4-ol is ultimately achieved via the limonene degradation pathway (Petasch *et al*. 2014).

The two-step purification protocols used in this study to isolate and characterize the alcohol dehydratases successfully enriched both enzymatic activities and allowed to evaluate some of their properties. However, it did not allow the identification of the catalytic proteins. Furthermore, both enzymes lost between 95 to 99% of the total enzymatic activity during purification. Therefore, optimization of the purification protocols is necessary in order to increase both enzyme purity and recovery. Considering that both enzymes preserved some level of catalytic activity after anion exchange chromatography (AEC) (between 4 and 13%), this purification step can be considered for

optimization. During the experimental phase of this project we used the same AEC column, the same binding and elution buffers, and similar purification regimes for both enzymes. Two main variables influence protein separation on AEC: the pH and the salinity of the buffer system. We kept the pH constant while the salinity was gradually increased to elute the bound proteins. Typically, longer salinity gradients yield higher protein purity but lower catalytic activity recovery and vice versa (de Medeiros *et al*. 2012; Luo and Hsu 1997). Thus, I suggest conducting a first AEC run where a step-wise increase of 50 to 100 mM KCl is applied. Here the bulk of accompanying proteins is eliminated while most the catalytic activity will be concentrated in one or two of the fractions collected. In a second AEC run the column is equilibrated at a slightly different pH, the active fraction from the previous run is equilibrated and injected, and finally further fractionation over a salinity gradient is conducted. The variation of pH in the second run will change the net charges of the protein mixtures and increase the probability of protein separation, while the gradual increase in salinity will provide a higher resolution. Alternatively, a cation exchanger can replace one of the AEC runs.

Another possible cause for the loss of catalytic activity during purification may be associated to protein hydrophobicity. Many enzymes active on monoterpenes known to date are highly hydrophobic (Brodkorb *et al*. 2010; Lüddeke *et al*. 2012b; Marmulla 2015). These carry hydrophobic pockets and surface patches that facilitate their interaction with the substrate and with the hydrophobic structures where monoterpenes tend to accumulate (i.e. cellular membranes). In general, hydrophobic proteins tend to aggregate and precipitate out of solution when brought above a threshold concentration or when exposed to kosmotropic ions (Wingfield 2001; Zhang *et al*. 2017). To avoid precipitation the effect of the addition of co-solvents such as glycerol, non-denaturing detergents or amino acids (e.g. arginine) can be tested. This hydrophobicity was evident when hydrophobic interaction chromatography (HIC) was used. The purification of the α-terpineol/terpinen-4-ol dehydratase activity required the use of a butyl sepharose column, since no enzymatic activity was recovered from the more hydrophobic phenyl sepharose. Although the active proteins eluted within the gradient applied to the butyl sepharose, protein precipitation in the hydrophobic environment or tight association to the column material may be the cause for the observed 90% loss in catalytic activity. As for the linalool cyclase which had total activity loss during HIC, the use of a less kosmotropic salt

such as KCl in the binding buffer instead of ammonium sulfate may prevent excessive protein aggregation and/or strong column association.

6.1.3 Limonene dehydrogenase: a central enzyme in the anaerobic monoterpene metabolism

A limonene dehydrogenase activity was purified and characterized from anaerobically-grown *C. defragrans* [**Chapter III**]. The reverse reaction, the reduction of perillyl alcohol to limonene with a thiol as electron donor, was also observed although it does not seem to be the main physiological role of the enzyme. The limonene dehydrogenase is a cytoplasmic heterodimer composed of proteins CtmA and CtmB. These proteins share a 27% amino acid composition and a 41% similarity (Figure 2), and belong to the FAD-dependent oxidoreductases within COG1233. The experimental evidence we gathered suggest that as expressed by *C. defragrans* CtmAB may carry a covalently-bound flavin. Though, the flavinylation site was not detected in mass spectra. Typically, the covalent association between flavins and enzymes raises the mid-redox potential by 50 to 60 mV to a more positive reduction potential which increases the thermodynamic driving force of the reactions catalyzed (Fraaije *et al*. 1999; Heuts *et al*. 2009; Huang *et al*. 2008). There are seven known types of covalent flavinylation: 8α-N3-histidyl–FAD/FMN, 8α-N1-histidyl–FAD/FMN, 8α-O-tyrosyl–FAD, 8α-S-cysteinyl–FAD, 6-S-cysteinyl–FMN, 8α-N1-histidyl-6-S-cysteinyl–FAD/FMN, and phosphoester-threonyl–FMN (Starbird *et al*. 2001). The most abundant covalent flavin attachment is the one in which FAD is bound to a histidine.

The overexpression of CtmA, CtmB and CtmAB in *E. coli* yielded only partially active enzyme due to incorrect folding and incomplete flavinylation. Luckily, the limonene dehydrogenase is highly induced during *C. defragrans*' growth on monoterpenes (Petasch *et al*. 2014). This allowed us to obtain enough purified enzyme from the native host to conduct kinetic experiments. In fact, the level of purity reached with our purification protocol can be used for attempting protein crystallization. Nonetheless, high scale production of CtmAB for eventual biotechnological applications will require setting up a suitable heterologous overexpression platform. Perillyl alcohol, the product of the CtmAB, has a significant market given both its organoleptic and anticarcinogenic properties (Gelb *et al*. 1995; Ma *et al*. 2016; Wagner and Elmadfa 2003; Zafeer *et al*. 2018). Due to its scarcity in nature and its

high demand, perillyl alcohol prices 10 to 100 times higher than other highly valuable monoterpenes such as menthol and carvone (Alonso-Gutierrez *et al*. 2013; Duetz *et al*. 2003). In consequence, an active search for novel (bio)catalysts for perillyl alcohol production is currently underway (Alonso-Gutierrez *et al*. 2013; Immethun *et al*. 2013; Mlodzik *et al*. 2016; van Beilen *et al*. 2005).

```
CtmA      MANPKSEYDVIIVGGGLNGLATGAYLQKAGLSVGIFERRDESGTFCATEEVLFPGVKLNL  60
CtmB      -MSEVKQCDVVVIGAGHNGLTTGAYLARAGAKVLVVERRHETGGALVTEE--FSGFRFNL  57
            .  .: **:::*.* ***:***** :** .* :.***.*:*   .***  * *.::**

CtmA      HASLLV-THFGPAMVDLELEKFGLELCKPAGAEYGYFYPFLDGNAAMFAHYDARKTYEMW  119
CtmB      HATYMMMLDVAPPYKDLGLEADGCVYIRPDVAAS----ILKKDGTAVTLHGDLEKSVESI  113
          **: ::  ...*   ** **  *    :*  *       : ...:*:  * * .*: *

CtmA      QRISPKDAETYRKVANFLGPRQDVILQQALCSKHTDE-----SFL-----QFLDEFSDVP  169
CtmB      RRISPRDAERFREIYLEYKQMSDEYLIPATYGKPVGSAQLAGTYMETELGKKILEVSELT  173
          :****:*** :*::       .*  *  *  .* ...     :::     : : *.*::

CtmA      V--FPKDWLFMSGFEFVENLFEHEQIRVGLLS---SAAMAADDLKSRLAGPLSILAALCG  224
CtmB      PYQICQSWGFET-----------PELGALLLYLICMWGIDPTETNSSYLVPL-----YFN  217
             : :.* * :             :: . **      .:   : :*    **       .

CtmA      FTSNFYTARGGSHDVVHALVRCFVLHGGKIFYNCPVEKIIIEDKKAKGIVLSSISCYPDA  284
CtmB      RMLNATLVRGGSHRLSSTLQKAGILAGMEVMENHEVKRIIMEDGAAVGVEVAPTGTDGPL  277
             *   .***** :  :* :. :* * ::: *  *::**:**  * *: ::  .

CtmA      EFKAGKAVISDLSAQTTFLGLVGEEHLSVSAR---ASLKRYDYRGGTLFTNYYVMNERPD  341
CtmB      IRIDAKSIVTSTDPTTTFGTFISEEEMQQRSKLCLNTARNWEWEHSSLFLCHLGLRKKPR  337
              .*::::. .  ***  ::.**.:.  ::    : :.:::. .:**  :  :.::*

CtmA      FACAQKFPEANNTYSFNFGAETVDQAADLFDRCDVRGVLPDPPVAWGGCANYCIADPTQA  401
CtmB      FKAEDQDPAVQTAFIRVFGVESPEDVVKHFNEVMEGHLLHDI----GHVTFTTDLDPNQA  393
          * . :: * .:.::   **.*: ::... *:.     :* *     *  :     **.**

CtmA      ----PPGMYTVMSWCFVPYKLNSLGGPGAWDDIRESYADKAEEVLVQYLPNLKTAKVARY  457
CtmB      PQETEPGSAVARIEAVVPY----APAQGDWADVAGPYGDRLIAKLAEYMVDFDPADIIRR  449
               **  ..   ..***      . * * *:   *.*:    *.:*: ::. *.: *

CtmA      VNTPHDYVRRNAH-SFGNMHPSGATTEAQMWSWKPFAGCDAPRTPIDSLYICQSMGMS-N  515
CtmB      YQYTPVYIEMKIPQMKRGSFKHGAYVMTQMGYSRPNVQCSSNKTPIKGLYVCGASTFPGG  509
           :    *:. :      . .  ** . :**   :* . *.: :***..**:* :  :  .

CtmA      FTHLGAAYVAASELMGDLGIERPDWWRAKAMDGAKELWRREGVERRTSVD    565
CtmB      MITFGGGYNAAKTVAQDMGL--NIWWTEPDEVIAA---REKGLLL-----    549
          :  :*..* **. :  *:*:    **       *    *.:*:
```

Figure 2. Alignment of the limonene dehydrogenase proteins: CtmA and CtmB. Asterisks "*" below the alignment indicate fully conserved amino acid residues; colon ":" and period "." indicate amino acid substitutions with strongly and weakly conserved properties, respectively. The alignment was prepared with Clustal Omega (Sievers *et al*. 2011).

Similar to CtmAB, other anaerobic hydroxylases, such as those acting on cholesterol, ethylbenzene and *p*-cresol utilize water as source of the hydroxyl moiety (Boll and Heider 2010; Chiang *et al*. 2007; Heider *et al*. 2016). Interestingly, unlike aerobic hydroxylases these enzymes produce, rather than consume, reducing equivalents during hydroxylation (Cunane *et al*. 2005; Hille 2005). The mechanism behind the oxidative-half reactions in anaerobic hydroxylases ranges from two-single electron transfers in molybdenum enzymes (i.e. cholesterol and ethylbenzene hydroxylases)

(Szaleniec *et al*. 2010) to a hydride transfer in the flavocytochrome c enzymes (i.e. *p*-cresol methylhydroxylase) (Cunane *et al*. 2005). The latter has also been proposed as the mechanism for all described phytoene dehydrogenases and the one we hypothesize for CtmAB. The reaction would start by the abstraction of a hydride from the primary methyl group, followed by the transfer onto the oxidized flavin. The resulting carbocation would be then stabilized by water addition and proton transfer yielding perillyl alcohol. The cycle is completed by re-oxidation of the flavin with the supplied ferrocenium ions. The reduction potential of ferrocenium (E°' = +380 mV) by CtmAB coincides with other phytoene dehydrogenases which also utilize *in vitro* electron sinks with high redox potentials, such as oxygen and benzoquinones (Ahn and Kim 2015; Schaub *et al*. 2012). To date, the physiological electron acceptor for CtmAB is not known. However, its co-localization with genes encoding for electron transfer flavoproteins (ETF) (CDM25301 and CDM25302) suggests two single-electron transfers from CtmAB via the ETFs to a flavoprotein:ubiquinone oxidoreductase (CDM23589) (Petasch *et al*. 2014). ETFs are single-electron shuttles essential for the metabolism of fatty acids and amino acids since they transfer the generated reducing equivalents to the respiratory chain (Costas *et al*. 2017; Ghisla and Thorpe 2004; Lehman *et al*. 1990; Thorpe and Kim 1995; Watmough and Frerman 2010).

CtmAB exhibited ferrocenium reducing activity while oxidizing a wide range of monocyclic monoterpenes carrying an allylic methyl group. The substrates included α-terpinene and terpinolene. These two monocyclic dienes are the main catalytic products of linalool, α-terpineol, terpinen-4-ol, α-pinene, 3-carene and sabinene biotransformations occurring in *C. defragrans* [as described in **Chapters II** and **IV]**. The hydroxylation of these monocyclic intermediates by CtmAB, most likely to perillyl alcohol, integrates the metabolism of most if not all acyclic, monocyclic and bicyclic substrates used by *C. defragrans* in a single pathway: the limonene degradation pathway (Figure 3) (Petasch *et al*. 2014). Such premise explains the metabolic plasticity of *C. defragrans* towards monoterpene substrates.

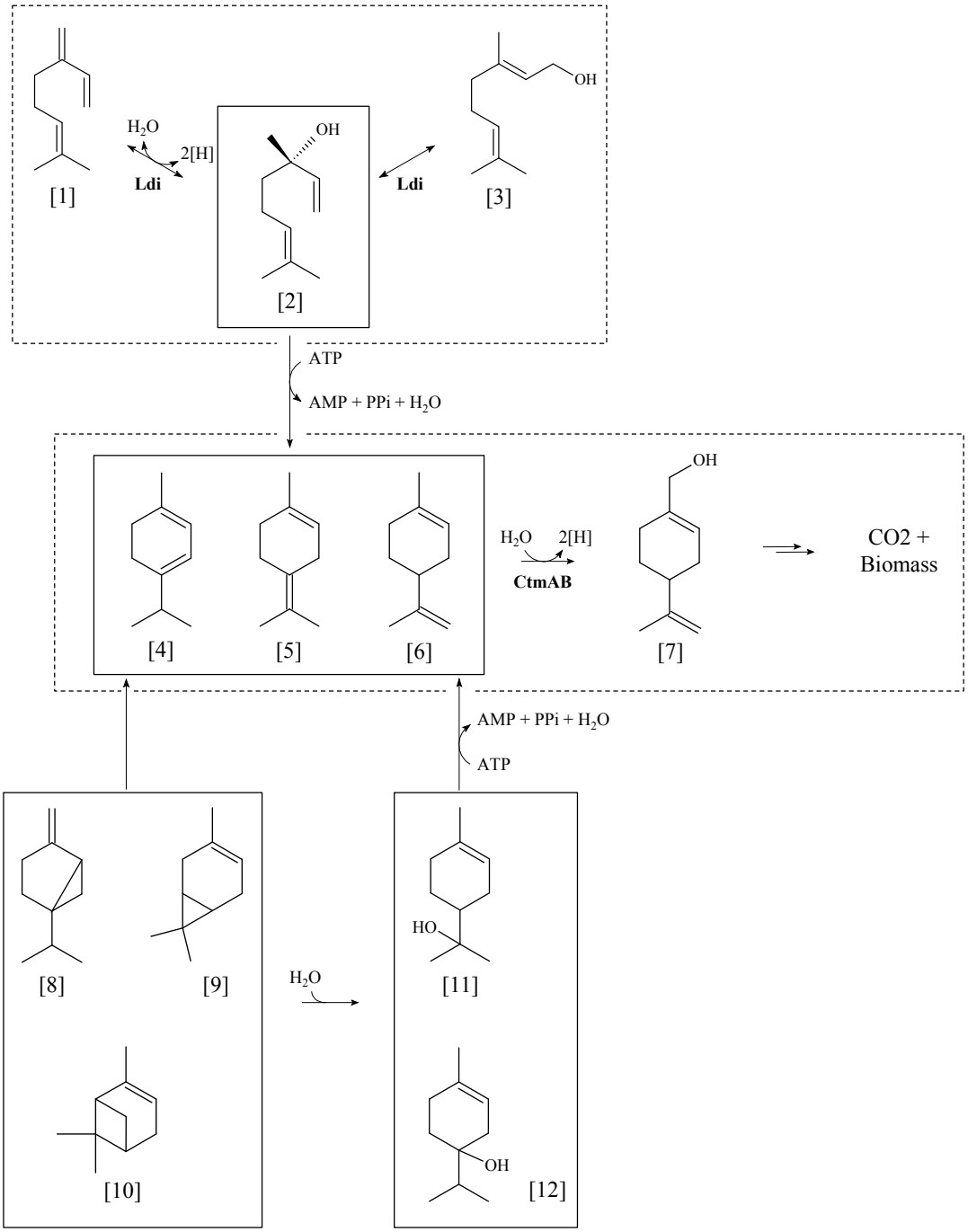

Figure 3. Unified pathway for the metabolism of acyclic, monocyclic and bicyclic monoterpenes in *C. defragrans* 65Phen. Acyclic monoterpenes β-myrcene [1] and geraniol [3] are enantiospecifically transformed into (*S*)-(+)-linalool [2] by the linalool dehydratase/isomerase [Ldi]. Linalool is transformed in an ATP-dependent reaction to the monocyclic monoterpenes α-terpinene [4] and terpinolene [5]. These together with limonene [6] are substrates of the limonene dehydrogenase [CtmAB] which transformed them into perillyl alcohol [7]. The latter is further transformed and mineralized by enzymes encoded in the monoterpene-specialized genomic island and then by enzymes

of the central metabolism. The bicyclic monoterpenes sabinene [8], 3-carene [9] and α-pinene [10] are also transformed into monocyclic monoterpene dienes [4, 5 and 6] either directly or in an ATP-dependent process involving the formation and dehydration of the monocyclic monoterpene alcohol α-terpineol [11] or terpinen-4-ol [12.]

In the recently described pathway, limonene is successively oxidized via perillyl alcohol and perillyl aldehyde to perillic acid (Petasch *et al*. 2014). Then a series of enzymatic steps catalyzed by proteins GeoC and MrcDEF result in the formation of the linear compound 3-isopropenyl-pimelyl-CoA. Up to that point, all enzymes are encoded in a genetic island found in *C. defragrans*' genome (Petasch *et al*. 2014). Seemingly, the aim of the enzymes in the island is to functionalize and utterly prepare the monoterpene substrate for further degradation via β-oxidation and amino acid catabolism. A similar strategy has been proposed for the degradation of the acyclic monoterpenes linalool and citronellol in *Thauera linaloolentis* 47Lol and several *Pseudomonas* strains (Förster-Fromme and Jendrossek 2010; Marmulla *et al*. 2016a). In these organisms, the monoterpenes are oxidized and then broken down in a β-oxidation-like manner to one acetate, two acetyl-CoA units and one methylcrotonyl-CoA (C_5). The latter is further degraded by enzymes of the leucine isovalerate utilization (Liu) pathway (Förster-Fromme *et al*. 2006; Marmulla *et al*. 2016a). So far, evidence for the utilization of the Liu pathway for monoterpene metabolism has not been found in *C. defragrans*, e.g. in the proteomic study of Petasch *et al*. (2014). The reason may be the outcome of the β-oxidation which in *C. defragrans* would purportedly be methacrylyl-CoA (C_4), instead of methylcrotonyl-CoA (C_5) (Petasch *et al*. 2014). Methacrylyl-CoA is oxidized and decarboxylated in the valine degradation pathway to propionyl-CoA, one of the most common products of polyunsaturated fatty acid degradation in bacteria (Luo *et al*. 2014). Finally, propionyl-CoA may be integrated into the central metabolism via the methylcitrate cycle.

6.2 A monoterpene efflux exporter as mechanism of tolerance

In **Chapter II** several transposon insertions within or contiguous to genes predicted as outer membrane components or membrane permeases resulted in defective growth on monoterpenes. The phenotype of such insertions, as it has been pointed out previously, most likely accounts for the

toxicity of the monoterpene substrates (Marmulla *et al*. 2016a; Petasch *et al*. 2014). In **Chapter V** a putative RND efflux complex active on monoterpene substrates was characterized. The expression of proteins from this RND transporter is highly up-regulated in monoterpene-grown *C. defragrans* (Petasch *et al*. 2014; Puentes-Cala *et al*. 2018), while the deletion of genes *ameABCD* affects growth on monoterpene hydrocarbons, but not on oxygen-functionalized monoterpenes. All in all, this inducible RND efflux transporter acts as a line of defense against monoterpene toxicity in *C. defragrans* complementing other detoxification mechanisms known in this organism such as the modification of cell membrane composition and monoterpene biotransformation (Foss *et al*. 1998).

The exact roles of the periplasmic proteins AmeB and AmeC in the complex still need to be clarified. Although it was demonstrated that AmeB is vital for growth of *C. defragrans* on monoterpenes (Petasch *et al*. 2014), its eventual association with AmeC as periplasmic components is unclear. The generation and characterization of deletion mutants lacking *ameB* or *ameC* may help resolve these questions. Also, I suggest the construction of genetic variants of the Δ*ameABCD* mutant for testing monoterpene growth and tolerance, as well as for conducting further Nile Red accumulation experiments. The Δ*ameABCD* mutant can be complemented in *trans* with the individual genes of the transporter. Complementation with plasmids carrying the RND complex with only one of the periplasmic proteins may bring further evidence as to define the role of these in detoxification. Likewise, variants carrying only *ameBCD* (lacking the outer membrane pore) may show whether association with other outer membrane proteins is possible.

References

Ahn JW, Kim KJ (2015) Crystal structure of 1′-OH-carotenoid 3,4-desaturase from *Nonlabens dokdonensis* DSW-6 Enzyme Microb Technol 77:29-37

Alonso-Gutierrez J, Chan R, Batth TS, Adams PD, Keasling JD, Petzold CJ, Lee TS (2013) Metabolic engineering of *Escherichia coli* for limonene and perillyl alcohol production. Metab Eng 19:33-41

Arachea BT, Sun Z, Potente N, Malik R, Isailovic D, Viola RE (2012) Detergent selection for enhanced extraction of membrane proteins. Protein Expr Purif 86:12-20

Arbuzov BA, Isaeva ZG (1976) Molecular-rearrangements in series of carane derivatives. Russ Chem Rev 45:674-683

Banthorpe DV, Whittaker D (1966) Rearrangements of pinane derivatives. Q Rev Chem Soc 20:373-387

Boll M, Heider J (2010) Anaerobic degradation of hydrocarbons: mechanisms of C–H-bond activation in the absence of oxygen. In: Timmis KN (ed) Handbook of hydrocarbon and lipid microbiology. Springer Berlin Heidelberg, Berlin, Heidelberg, pp 1011-1024

Brodkorb D, Gottschall M, Marmulla R, Lüddeke F, Harder J (2010) Linalool dehydratase-isomerase, a bifunctional enzyme in the anaerobic degradation of monoterpenes J Biol Chem 285:30436-30442

Chiang YR, Ismail W, Muller M, Fuchs G (2007) Initial steps in the anoxic metabolism of cholesterol by the denitrifying *Sterolibacterium denitrificans.* J Biol Chem 282:13240-13249

Costas AMG, Poudel S, Miller AF, Schut GJ, Ledbetter RN, Fixen KR, Seefeldt LC, Adams MWW, Harwood CS, Boyd ES, Peters JW (2017) Defining electron bifurcation in the electron-transferring flavoprotein family. J Bacteriol 199:e00440-17

Cunane LM, Chen ZW, McIntire WS, Mathews FS (2005) *p*-cresol methylhydroxylase: alteration of the structure of the flavoprotein subunit upon its binding to the cytochrome subunit. Biochemistry 44:2963-2973

de Medeiros FO, Burkert CAV, Kalil SJ (2012) Purification of beta-galactosidase by ion exchange chromatography: elution optimization using an experimental design. Chem Eng Technol 35:911-918

Duetz WA, Bouwmeester H, van Beilen JB, Witholt B (2003) Biotransformation of limonene by bacteria, fungi, yeasts, and plants. Appl Microbiol Biotechnol 61:269-277

Fernandez-Martinez J, LaCava J, Rout MP (2016) Density gradient ultracentrifugation to isolate endogenous protein complexes after affinity capture. Cold Spring Harbor Protoc 2016:pdb.prot087957

Förster-Fromme K, Höschle B, Mack C, Bott M, Armbruster W, Jendrossek D (2006) Identification of genes and proteins necessary for catabolism of acyclic terpenes and leucine/isovalerate in *Pseudomonas aeruginosa*. Appl Environ Microbiol 72:4819-4828

Förster-Fromme K, Jendrossek D (2006) Identification and characterization of the acyclic terpene utilization gene cluster of *Pseudomonas citronellolis.* FEMS Microbiol Lett 264:220-225

Förster-Fromme K, Jendrossek D (2010) Catabolism of citronellol and related acyclic terpenoids in pseudomonads. Appl Microbiol Biot 87:859-869

Foss S, Heyen U, Harder J (1998) *Alcaligenes defragrans* sp. nov., description of four strains isolated on alkenoic monoterpenes ((+)-menthene, alpha-pinene, 2-carene, and alpha-phellandrene) and nitrate. Syst Appl Microbiol 21:237-244

Fraaije MW, van den Heuvel RHH, van Berkel WJH, Mattevi A (1999) Covalent flavinylation is essential for efficient redox catalysis in vanillyl-alcohol oxidase. J Biol Chem 274:35514-35520

Gainsford GJ, Hosie CF, Weston RJ (2001) Conversion of alpha-pinene to terpinyl acetate over H-beta zeolites. Appl Catal A Gen 209:269-277

Gelb MH, Tamanoi F, Yokoyama K, Ghomashchi F, Esson K, Gould MN (1995) The inhibition of protein prenyltransferases by oxygenated metabolites of limonene and perillyl alcohol. Cancer Lett 91:169-175

Ghisla S, Thorpe C (2004) Acyl-CoA dehydrogenases - a mechanistic overview. Eur J Biochem 271:494-508

Harder J, Marmulla R (2017) Catabolic pathways and enzymes involved in the anaerobic degradation of terpenes. In: Boll M (ed) Anaerobic utilization of hydrocarbons, oils, and lipids. Springer International Publishing, Cham, pp 1-15

Heider J, Szaleniec M, Sunwoldt K, Boll M (2016) Ethylbenzene dehydrogenase and related molybdenum enzymes involved in oxygen-independent alkyl chain hydroxylation. J Mol Microbiol Biotechnol 26:45-62

Heuts DP, Scrutton NS, McIntire WS, Fraaije MW (2009) What's in a covalent bond? On the role and formation of covalently bound flavin cofactors. FEBS J 276:3405-3427

Hille R (2005) Molybdenum-containing hydroxylases. Arch Biochem Biophys 433:107-116

Huang CH, Winkler A, Chen CL, Lai WL, Tsai YC, Macheroux P, Liaw SH (2008) Functional roles of the 6-*S*-cysteinyl, 8-alpha-N1-histidyl FAD in glucooligosaccharide oxidase from *Acremonium strictum*. J Biol Chem 283:30990-30996

Hylemon PB, Harder J (1998) Biotransformation of monoterpenes, bile acids, and other isoprenoids in anaerobic ecosystems. FEMS Microbiol Rev 22:475-488

Immethun CM, Hoynes-O'Connor AG, Balassy A, Moon TS (2013) Microbial production of isoprenoids enabled by synthetic biology. Front Microbiol 4:75-82

Lehman TC, Hale DE, Bhala A, Thorpe C (1990) An Acyl-Coenzyme A dehydrogenase assay utilizing the ferricenium ion. Anal Biochem 186:280-284

Lüddeke F, Dikfidan A, Harder J (2012a) Physiology of deletion mutants in the anaerobic beta-myrcene degradation pathway in *Castellaniella defragrans.* BMC Microbiol 12:192-202

Lüddeke F, Wülfing A, Timke M, Germer F, Weber J, Dikfidan A, Rahnfeld T, Linder D, Meyerdierks A, Harder J (2012b) Geraniol and geranial dehydrogenases induced in anaerobic monoterpene degradation by *Castellaniella defragrans.* Appl Environ Microbiol 78:2128-2136

Luo Q, Hiessl S, Poehlein A, Daniel R, Steinbuchel A (2014) insights into the microbial degradation of rubber and gutta-percha by analysis of the complete genome of *Nocardia nova* SH22a. Appl Environ Microbiol 80:3895-3907

Luo RG, Hsu JT (1997) Optimization of gradient profiles in ion-exchange chromatography for protein purification. Ind Eng Chem Res 36:444-450

Ma Y, Bian J, Zhang F (2016) Inhibition of perillyl alcohol on cell invasion and migration depends on the Notch signaling pathway in hepatoma cells. Mol Cell Biochem 411:307-315

Marmulla R (2015) The anaerobic linalool metabolism in the betaproteobacteria *Castellaniella defragrans* 65Phen and *Thauera linaloolentis* 47Lol. Disseration. University Bremen.

Marmulla R, Cala EP, Markert S, Schweder T, Harder J (2016a) The anaerobic linalool metabolism in *Thauera linaloolentis* 47 Lol. BMC Microbiol 16:76-83

Marmulla R, Safaric B, Markert S, Schweder T, Harder J (2016b) Linalool isomerase, a membrane-anchored enzyme in the anaerobic monoterpene degradation in *Thauera linaloolentis* 47Lol. BMC Biochem 17:6-16

Mlodzik J, Wroblewska A, Makuch E, Wrobel RJ, Michalkiewicz B (2016) Fe/EuroPh catalysts for limonene oxidation to 1,2-epoxylimonene, its diol, carveol, carvone and perillyl alcohol. Catal Today 268:111-120

Petasch J, Disch EM, Markert S, Becher D, Schweder T, Hüttel B, Reinhardt R, Harder J (2014) The oxygen-independent metabolism of cyclic monoterpenes in *Castellaniella defragrans* 65Phen. BMC Microbiol 14:164-176

Prive GG (2007) Detergents for the stabilization and crystallization of membrane proteins. Methods 41:388-397

Puentes-Cala E, Liebeke M, Markert S, Harder J (2018) Anaerobic degradation of bicyclic monoterpenes in *Castellaniella defragrans*. Metabolites 8:E12

Schaub P, Yu Q, Gemmecker S, Poussin-Courmontagne P, Mailliot J, McEwen AG, Ghisla S, Al-Babili S, Cavarelli J, Beyer P (2012) On the structure and function of the phytoene desaturase CRTI from *Pantoea ananatis*, a membrane-peripheral and FAD-dependent oxidase/isomerase. PloS one 7: e39550

Sievers F, Wilm A, Dineen D, Gibson TJ, Karplus K, Li W, Lopez R, McWilliam H, Remmert M, Söding J, Thompson JD, Higgins DG (2011) Fast, scalable generation of high-quality protein multiple sequence alignments using Clustal Omega Mol Syst Biol 7:539-544

Starbird CA, Maklashina E, Cecchini G, Iverson TM (2001) Flavoenzymes: covalent versus noncovalent. In: eLS. John Wiley & Sons, Ltd, pp:1-11

Szaleniec M, Borowski T, Schuhle K, Witko M, Heider J (2010) *Ab inito* modeling of ethylbenzene dehydrogenase reaction mechanism. J Am Chem Soc 132:6014-6024

Tadasa K, Fukazawa S, Kunimatsu M, Hayashi T (1976) Microbiological conversion of α-terpineol (2) Agr Biol Chem 40:1069-1073

Thorpe C, Kim JP (1995) Flavoprotein Structure and Mechanism .3. Structure and mechanism of action of the Acyl-Coa dehydrogenases. FASEB J 9:718-725

Traas PC (1982) 5 - Advances in the chemistry of some interesting cyclic monoterpene alcohols A2 - Theimer, Ernst T. In: Fragrance Chemistry. Academic Press, San Diego, pp 165-219

van Beilen JB, Holtackers R, Luscher D, Bauer U, Witholt B, Duetz WA (2005) Biocatalytic production of perillyl alcohol from limonene by using a novel *Mycobacterium* sp cytochrome P450 alkane hydroxylase expressed in *Pseudomonas putida*. Appl Environ Microbiol 71:1737-1744

Wagner KH, Elmadfa I (2003) Biological relevance of terpenoids. Overview focusing on mono-, di- and tetraterpenes. Ann Nutr Metab 47:95-106

Watmough NJ, Frerman FE (2010) The electron transfer flavoprotein ubiquinone oxidoreductases Biochim Biophys Acta 1797:1910-1916

Wingfield P (2001) Protein precipitation using ammonium sulfate. Curr Protoc Protein Sci Appendix 3:Appendix 3F

Yoo SK, Day DF (2002) Bacterial metabolism of α- and β-pinene and related monoterpenes by *Pseudomonas* sp. strain PIN. Process Biochem 37:739-745

Zafeer MF , Firdaus F, Ahmad F, Ullah R, Anis E, Waseem M, Ali A, Hossain MM (2018) Perillyl alcohol alleviates amyloid-beta peptides-induced mitochondrial dysfunction and cytotoxicity in SH-SY5Y cells. Int J Biol Macromol 109:1029-1038

Zhang DQ, Mu TH, Sun HN, Chen JW, Zhang M (2017) Comparative study of potato protein concentrates extracted using ammonium sulfate and isoelectric precipitation. Int J Food Prop 20:2113-2127

Appendix: Contributed work

The anaerobic linalool metabolism in *Thauera linaloolentis* 47 Lol

Robert Marmulla[1], Edinson Puentes Cala[1], Stephanie Markert[2], Thomas Schweder[2] and Jens Harder[1]*

[1]Dept. of Microbiology, Max Planck Institute for Marine Microbiology, Celsiusstr. 1, D-28359 Bremen, Germany.

[2]Dept. of Pharmaceutical Biotechnology, Institute for Pharmacy, University of Greifswald, Felix-Hausdorff-Str. 3, D-17487 Greifswald, Germany

*To whom correspondence should be addressed: Jens Harder, Dept. of Microbiology, Max Planck Institute for Marine Microbiology, Celsiusstr. 1, D-28359 Bremen, Germany, Tel.: +49 421 2028-750; Fax: +49 421 2028-790; e-mail: jharder@mpi-bremen.de

Published in *BMC Microbiology* (2016) 16:76. DOI: 10.1186/s12866-016-0693-8.

Marmulla *et al. BMC Microbiology* (2016) 16:76
DOI 10.1186/s12866-016-0693-8

BMC Microbiology

RESEARCH ARTICLE Open Access

The anaerobic linalool metabolism in *Thauera linaloolentis* 47 Lol

Robert Marmulla[1], Edinson Puentes Cala[1], Stephanie Markert[2], Thomas Schweder[2] and Jens Harder[1*]

Abstract

Background: The betaproteobacterium *Thauera linaloolentis* 47Lol^T was isolated on the tertiary monoterpene alcohol (*R,S*)-linalool as sole carbon and energy source under denitrifying conditions. Growth experiments indicated the formation of geraniol and geranial. Thus, a 3,1-hydroxyl-Δ^1-Δ^2-mutase (linalool isomerase) activity may initiate the degradation, followed by enzymes of the acyclic terpene utilization (Atu) and leucine/isovalerate utilization (Liu) pathways that were extensively studied in *Pseudomonas* spp. growing on citronellol or geraniol.

Results: A transposon mutagenesis yielded 39 transconjugants that could not grow anaerobically on linalool and nitrate in liquid medium. The deficiencies were apparently based on gene functions required to overcome the toxicity of linalool, but not due to inactivation of genes in the degradation pathway. Growing cultures formed geraniol and geranial transiently, but also geranic acid. Analysis of expressed proteins detected several enzymes of the Atu and Liu pathways. The draft genome of *T. linaloolentis* 47Lol^T had *atu* and *liu* genes with homology to those of *Pseudomonas* spp..

Conclusion: The in comparison to monoterpenes larger toxicity of monoterpene alcohols is defeated by several modifications of the cellular structure and metabolism in *Thauera linaloolentis* 47Lol^T. The acyclic terpene utilization pathway is used in *T. linaloolentis* 47Lol^T during growth on (*R,S*)-linalool and nitrate under anoxic conditions. This is the first experimental verification of an active Atu pathway outside of the genus *Pseudomonas*.

Keywords: Monoterpene, Linalool, Geraniol, Acyclic terpene utilization

Background

Linalool ($C_{10}H_{18}O$, 3,7-dimethylocta-1,6-dien-3-ol), a tertiary monoterpene alcohol, is the main constituent in essential oils of lavender and coriander. It is also a fragrance of flowers [1, 2]. As tertiary alcohols cannot be directly oxidized to ketones, microorganisms initiate their metabolism with oxidation reactions by oxygenases at other parts of the molecule [3] or with isomerizations without molecular oxygen. The latter case has been described for the betaproteobacterium *Castellaniella defragrans* 65Phen. A linalool dehydratase/isomerase metabolizes (*S*)-linalool to geraniol [4, 5]. The further degradation pathway to geranic acid is catalyzed by a NAD^+-dependent geraniol and a geranial dehydrogenase (GeoA, GeoB) [6]. However, a pathway for geranic acid degradation was not found in the genome of *C. defragrans* 65Phen [7]. Expected were genes and operons as described for the degradation of the monoterpene alcohols geraniol and citronellol in *Pseudomonas aeruginosa* PAO1. In this strain, oxidation of the alcohols to their corresponding carboxylic acids and the oxidation of citronellic acid to geranic acid is followed by activation as CoA thioester (Fig. 1). The tertiary carbon atom is transformed into a secondary carbon atom by carboxylation of the β-methyl group as initial reaction. Hydration on the C3 atom yields 3-hydroxy-3-isohexenylglutaryl-CoA followed by acetate cleavage which removes the methyl group initially present at the tertiary carbon atom. 7-methyl-3-oxo-6-octenoyl-CoA is the product of the pathway that was named acyclic terpene utilization (Atu). For several *Pseudomonas* species the enzymes were characterized or tentatively identified: citronellol/citronellal dehydrogenase (AtuB and AtuG), citronellyl-CoA dehydrogenase (AtuD), long-chain acyl-CoA synthase (AtuH), geranyl-CoA carboxylase (AtuC and AtuF), isohexenyl-glutaconyl-CoA hydratase (AtuE) and 3-hydroxy-3-isohexenylglutaryl-

* Correspondence: jharder@mpi-bremen.de
[1]Department of Microbiology, Max Planck Institute for Marine Microbiology, Celsiusstr. 1, D-28359 Bremen, Germany
Full list of author information is available at the end of the article

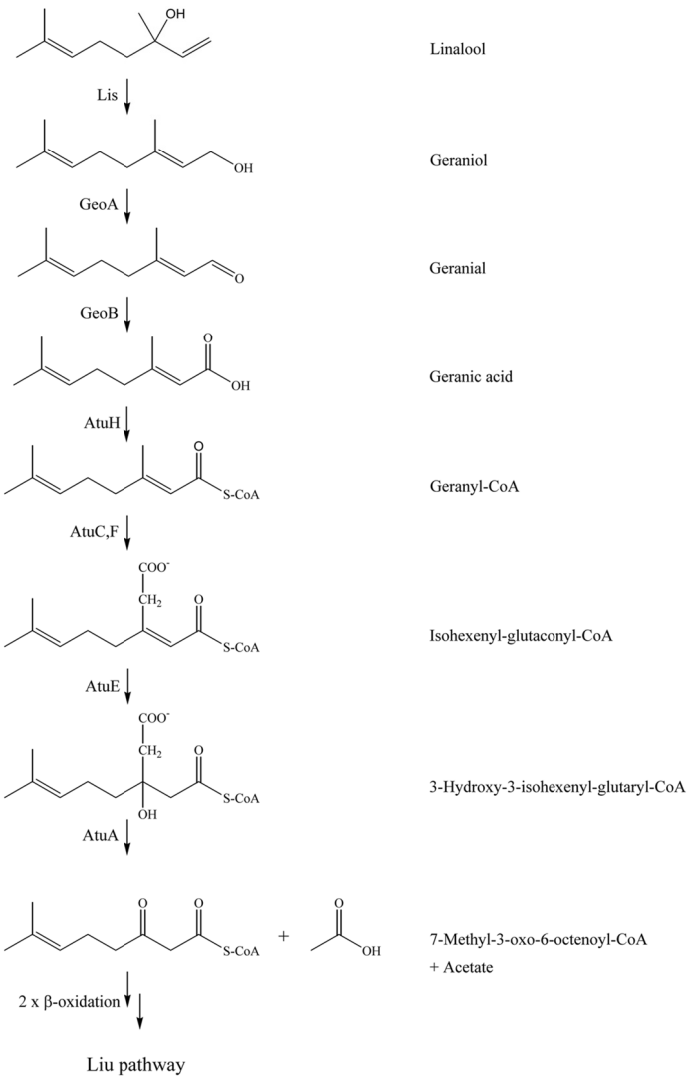

Fig. 1 Proposed pathway for the linalool metabolism in *T. linaloolentis* 47Lol^T, based on the acyclic terpene utilization pathway (Atu) in *Pseudomonas* spp. (adapted from [9]). Linalool isomerase (Lis), geraniol dehydrogenase (GeoA), geranial dehydrogenase (GeoB)

CoA:acetate lyase (AtuA). The corresponding genes are arranged in an operon like structure (*atuABCDEFGH*) under the control of a transcriptional regulator (AtuR) [8–11]. 7-methyl-3-oxo-6-octenoyl-CoA undergoes two rounds of β-oxidation to two acetyl-CoA and 3-methyl-crotonyl-CoA. The latter enters the leucine/isovalerate utilization pathway (Liu) for complete mineralization [12].

The absence of the Atu pathway in the denitrifying *C. defragrans* 65Phen motivated us to search for the pathway in another denitrifying betaproteobacterium, *T. linaloolentis* 47Lol^T. It was isolated on linalool as sole carbon and energy source under denitrifying conditions and uses linalool and geraniol as growth substrates. It has a strictly respiratory metabolism, using molecular oxygen, nitrate, nitrite or nitrous oxide as terminal electron acceptor [13]. Growth studies revealed the regioselective formation of geraniol from linalool in the stationary phase, while linalool and geranial were detected in geraniol-grown cultures. These findings suggested the presence of a linalool isomerase, a 3,1-hydroxyl-Δ^1-Δ^2-mutase [14]. In this study, we attempted the identification of genes and proteins essential for the anaerobic linalool degradation by transposon mutagenesis and by mass spectrometry analyses of proteins.

Results and discussion

Transposon insertion mutagenesis

Five thousand nine hundred sixteen transconjugants were screened on solid medium for denitrifying growth on acetate or linalool as carbon source, presenting a gene coverage of 74 % for an average gene size of 1000 bp. 92 mutants had a growth deficiency on linalool, thus a mutation frequency of 0.0155 was observed. Transfer cultures in liquid medium on linalool and nitrate revealed for 53 of these transposon mutants a biomass yield equal to the wildtype, only 39 transconjugants lacked growth on linalool. The transposon insertion sites in the genome were identified by sequencing and comparison to the genome sequence. Surprisingly, genes of the Atu pathway were not inactivated by transposon insertions. The majority of the inactivated genes was affiliated to the following functional classifications (Additional file 1: Table S1): DNA modification/processing (10 mutants), cellular transport systems (7 mutants), membrane integrity (4 mutants), miscellaneous (7 mutants) and unclassified (11 mutants). In general, these genes, involved in biosynthesis and repair, have to be seen as reflection of the cell toxicity of monoterpenes rather than the involvement in the biodegradation. Monoterpene alcohols exhibit usually a higher toxicity than the pure hydrocarbons. Once these compounds have passed the polar part of the lipopolysaccharide layer (LPS), they can integrate into the outer and inner membranes as well as the hydrophobic core of proteins. The amphiphilic monoterpene alcohols may act as surfactants. Destabilization of the membrane system and cellular structures causes ion leakages and a collapse of the proton motive force. Effects on proteins and on enzyme activities have been reported [15–17]. As defense against the penetration and accumulation of lipophilic substances, Gram-negative bacteria alter the composition and structure of their outer membrane (OM) and the lipopolysaccharide layer [18, 19], e.g., a change in membrane composition from saturated fatty acids to cyclopropane-containing fatty acids has been observed from acetate-grown to monoterpene-grown cells of *C. defragrans* 65Phen [20]. Among the transconjugants were three mutants affected in LPS core and O-antigen synthesis or modification, while another mutant was affected in a penicillin-binding protein (PDB 2) involved in peptidoglycan synthesis during cell growth and division [21, 22]. Bacteria counteract the toxic effects of monoterpenes by active export with energy-driven transporters. Well known examples for such transport systems are multidrug resistance (MDR) or resistance-nodulation-cell division (RND) efflux pumps, however the substrate range of the exporters is often not known [23–25]. We obtained linalool-growth deficient transconjugants with insertion into an ABC-type multidrug transporter or branched-chain amino acid transporters (three mutants). Ten insertions were in genes involved in DNA modification and transcriptional control. Two transconjugants had inactivated a putative transcriptional repressor of the TetR family (NCBI:ENO85695) that had a different domain order, but still an overall 38 % identity on the amino acid level (blastp) to AtuR (NCBI:-BAT64851), a specific transcriptional regulator for the acyclic terpene utilization in *Pseudomonas* spp. [26]. However, the *atu* genes in 47Lol^T are not arranged in the operon structure of *Pseudomonas* and are distant to the repressor gene. Insertion mutants of *P. aeruginosa* showed a consecutive basal expression of Atu proteins [26]. Thus the transcriptional role of this putative repressor remains unclear. Another transconjugant had an insertion in a transcriptional regulator of the ModE family, known to be involved in molybdenum uptake and incorporation [27]. The oxidation of geraniol to geranic acid in *P. aeruginosa* PAO1 is dependent on molybdenum, but other *Pseudomonas* species grow on geraniol and express the Atu pathway without evidence for a molybdenum requirement [10].

The high frequency of transconjugants with a deficiency in growth on linalool coincides with related studies that revealed distinct changes in the transcriptome and proteome in cells switching the growth substrate from non-toxic aliphatic short chain acids to monoterpenes. *Pseudomonas* sp. M1 changed the expression of nearly 30 % of the genome in response to a change from lactate to myrcene, including genes involved in the Atu-pathway, citric acid cycle and β-oxidation, genes for a restructuring of the LPS layer and membranes and an up-regulation of nitrate-respiration gene clusters [28]. The toxicity of monoterpenes was also reflected in the proteomes of *C. defragrans* 65Phen cells grown on acetate and α-phellandrene: among the 107 identified induced proteins were several transporters and membrane biosynthesis proteins [7]. For this organism, a similar transposon mutagenesis identified the central degradation pathway for monoterpenes [7], but these alkenes are less toxic than monoterpene alcohols [6].

The lack of mutants in the catabolic pathway may also indicate the presence of isoenzymes or a second pathway for the degradation of linalool. As second pathway, a linalool kinase/monoterpene synthase together with a degradation of cyclic monoterpenes may be considered for anoxic conditions. We did not detect isoenzymes of the acyclic terpene utilization (Atu) and leucin isovalerate utilization (Liu) pathway (see Table 1). Candidate genes for a second pathway were also not found: monoterpene synthases or the *ctm* operon that was recently identified for limonene degradation [7]. The cytochrome P450 enzyme linalool 8-monooxygenase was also not present, albeit the genome contains mono- and dioxygenases. We tested growth of the transposon mutants on linalool

Table 1 Genes involved in the acyclic terpene utilization (Atu) and leucin isovalerate utilization (Liu) pathway

Enzyme	NCBI accession	Length [AA]	AA similarity [%]	E-value	Protein identification by MS
Linalool isomerase[a]	ENO87364	644	20	3E-10	Yes
Geraniol dehydrogenase[a] (GeoA)	ENO84122	366	46	7E-96	Yes
Geranial dehydrogenase[a] (GeoB)	ENO84123	456	31	7E-39	No
Acyl-CoA synthase[b] (AtuH)	ENO87356	545	24	1E-15	No
Geranyl-CoA carboxylase[b] beta-subunit (AtuC)	ENO87361	545	54	0	Yes
Geranyl-CoA carboxylase[b] alpha subunit (AtuF)	ENO87362	705	52	0	Yes
Isohexenyl-glutaconyl-CoA hydratase[b] (AtuE)	ENO87363	258	30	7E-27	No
3-Hydroxy-3-isohexenylglutaryl-CoA:acetate lyase[b] (AtuA)	ENO84124	615	52	0	Yes
3-Methylcrotonyl-CoA carboxylase[b] beta-subunit (LiuB)	ENO88226	535	72	0	Yes
3-Methylcrotonyl-CoA carboxylase[b] alpha subunit (LiuD)	ENO88223	668	53	0	Yes
3-Methylglutaconyl-CoA hydratase[b] (LiuC)	ENO88225	265	44	3E-73	No
Hydroxymethylglutaryl-CoA lyase[b] (LiuE)	ENO88221	312	63	2E-129	No

Genes were identified by amino acids alignments using *C. defragrans* 65Phen[a] and *P. aeruginosa* PAO1[b] sequences as references. Proteins identified in the proteomic approach were analyzed by SDS-PAGE coupled to MALDI-ToF MS (Additional file 2: Figure S1)

only under denitrifying conditions, thus the linalool metabolism in the presence of oxygen will be studied in the future.

Characterization of growth on linalool

T. linaloolentis 47Lol^T was grown on linalool under denitrifying conditions. Besides the previously demonstrated formation of geraniol and geranial as metabolites [14] we established the detection of geranic acid (Fig. 2a,b). Geraniol and geranial accumulated transiently to 7 and 10 μM, while geranic acid accumulated up to 200 μM. Low cellular concentrations of the toxic geraniol and geranial are due to high affinities of the corresponding enzymes, which is part of a cellular defense [29]. Activities of the intial enzymes - linalool isomerase, geraniol dehydrogenase (GeoA) and geranial dehydrogenase (GeoB) - were measured in cell-free protein extracts of linalool-grown cultures. Linalool isomerase was measured for the thermodynamically favored backward reaction from geraniol to linalool and showed an activity of 260 pkat * mg protein^{-1}. NAD^+-reductase activity for geraniol and citral (mixture of geranial and neral) were 269 ± 51 pkat * mg protein^{-1} and 247 ± 107 pkat * mg protein^{-1}, respectively. Abundant proteins in the cell-free protein extract were identified by SDS-PAGE and MALDI-ToF-based mass spectrometric analysis (Additional file 2: Figure S1). Proteins annotated as linalool isomerase, geraniol dehydrogenase, the two subunits of geranyl-CoA carboxylase as well as a 3-hydroxy-3-isohexenylglutaryl-CoA:acetate lyase were identified together with

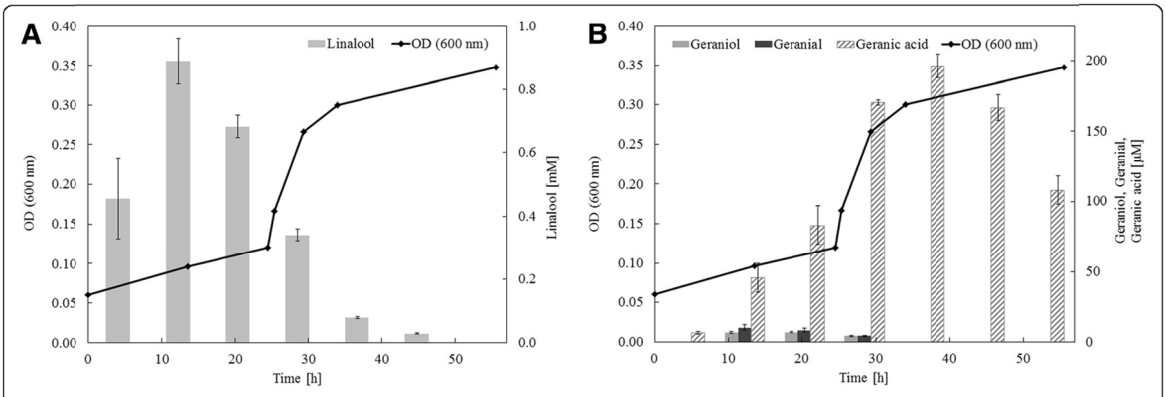

Fig. 2 Growth of *T. linaloolentis* 47Lol^T on 2 mM (*R,S*)-linalool under denitrifying conditions. **a** Optical density at 600 nm as a measure for growth and linalool concentration in mM, **b** Optical density at 600 nm as a measure for growth and geraniol, geranial and geranic acid concentration in μM. Experiment was performed in duplicates. Initial increase in linalool concentration is due to time-dependent dissolution of linalool in medium. Linalool decreased accompanied with an increase in optical density. Geraniol and geranial accumulated only transiently, while geranic acid accumulated up to 200 μM

the two subunits of the methylcrotonyl-CoA carboxylase and the isovaleryl-CoA dehydrogenase of the leucine degradation pathway (*liu* operon).

Genome annotation

Two publicly available draft genomes of *T. linaloolentis* 47Lol^T were assembled and yielded a draft genome with 23 contigs of 4,402,076 bp, an overall G + C content of 66.6 %, 4084 open reading frames, 46 transfer RNA genes and 1 ribosomal RNA operon. The genome completely covers central metabolic pathways, e.g. citric acid cycle, β-oxidation of fatty acids, oxygen respiration and denitrification. Genetic information from *P. citronellolis*, *P. aeruginosa* PAO1 (Atu and Liu pathway) and *C. defragrans* 65Phen (linalool isomerization and geraniol/geranial oxidation) were used to identify homologous genes in *T. linaloolentis* 47Lol^T (Table 1).

Annotations were fully supported by the aforementioned protein identification. One result of the reassembly was the formation of two large contigs that contained all genes of the Atu and Liu pathways over a region of 24 and 9.1 kb, respectively. The *atu* genes were organized with the putative linalool isomerase gene *lis* downstream of *atuCFE* and the genes for the geraniol oxidation *geoAB* upstream of *atuA* (Fig. 3). The genes in between were annotated as hypothetical proteins. Gene homologs for *atuB* and *atuG*, the putative citronellol and citronellal dehydrogenases, were identified in the draft genome but did not show significant similarity in a reciprocal best match analysis.

Conclusion

A transposon mutagenesis targeting the degradation pathway for linalool yielded mutants defective in the defense against the toxic monoterpene alcohol. Enzyme activities of a linalool isomerase, geraniol and geranial dehydrogenases together with the formation of geranic acid demonstrated the initial degradation pathway. Mass spectrometry identified the carboxylases of Atu and Liu pathways which indicated the utilization of these pathways for geranic acid degradation. The draft genome contained the *atu* genes together with candidate genes for the initial degradation pathway. To our knowledge, this is the first description of an active Atu pathway outside of the genus *Pseudomonas* and under anoxic conditions.

Methods

Bacterial strains and cultivation conditions

T. linaloolentis 47Lol^T (= CCUG 41526^T = CIP 105981^T = DSM 12138^T = IAM 15112^T = JCM 21573^T = NBRC 102519^T) was isolated and maintained in our laboratory [13]. For this study, the strain was cultivated under anaerobic, denitrifying conditions in artificial fresh water (AFW) medium. Medium was prepared as described by Foss et al. [20] with modifications. Carbonate buffer was replaced by 10 mM Na_2HPO_4/NaH_2PO_4 and vitamins were omitted. The headspace contained nitrogen gas only. 20 mM Acetate or 2 mM (*R,S*)-linalool were used as growth substrates. Growth experiments were performed in 10 mL cultures, incubated at 28 °C under mild shaking (90 rpm). Growth occurred homogenous and was estimated by measuring the optical density at 600 nm. Monoterpenes were purchased from Sigma-Aldrich (Taufkirchen, Germany) and were of 95 to 97 % purity. Geranial was provided as citral; the mixture of geranial and neral.

Solid AFW medium (0.5 g L^{-1} KH_2PO_4, 0.5 g L^{-1} NH_4Cl, 0.5 g L^{-1} $MgSO_4$ x 7 H_2O, 0.1 g L^{-1} $CaCl_2$ x 2 H_2O, 0.85 g L^{-1} $NaNO_3$, 11.9 g L^{-1} HEPES, 15 g L^{-1}

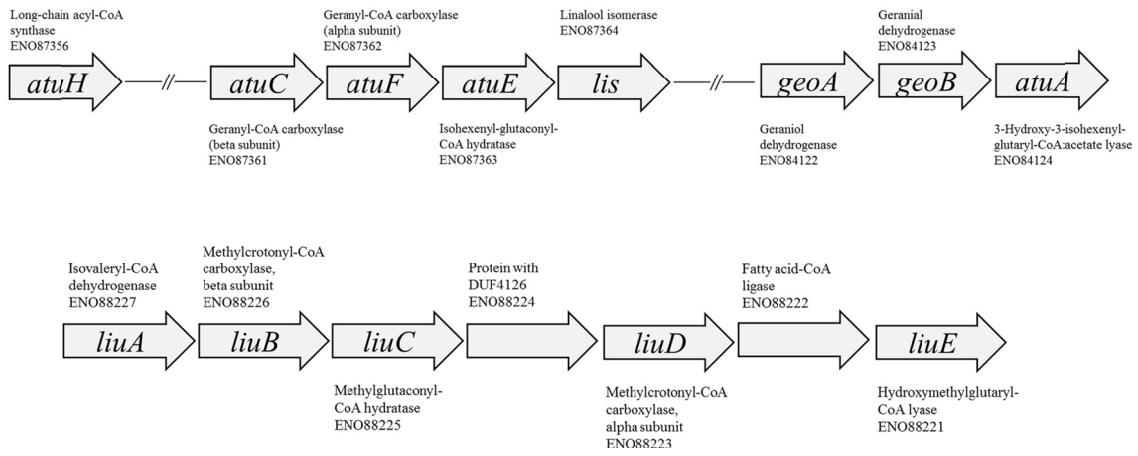

Fig. 3 Gene arrangement of acyclic terpene utilization (*atu*) and leucine isovalerate utilization (*liu*) pathway genes in the draft genome of *T. linaloolentis* 47Lol^T. Annotation and NCBI accession numbers are indicated. Gaps size between *atuH* and *atuC* is 3488 bp and gap size between *lis* and *geoA* is 7617 bp. The *atu* genes are located on a 388748 bp large contig, while the *liu* genes are located on a 205711 bp contig

agar, pH 7.2) was mixed, autoclaved and supplemented with trace-element and selenite-tungstate stock solutions as described [20]. Plates contained either 2 mM (*R,S*)-linalool or 50 mM acetate as carbon source. Liquid brain heart infusion (BHI) medium (12 g L^{-1} brain heart infusion, 10 g L^{-1} peptone, 4 g L^{-1} hydrolyzed casein, 5 g L^{-1} NaCl, 2 g L^{-1} glucose, 2.5 g L^{-1} Na_2HPO_4, 0.2 g L^{-1} $NaNO_3$, pH 7.4) was used to yield higher biomass for genomic DNA extraction. Antibiotics were provided from stock solutions in the following working concentrations: 25-50 μg mL^{-1} kanamycin, 50 μg mL^{-1} rifampicin, 1 μg mL^{-1} ofloxacin.

Transposon insertion mutagenesis

Transposon insertion mutagenesis was performed by using the mini-Tn5 plasmid and biparental conjugation as described by Larsen et al. [30]. Two spontaneous *T. linaloolentis* 47Lol^T mutants resistant to the antibiotics ofloxacin (47Lol-OF) or rifampicin (47Lol-RIF) were obtained by repeated culturing of the wildtype in anoxic medium on 20 mM acetate and 10 mM nitrate in the presence of various concentrations of the antibiotics (20 – 200 μg mL^{-1} rifampicin, 0.05 – 0.15 μg mL^{-1} ofloxacin). *Escherichia coli* BW20767 [31] harboring the pRL27 plasmid with the mini-Tn5 transposon was grown overnight in lysogeny broth with 50 μg mL^{-1} kanamycin at 37 °C. Cells were collected by centrifugation (8000 x *g*, 5 min) and washed twice with fresh medium without antibiotic. The cells were resuspended in medium, diluted to an optical density (600 nm) of 1 and mixed in a donor:recipient ratio of 1:3. 200 μL of this mixture were incubated on AFW-plates (50 mM acetate, no antibiotics) at 28 °C for 24 h aerobically. Cells were resuspended in 1 mL AFW and diluted twofold and tenfold and plated on AFW-plates containing 50 mM acetate, kanamycin and rifampicin or ofloxacin. The plates were incubated for up to 5 days aerobically at 28 °C. Colonies were randomly screened for transposon-integration in the genome by PCR with the primer pair pRL27 Tn5_F (CGTTACATCC CTGGCTTGTT) and pRL27 Tn5_R (TGAAGAAGGTG TTGCTGA) [7]. Transconjugants were replica-plated on AFW-plates containing either 20 mM acetate or 2 mM (*R,S*)-linalool and nitrate. Colonies showing deficiency for anaerobic growth on linalool were selected and transferred into liquid culture and a second anoxic screening on acetate and linalool in the presence of nitrate was performed. Cultures deficient in growth on linalool were selected for further analysis. Genomic DNA was prepared to determine the location of transposon insertion and to identify the affected gene by direct sequencing. Mutants were grown in 10 mL BHI medium overnight. Biomass was collected by centrifugation (4500 x *g*, 10 min), resuspended in 150 μL buffer (Tris-Cl 50 mM, 10 mM EDTA, pH 8, 50 units RNase A) and treated with 150 μL lysis buffer (200 mM NaOH, 1 % w/v SDS). After mixing and incubation at 96 °C for 20 min the solution was neutralized by addition of 225 μL neutralization buffer (3 M sodium acetate, pH 5.5). Precipitates were removed by centrifugation (20000 × *g*, 10 min). Genomic DNA was precipitated from the supernatant by addition of ice-cold isopropanol to a content of 50 % (v/v), incubation at −20 °C for 60 min and centrifugation (20000 × *g*, 20 min, 4 °C). The DNA pellet was washed with 70 % (v/v) ice-cold ethanol, centrifuged and dissolved in 40 μL water. Sequencing reactions were performed with the BigDye Terminator v3.1 Cycle Sequencing Kit (Applied Biosystems by Thermo Fisher Scientific, Waltham, USA), gDNA (1 – 3 μg) as template and the primer pair tnpRL 17_1 (AACAAGCCAGGGATG-TAA) and tnpRL 13_2 (CAGCAACACCTTCTTCACGA) [30] using the following program: 96 °C for 20 s, 99 cycles of 96 °C for 10 s, 56 °C for 5 s, 60 °C for 4 min. Amplicons were analyzed with an ABI Prism 3130*xl* Genetic Analyzer (Applied Biosystems by Thermo Fisher Scientific, Waltham, USA). The probability of coverage of a gene by a mutant was calculated for a genome size of 4402076 bases with:

$$P = 1 - \left(1 - \frac{average\ gene\ size}{genome\ size}\right)^{number\ of\ mutans}$$

Metabolite analysis

T. linaloolentis 47Lol^T was cultivated on 1.5 mM (*R,S*)-linalool and 10 mM nitrate in duplicate cultures. Inoculum was 2 % (v/v) of a linalool-adapted culture. Two cultures with similar optical densities were sampled for metabolite extraction, covering growth over the lag-phase, exponential phase to the entry into the stationary phase. 10 mL culture liquid was transferred to a 15 mL plastic tube, 3 g of NaCl and 250 μL of n-hexane were added. The sample was mixed by vortexing for 30 s and 10 min incubation on a tilting shaker. Phase separation was achieved by 10 min centrifugation (3500 × *g*, 10 min, 5 °C). The clear hexane phase was recovered into a GC-vial. 1 μL sample was analyzed by gas chromatography with flame ionization detection (Shimadzu GC-14A, Shimadzu, Duisburg, Germany) on a Hydrodex-β-6TBDM column (25 m × 0.25 mm, Macherey-Nagel, Düren, Germany) with the following temperature program: injection port 200 °C, detection port 250 °C, initial column temperature 60 °C for 1 min, increasing to 130 °C at a rate of 5 °C min^{-1}, keeping 130 °C for 0.5 min, followed by an increase to 230 °C at 20 °C min^{-1} and hold for 4 min. To determine the geranic acid concentration, 50 μL of the hexane phase were mixed with 50 μL 1 mM NaOH and the hexane was allowed to evaporate. 5 μL of 20 mM phosphoric acid were added and the sample was analyzed by an Acquity UPLC H-class system (Waters Corporation, Milford, USA). 1 μL sample was separated on a reverse phase (BEH C18, 1.7 μm, 2.1 ×

50 mm) column with 1 mM H_3PO_4 at 0.6 mL min^{-1} in a water-acetonitrile gradient from 10 to 70 % acetonitrile (v/v) at 30 °C. UV detection was performed at 221 nm.

Geraniol-, Geranial dehydrogenase and Linalool isomerase assays

Soluble protein extract of *T. linaloolentis* 47Lol^T was prepared from biomass suspension in Tris-Cl buffer (40 mM, pH 8.0) by passing through an One-Shot cell disruptor (Constant Systems Ltd., Daventry, UK) at 1.7 GPa two times, followed by ultracentrifugation (150000 × *g*, 30 min, 4 °C). The clarified supernatant was used for further experiments. Geraniol- and Geranial dehydrogenase activities were determined by absorption measurement of NADH formation at 340 nm on a Beckman DU640 Spectrophotometer (Beckman Coulter, Brea, USA) as described previously [6]. Soluble protein extract was dialyzed against Tris-Cl buffer (VISKING dialysis tubing, 14 kDa cutoff, Serva, Heidelberg, Germany). The final assay (1 mL) was performed in a quartz cuvette at 22 °C and contained 1 mM geraniol or 1.5 mM citral, 1 mM NAD^+ (final concentrations) and various amounts of protein. Reactions were started by addition of NAD^+. Rates were calculated based on a molar extinction coefficient of 6220 M^{-1} cm^{-1}. Linalool isomerase activity was determined in soluble protein extracts. Glass vials (4 mL) with 300 to 500 µL sample were reduced with 5 mM dithionite, closed with butyl rubber stoppers and flushed with nitrogen gas for 3 min, to provide anoxic conditions. Samples were incubated for 20 min at room temperature. The reaction was started by addition of 200 µL geraniol (200 mM) in 2,2,4,4,6,8,8-heptamethylnonane (HMN) through a needle and incubated for 14 to 16 h at 28 °C under mild shaking. Product formation was determined in samples from the HMN phase by gas chromatography with flame ionization detection (PerkinElmer Auto System XL, Überlingen, Germany) on an Optima-5column (30 m × 0.32 mm, 0.25 µm film thickness; Macherey-Nagel, Düren, Germany) with the following temperature program: injection port 250 °C, detection port 350 °C, initial column temperature 40 °C for 2 min, increasing to 100 °C at a rate of 4 °C min^{-1}, keeping 100 °C for 0.1 min, followed by an increase to 320 °C at 45 °C min^{-1} and hold for 3 min. The split ratio was set to 1:9.

Proteomics by MALDI-ToF MS

T. linaloolentis 47Lol^T cultures were grown on (*R,S*)-linalool to the late exponential phase and harvested by centrifugation. Cells were suspended in Tris-Cl buffer (40 mM, pH 8.0) and soluble protein extract was prepared as described above. Protein samples, obtained from individual purifications, were analyzed by SDS-PAGE coupled with matrix-assisted laser desorption/ionization time of flight (MALDI-ToF) mass spectrometry (MS). Protein bands in gels were excised manually, and the Ettan Spot Handling Workstation (GE Healthcare, Freiburg, Germany) was used for trypsin digestion and embedding of the resulting peptide solutions in an α-cyano-4-hydroxycinnamic acid matrix for spotting onto MALDI targets. MALDI-ToF MS analysis was performed on an AB SCIEX TOF/TOF™ 5800 Analyzer (Sciex, Ontario, Canada) [32]. Spectra in a mass range from 900 to 3700 Da (focus 1700 Da) were recorded and analyzed by GPS Explorer™ Software Version 3.6 (build 332, Applied Biosystems by Thermo Fisher Scientific, Waltham, USA) and the Mascot search engine version 2.4.0 (Matrix Science Ltd, London, UK) using the RAST draft genome as reference.

Draft genome and gene analysis

Two publicly available sequencing datasets for *T. linaloolentis* 47Lol^T, ASM31020 (4.199 Mbp on 220 contigs, available since November 2012) and ASM62130 (4.214 Mbp on 46 contigs, available since April 2014), were merged using Sequencher 4.6 (Gene Codes, Ann Arbor, USA) with a minimum match percentage of 95 % and a minimum overlap of 50 bases. The resulting draft genome was uploaded to RAST for further analysis [33, 34]. Known genes from *Castellaniella defragrans* 65Phen, *Pseudomonas aeruginosa* PAO1 and *P. citronellolis*, encoding enzymes involved in the linalool and geraniol metabolism, were used to identify homologs in *T. linaloolentis* 47Lol^T. Overall similarity of the identified genes to their homologs was determined by blastp [35].

Ethics approval and consent to participate

Consent for publication

Not applicable.

Availability of data and materials

The datasets supporting the conclusions of this article are included within the article and its additional files.

Additional files

Additional file 1: Table S1. Transposon insertion mutants. The table presents the transposon insertion mutants (name, NCBI accession number of protein, annotation). (DOCX 22 kb)

Additional file 2: Figure S1. SDS-PAGEs (A, B) of cell-free protein extracts of *T. linaloolentis* 47Lol^T grown on 1 mM (*R,S*)-linalool and 10 mM nitrate to the late exponential phase. Indicated bands were extracted and analyzed by MALDI-ToF MS. Marker is given in kDa. (1) AtuF - geranyl-CoA carboxylase alpha subunit, (2) LiuD - methylcrotonyl-CoA carboxylase biotin-containing subunit, (3) AtuA - 3-hydroxy-3-isohexenylglutaryl-CoA:acetate lyase, (4) AtuC - geranyl-CoA carboxylase beta subunit, (5) LiuA - Isovaleryl-CoA dehydrogenase, (6) GeoA - geraniol dehydrogenase, (7) Lis - linalool isomerase, (8) LiuB - methylcrotonyl-CoA carboxylase carboxyl transfer subunit. (PNG 263 kb)

Abbreviation

LPS: lipopolysaccharide.

Competing interests
The authors declare that they have no competing interests.

Authors' contributions
RM, EPC and JH participated in the design of the study. RM carried out growth experiments, enzyme measurements and bioinformatic work. EPC performed the transposon mutagenesis experiment. SM and TS conducted mass-spectrometry based protein identifications and analyzed data. RM and JH drafted the manuscript. All authors read and approved the final manuscript.

Acknowledgments
We thank Dirk Albrecht for MALDI-ToF measurements and Tina Trautmann for technical assistance.

Funding
This study was financed by the Max Planck Society.

Author details
[1]Department of Microbiology, Max Planck Institute for Marine Microbiology, Celsiusstr. 1, D-28359 Bremen, Germany. [2]Department of Pharmaceutical Biotechnology, Institute for Pharmacy, University of Greifswald, Felix-Hausdorff-Str. 3, D-17487 Greifswald, Germany.

Received: 9 November 2015 Accepted: 14 April 2016
Published online: 27 April 2016

References

1. Kesselmeier J, Staudt M. Biogenic volatile organic compounds (VOC): An overview on emission, physiology and ecology. J Atmos Chem. 1999;33:23–88.
2. Sharkey TD, Yeh S. Isoprene emission from plants. Annu Rev Plant Physiol Plant Mol Biol. 2001;52:407–36.
3. Marmulla R, Harder J. Microbial monoterpene transformations – A review. Front Microbiol. 2014;5:346.
4. Brodkorb D, Gottschall M, Marmulla R, Lüddeke F, Harder J. Linalool dehydratase-isomerase, a bifunctional enzyme in the anaerobic degradation of monoterpenes. J Biol Chem. 2010;285:30436–42.
5. Lüddeke F, Harder J. Enantiospecific (S)-(+)-linalool formation from beta-myrcene by linalool dehydratase-isomerase. Z Naturforsch, C: Biosci. 2011;66:409–12.
6. Lüddeke F, Wülfing A, Timke M, Germer F, Weber J, Dikfidan A, Rahnfeld T, Linder D, Meyerdierks A, Harder J. Geraniol and geranial dehydrogenases induced in anaerobic monoterpene degradation by *Castellaniella defragrans*. Appl Environ Microbiol. 2012;78:2128–36.
7. Petasch J, Disch E-M, Markert S, Becher D, Schweder T, Hüttel B, Reinhardt R, Harder J. The oxygen-independent metabolism of cyclic monoterpenes in *Castellaniella defragrans* 65Phen. BMC Microbiol. 2014;14:164.
8. Förster-Fromme K, Jendrossek D. Identification and characterization of the acyclic terpene utilization gene cluster of *Pseudomonas citronellolis*. FEMS Microbiol Lett. 2006;264:220–5.
9. Förster-Fromme K, Jendrossek D. Catabolism of citronellol and related acyclic terpenoids in pseudomonads. Appl Microbiol Biotechnol. 2010;87:859–69.
10. Höschle B, Jendrossek D. Utilization of geraniol is dependent on molybdenum in *Pseudomonas aeruginosa*: evidence for different metabolic routes for oxidation of geraniol and citronellol. Microbiology. 2005;151:2277–83.
11. Poudel N, Pfannstiel J, Simon O, Walter N, Papageorgiou AC, Jendrossek D. *Pseudomonas aeruginosa* isohexenyl glutaconyl-CoA hydratase (AtuE) is upregulated in citronellate-grown cells and belongs to the crotonase family. Appl Environ Microbiol. 2015;81:6558–66.
12. Förster-Fromme K, Höschle B, Mack C, Bott M, Armbruster W, Jendrossek D. Identification of genes and proteins necessary for catabolism of acyclic terpenes and leucine/isovalerate in *Pseudomonas aeruginosa*. Appl Environ Microbiol. 2006;72:4819–28.
13. Foss S, Harder J. *Thauera linaloolentis* sp. nov. and *Thauera terpenica* sp. nov., isolated on oxygen-containing monoterpenes (linalool, menthol, and eucalyptol) and nitrate. Syst Appl Microbiol. 1998;21:365–73.
14. Foss S, Harder J. Microbial transformation of a tertiary allylalcohol: Regioselective isomerisation of linalool to geraniol without nerol formation. FEMS Microbiol Lett. 1997;149:71–5.
15. Nazzaro F, Fratianni F, De Martino L, Coppola R, De Feo V. Effect of essential oils on pathogenic bacteria. Pharmaceuticals. 2013;6:1451–74.
16. Bakkali F, Averbeck S, Averbeck D, Waomar M. Biological effects of essential oils - A review. Food Chem Toxicol. 2008;46:446–75.
17. Sikkema J, Debont JAM, Poolman B. Mechanisms of membrane toxicity of hydrocarbons. Microbiol Rev. 1995;59:201–22.
18. Nikaido H. Molecular basis of bacterial outer membrane permeability revisited. Microbiol Mol Biol Rev. 2003;67:593–656.
19. van den Berg B. Going forward laterally: Transmembrane passage of hydrophobic molecules through protein channel walls. ChemBioChem. 2010;11:1339–43.
20. Foss S, Heyen U, Harder J. *Alcaligenes defragrans* sp. nov., description of four strains isolated on alkenoic monoterpenes ((+)-menthene, alpha-pinene, 2-carene, and alpha-phellandrene) and nitrate. Syst Appl Microbiol. 1998;21:237–44.
21. Macheboeuf P, Contreras-Martel C, Job V, Dideberg O, Dessen A. Penicillin binding proteins: key players in bacterial cell cycle and drug resistance processes. FEMS Microbiol Rev. 2006;30:673–91.
22. Sauvage E, Kerff F, Terrak M, Ayala JA, Charlier P. The penicillin-binding proteins: structure and role in peptidoglycan biosynthesis. FEMS Microbiol Rev. 2008;32:234–58.
23. Lubelski J, Konings WN, Driessen AJM. Distribution and physiology of ABC-type transporters contributing to multidrug resistance in bacteria. Microbiol Mol Biol Rev. 2007;71:463–76.
24. Martinez JL, Sánchez MB, Martínez-Solano L, Hernandez A, Garmendia L, Fajardo A, Alvarez-Ortega C. Functional role of bacterial multidrug efflux pumps in microbial natural ecosystems. FEMS Microbiol Rev. 2009;33:430–49.
25. Ramos JL, Duque E, Gallegos M-T, Godoy P, Ramos-González MI, Rojas A, Terán W, Segura A. Mechanisms of solvent tolerance in Gram-negative bacteria. Annu Rev Microbiol. 2002;56:743–68.
26. Förster-Fromme K, Jendrossek D. AtuR is a repressor of acyclic terpene utilization (Atu) gene cluster expression and specifically binds to two 13 bp inverted repeat sequences of the atuA-atuR intergenic region. FEMS Microbiol Lett. 2010;308:166–74.
27. Grunden AM, Self WT, Villain M, Bialock JE, Shanmugam KT. An analysis of the binding of repressor protein ModE to modABCD (Molybdate transport) operator/promoter DNA of *Escherichia coli*. J Biol Chem. 1999;274:24308–15.
28. Soares-Castro P, Santos PM. Deciphering the genome repertoire of *Pseudomonas* sp. M[+] toward β-myrcene biotransformation. Genome Biol Evol. 2015;7:1–17.
29. Kim JM, Marshall MR, Cornell JA, III JFP, Wei CI. Antibacterial activity of carvacrol, citral, and geraniol against *Salmonella typhimurium* in culture medium and on fish cubes. J Food Sci. 1995;60:1364–8.
30. Larsen R, Wilson M, Guss A, Metcalf W. Genetic analysis of pigment biosynthesis in *Xanthobacter autotrophicus* Py2 using a new, highly efficient transposon mutagenesis system that is functional in a wide variety of bacteria. Arch Microbiol. 2002;178:193–201.
31. Metcalf WW, Jiang W, Daniels LL, Kim S-K, Haldimann A, Wanner BL. Conditionally replicative and conjugative plasmids carrying *lacZα* for cloning, mutagenesis, and allele replacement in bacteria. Plasmid. 1996;35:1–13.
32. Wolf C, Hochgräfe F, Kusch H, Albrecht D, Hecker M, Engelmann S. Proteomic analysis of antioxidant strategies of *Staphylococcus aureus*: Diverse responses to different oxidants. Proteomics. 2008;8:3139–53.
33. Aziz RK, Bartels D, Best AA, DeJongh M, Disz T, Edwards RA, Formsma K, Gerdes S, Glass EM, Kubal M, et al. The RAST server: Rapid annotations using subsystems technology. BMC Genomics. 2008;9.
34. Overbeek R, Olson R, Pusch GD, Olsen GJ, Davis JJ, Disz T, Edwards RA, Gerdes S, Parrello B, Shukla M, et al. The SEED and the Rapid Annotation of microbial genomes using Subsystems Technology (RAST). Nucleic Acids Res. 2014;42:D206–14.
35. Altschul SF, Gish W, Miller W, Myers EW, Lipman DJ. Basic local alignment search tool. J Mol Biol. 1990;215:403–10.

Supplementary material

The anaerobic linalool metabolism in *Thauera linaloolentis* 47 Lol

Robert Marmulla[1], Edinson Puentes Cala[1], Stephanie Markert[2], Thomas Schweder[2] and Jens Harder[1]*

[1]Dept. of Microbiology, Max Planck Institute for Marine Microbiology, Celsiusstr. 1, D-28359 Bremen, Germany.

[2]Dept. of Pharmaceutical Biotechnology, Institute for Pharmacy, University of Greifswald, Felix-Hausdorff-Str. 3, D-17487 Greifswald, Germany

*To whom correspondence should be addressed: Jens Harder, Dept. of Microbiology, Max Planck Institute for Marine Microbiology, Celsiusstr. 1, D-28359 Bremen, Germany, Tel.: +49 421 2028-750; Fax: +49 421 2028-790; e-mail: jharder@mpi-bremen.de

Table S1: Transposon insertion mutants. The table presents the transposon insertion mutants (name, NCBI accession number of protein, annotation

Mutant	Length [bp]	NCBI accession	Protein annotation	Probable function
			DNA modification / transcriptional control	
18	309	ENO90120	Integration host factor, α-subunit	Transcription regulation
36	2124	ENO88423	DNA-repair protein; Type III restriction enzyme	DNA repair mechanism
41	813	ENO89557	DNA-binding domain of ModE	Transcription regulation (molybdenum metabolism)
47	675	ENO85695	Trancriptional regulator, TetR family	Transcription regulation
63	294	ENO87982	XRE family transcriptional regulator	Transcription regulation (response to xenobiotics)
64	675	ENO85695	Trancriptional regulator, TetR family	Transcription regulation
83	1074	ENO88415	DNA sulfur modification protein DndB	DNA binding and recognition of modification sites
88	2568	ENO89640	PAS/PAC sensor hybrid histidine kinase	Signaling and transcription regulation

Mutant	Length [bp]	NCBI accession	Protein annotation	Probable function
91	1542	ENO89296	ATP-dependent endonuclease family protein	DNA repair mechanism
93	903	ENO82884	Integrase core domain (Transposase)	DNA mobility
			Transport	
37	2433	ENO85793	TonB-dependent siderophore receptor (FpvA)	Transport
38	2430	ENO90450	TonB-dependent siderophore receptor	Transport
60	1332	ENO85236	Branched-chain amino acid transport system permease protein LivM	Branched-chain amino acid transport
69	705	ENO88656	Membrane protein belonging to the AzlC superfamily	Branched-chain amino acid transport
73	705	ENO88656	Membrane protein belonging to the AzlC superfamily	Branched-chain amino acid transport
80	1140	ENO86020	ABC-type multidrug transprort system	Transport
81	2475	ENO86288	TonB-dependent siderophore receptor	Transport

Mutant	Length [bp]	NCBI accession	Protein annotation	Probable function
			Membrane integrity	
21	1971	ENO84346	Penicillin-binding protein 2	Peptidoglycan synthesis (cell elongation)
52	963	ENO84489	ADP-L-glycero-D-manno-heptose-6-epimerase (EC 5.1.3.20)	Lipooligosaccharide core biosynthesis
68	1386	ENO89893	UDP-phosphate galactose phosphotransferase	Lipopolysachharide O-antigen synthesis
85	1386	ENO89893	UDP-phosphate galactose phosphotransferase	Lipopolysachharide O-antigen synthesis
			Miscellaneous	
54	1548	ENO84316	ATP-dependent RNA helicase	RNA metabolism
58	264	ENO89266	Lysophospholipase (EC 3.1.1.5)	Phospholipid metabolism
61	16533	ENO89831	Putative large exoprotein involved in heme utilization or adhesion of ShlA/HecA/FhaA family	Similarity to hemagglutinin-like protein; involved in cell adhesion
62	1041	ENO84082	Peptidase Gluzincin family (MA2)	Protein metabolism
66	1146	ENO84083	Fic (Filamentation induced by cAMP) family protein	Regulatory mechanism of cell division, folate metabolism

Mutant	Length [bp]	NCBI accession	Protein annotation	Probable function
67	504	ENO85121	Putative phasin protein	Surface proteins of intracellular storage granules
87	504	ENO85121	Putative phasin protein	Surface proteins of intracellular storage granules
			Unclassified	
28	7296	ENO88318*	Hypothetical protein	unknown
43	1812	ENO90436*	Putative ATP and DNA-binding domain	DNA metabolism
46	1209	ENO90599	Membrane protein, Acyltransferase	unknown
53	1524; 927	ENO87300; ENO87299	Reverse transcriptase; Threonine dehydratase	Unknown; Amino acid metabolism
55	1104	ENO86348	Hypothetical protein	unknown
70	525	ENO88413	Hypothetical protein	Motif for dnd system-associated protein 4 within DNA sulfur modification system
71	1179	ENO87344	von Willebrand factor A containing CoxE domain-like protein	unknown

Mutant	Length [bp]	NCBI accession	Protein annotation	Probable function
76 [#]				
77	819	ENO89891	Similarity to labA-like proteins (NYN domain)	Unknown (might be involved in RNA core metabolism; RNA processome)
79	1170	ENO89611	Hypothetical protein	Unknown (DUF2863)
84	1104	ENO86348	Hypothetical protein	Unknown

***** DNA sequence identical but translation is incorrect in NCBI

[#] no sequence was obtained from the sequencing for mutant 76

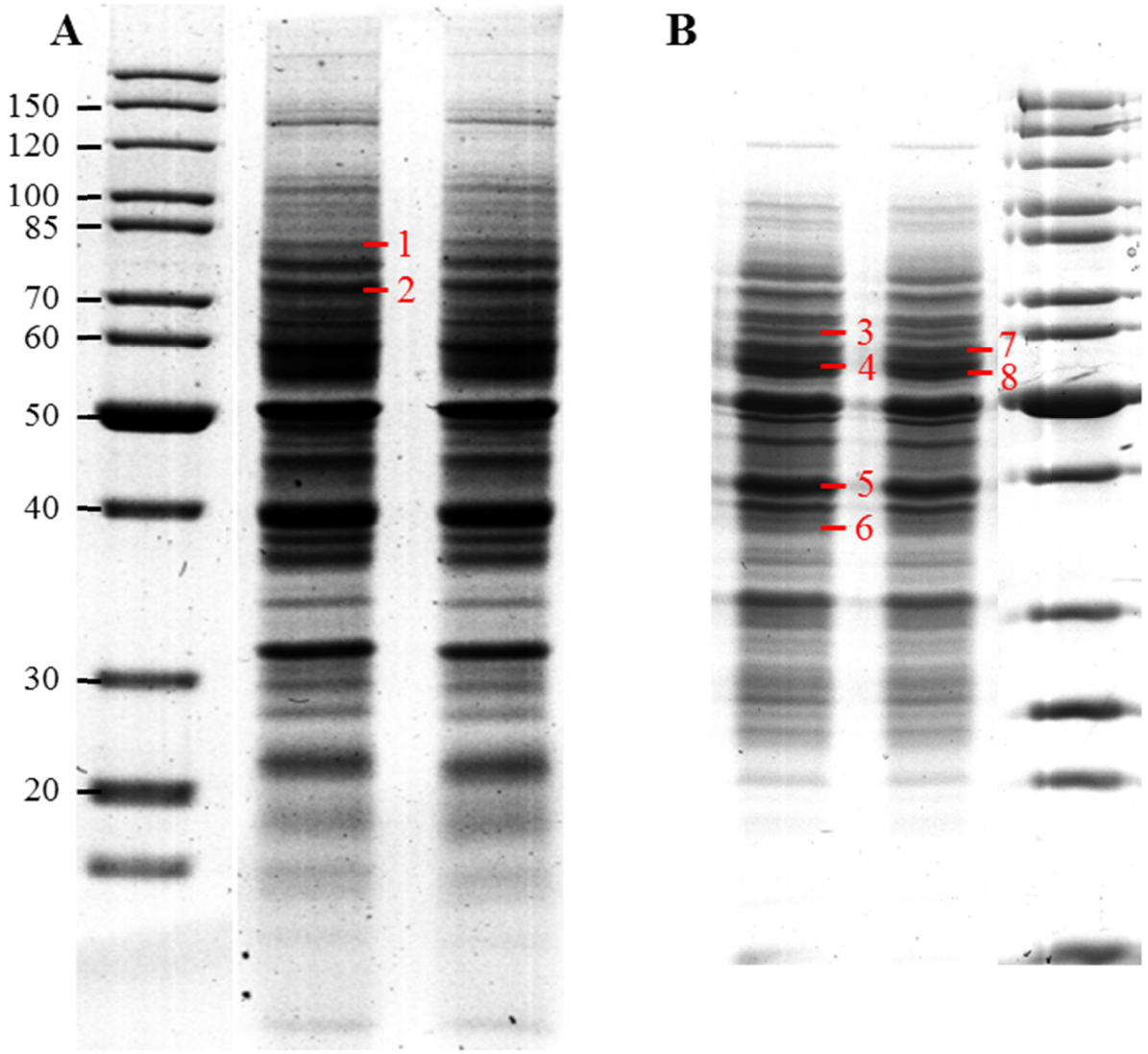

Figure S1. SDS-PAGEs (A, B) of cell-free protein extracts of *T. linaloolentis* 47Lol^T grown on 1 mM (*R,S*)-linalool and 10 mM nitrate to the late exponential phase. Indicated bands were extracted and analyzed by MALDI-ToF MS. Marker is given in kDa. (1) AtuF - geranyl-CoA carboxylase alpha subunit, (2) LiuD - methylcrotonyl-CoA carboxylase biotin-containing subunit, (**3**) AtuA - 3-hydroxy-3-isohexenylglutaryl-CoA:acetate lyase, (4) AtuC - geranyl-CoA carboxylase beta subunit, (5) LiuA - Isovaleryl-CoA dehydrogenase, (6) GeoA - geraniol dehydrogenase, (7) Lis - linalool isomerase, (8) LiuB - methylcrotonyl-CoA carboxylase carboxyl transfer subunit.

Acknowledgements

I will be always grateful to Prof. Dr. Jens Harder not only for the chance to work under his supervision during this doctoral thesis, but for his teachings in microbiology, chemistry, biochemistry, oceanography and many others, and in general for the numerous teachings about science and its perks. I particularly appreciate your support while I was struggling for funding here and there and above all for your constant disposition to talk to us, your students, and for keeping your door always open. Thanks for taking the time for reading and correcting over and over my always improvable writings. And thanks as well for presiding my defense's examination board and for the funny way I know you are gonna introduce me to the audience on that day.

Special thanks to Prof. Dr. Michael Friedrich for accepting to be the second reviewer of my thesis in rather short notice. Also for being a major source of inspiration: your lectures have encouraged me to continue exploring the fascinating world of prokaryotes!

Prof. Dr. Rudolf Amann and Dr. Jan-Hendrik Hehemann, I thank you both for accepting to be part of my examination board. Also, thanks for your support over the last years. I am very grateful and honored to have had the chance to interact with you.

Dear Prof. Dr. Ulrich Fischer thank you very much for your constructive input during the committee meetings. I am very glad that I had the chance to count with your expertise.

A special thank you goes to Prof. Dr. Matthias Ulrich for his support during both my master and PhD thesis.

I thank Tanja Fischer and Hagen Buck-Wiese for the representative student in my examination board.

A big thank you to an army of bachelor and master students with whom I had the privilege to work: Radhika, Nelissa, Anastasia, Paola, Sara, Norah, Chad, Yoga, Stefano and Elizabeth.

A special mention to a lot of marmics that have positively influenced me and taught me so much along the way: Jenny, Robert, Tanja, Burak, Olie, Anni and all other Garlics. Love all you guys. I hope you come visit us in Colombia one day.

A big thank you goes also to Christina, Ramona, Ingrid and Daniela, our lovely lab technicians, for introducing me into the lab's do's and don'ts, for your constant support and for the always interesting conversations in German ;). I'm gonna miss you.

Finally, I want to thank the MARMIC program, its faculty members and specially Anita, Karl-Heinz and Christiane for making these last few years one the most fruitful periods of my life.

Quiero expresar también mis sinceros agradecimientos y aprecio a la Corporación para la Investigación de la Corrosión –CIC–, especialmente al Dr. Jorge Hdo. Panqueva, por su inmenso apoyo y su gran visión. Se quedarían cortas todas las páginas de esta tesis para agradecerle a Ud. y a todos mis compañeros en la CIC.

Mis agradecimientos también a COLCIENCIAS y al MEN por su apoyo financiero. Continuemos así hasta alcanzar una masa crítica de profesionales que inclinen la balanza en nuestro bello país.

Mis agradecimientos a mi amada madre y a mis hermanos por ser una inmensa fuente de inspiración y por ponerme una sonrisa en el rostro que me alcanza hasta la siguiente llamada telefónica.

A Genis, Sina, Luc y Mateo, gracias por estar ahí siempre y ayudarme a mantener la moral alta. Un abrazo para los cuatro.

Ich hätte das alles hier nicht schaffen können, ohne meine alle Schönste. Meine letzten 6 Jahre und nächsten 60 hätten ohne dich keinen Sinn! Ich danke dir meine Jenny. Auch für Tweety!

Universität Bremen

Name: Edinson Andrés Puentes Cala **Ort, Datum:** Bremen, 7. März 2018

Anschrift: Ottilie-Hoffmann-Str. 73, 28213 Bremen

ERKLÄRUNG

.

Hiermit erkläre ich, dass ich die Doktorarbeit mit dem Titel:

„The anaerobic monoterpene metabolism in *Castellaniella defragrans* 65Phen"

selbstständig verfasst und geschrieben habe und außer den angegebenen Quellen keine weiteren Hilfsmittel verwendet habe.

Ebenfalls erkläre ich hiermit, dass es sich bei den von mir abgegebenen Arbeiten um drei identische Exemplare handelt.

_____

(Unterschrift)